

UVM ScholarWorks

Characterization of Unsaturated Soils Using Acoustic Techniques

Item Type	dissertation;article
Authors	George, Lindsay
Download date	2026-06-18 08:25:31
Link to Item	https://hdl.handle.net/20.500.14849/4890

**CHARACTERIZATION OF UNSATURATED SOILS
USING ACOUSTIC TECHNIQUES**

A Dissertation Presented

by

Lindsay A. George

to

The Faculty of the Graduate College

of

The University of Vermont

**In Partial Fulfillment of the Requirements
for the Degree of Doctor of Philosophy
Specializing in Civil and Environmental Engineering**

February, 2009

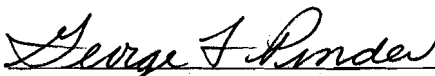
Accepted by the Faculty of the Graduate College, The University of Vermont, in partial fulfillment of the requirements for the degree of Doctor of Philosophy, specializing in Civil and Environmental Engineering.

Dissertation Examination Committee:

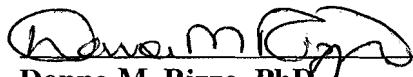


Advisor

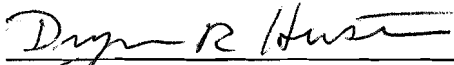
Mandar M. Dewoolkar, PhD



George F. Pinder, PhD



Donna M. Rizzo, PhD



Chairperson

Dryver R. Huston, PhD



Frances E. Carr, Ph.D.

Vice President for Research
and Dean of Graduate Studies

Date: November 21, 2008

ABSTRACT

Recently there has been a great interest in the ability to relate the hydro-mechanical properties of soils to their acoustic response. This ability could enhance high resolution non-destructive evaluation of the shallow subsurface, and would have applications in a variety of fields including groundwater and contaminant hydrogeology, oil recovery, soil dynamics, and the detection of buried objects. Groundwater hydrologists and environmental engineers are challenged with the task of characterizing the material, mechanical and hydraulic properties of the subsurface with limited information generally collected from discrete points. Geophysical testing offers a suite of measurement techniques that allow for the non destructive evaluation of potentially large areas in a continuous manner. Acoustic testing is one geophysical method used by many professions to characterize the subsurface.

Unsaturated and multiphase flow modeling relies on the relationship between the capillary pressure and the level of saturation of the porous media. It has been previously suggested that this relationship may be non-unique and rate dependent. A theory which relates this dynamic relationship to the acoustic properties of the soil was developed by others. This research attempts to experimentally verify this theory by meeting the following three objectives: (1) develop an apparatus and procedure to collect acoustic waveforms on laboratory sized unsaturated soil samples, (2) develop a forward modeling technique using a one-dimensional wave propagation model as an alternative analysis method for waves collected on relatively small laboratory specimens, and (3) apply the theory to the measured acoustic data in an attempt to predict the dynamic behavior of the capillary pressure relationship.

The acoustic data collected showed variation in compressional wave velocity and attenuation with saturation, and the trends were consistent with data collected by others in partially saturated rocks. The forward modeling technique was shown to provide objective results with reasonable accuracy and low computational time. The dynamic effects predicted with these acoustic measurements did not sufficiently explain the dynamic behavior seen in the laboratory. This is attributed to other causes of significant attenuation not accounted for in the wave propagation theory that was evaluated.

CITATIONS

Material from this dissertation was submitted for publication in Vadose Zone Journal on October 4, 2008 in the following form:

George, L. A., Dewoolkar, M. M., and Znidarcic, D. (In Review) Simultaneous laboratory measurement of acoustic and hydraulic properties of unsaturated soils. Vadose Zone Journal.

AND

Material from this dissertation has been submitted for publication to Geotechnical Testing Journal on November 10, 2008 in the following form:

George, L. A. and Dewoolkar, M. M. (In Review) Interpretation of Compressional and Shear waves in laboratory unsaturated soils using a forward modeling technique. Geotechnical Testing Journal.

DEDICATION

This dissertation is dedicated to JD, my husband

ACKNOWLEDGEMENTS

There are many people I would like to thank for both the support and advice given during the completion of this dissertation. First, I would like to thank my advisor, Dr. Mandar Dewoolkar, for all of his advice and expertise over the past four years. I have really appreciated his efforts and the connections he helped establish to answer all of my questions. I would also like to thank Dr. Changfu Wei who introduced this subject to me, and continued to provide support, even after relocating to China. Dr. George Pinder also spent a very generous amount of time brainstorming with me about numerous unexpected experimental phenomenons.

There are a number of people who offered their expertise in different areas of this research whom I would like to thank. From New England Research, Dr. Greg Boitnott, Martin Smith and Dr. Mary Krasovec were invaluable resources of information on the acoustic equipment, analysis techniques and modeling software. Dr. Dobroslav Znidarcic of the University of Colorado at Boulder graciously opened his lab to me, and shared his experiences with unsaturated soil testing.

Finally, I would like to thank my family, friends, and fellow graduate students for their support and companionship through my years at the University of Vermont. Without all of the people mentioned this research would not have been possible.

TABLE OF CONTENTS

CITATIONS	ii
DEDICATION	iii
ACKNOWLEDGEMENTS	iv
LIST OF TABLES	x
LIST OF FIGURES	xi
LIST OF FIGURES	xi
LIST OF NOTATIONS	xiv
1. INTRODUCTION	1
1.1 Motivation	1
1.2 Research Overview and Objectives	2
1.3 Background	8
1.3.1 Flow in unsaturated soils	8
1.3.2 Experimental measurement of hydraulic properties	9
<i>1.3.2.1 Static Capillary Pressure function</i>	9
<i>1.3.2.2 Hydraulic conductivity as a function of saturation</i>	13
<i>1.3.2.3 Dynamic capillary pressure function</i>	14
1.3.3 Wave propagation in unsaturated soils	16
1.3.4 Elastic wave propagation – theory of mixtures with interfaces	20
1.3.5 Experimental measurement of acoustic properties	23
1.3.6 Dynamic capillary pressure function described with acoustic properties	24
1.3.7 Dynamic capillary pressure functions and implications	26

1.4 Organization of Dissertation	27
1.5 References	30
2. SIMULTANEOUS LABORATORY MEASUREMENT OF ACOUSTIC AND.....	41
HYDAULIC PROPERTIES OF UNSATURATED SOILS	41
2.1 ABSTRACT	41
2.2 INTRODUCTION	42
2.3 EXPERIMENTAL SETUP.....	46
2.4 MATERIAL AND METHODS	47
2.4.1 Soil Sample	47
2.4.2 Soil Water Characteristic Curve	48
2.4.3 Unsaturated Hydraulic Conductivity Function	51
2.4.4 Acoustic Properties	52
2.5 RESULTS	56
2.6 DISCUSSION	56
2.7 CONCLUSIONS.....	59
2.8 ACKNOWLEDGEMENTS.....	59
2.9 REFERENCES	60
3. INTERPRETATION OF COMPRESSIONAL AND SHEAR WAVES IN	
LABORATORY UNSATURATED SOIL SPECIMENS USING A FORWARD	
MODELING TECHNIQUE	81
3.1 Introduction.....	83
3.2 Background.....	85

3.2.1 Analysis Methods for Determining Velocity.....	85
3.2.2 Analysis Methods for Determining Attenuation.....	86
3.2.3 Forward Modeling Technique.....	92
3.3 Results.....	95
3.4 Verification with the two-dimensional model	97
3.5 Conclusions.....	99
3.6 Acknowledgements.....	99
3.7 References.....	101
4. PREDICTION OF CAPILLARY RELAXATION TIME OF UNSATURATED SOILS USING MEASURED ACOUSTIC VELOCITY AND ATTENUATION WITH VISCO- POROELASTIC THEORY.....	118
Abstract:.....	118
4.1 Introduction.....	119
4.2 Theoretical Background.....	124
4.2.1 Dynamic capillary pressure function	124
4.2.2 Wave propagation including the effects of local flow	127
4.3 Methods to measure static properties.....	129
4.4 Methods to measure the dynamic properties	131
4.5 Experimental Results and Predictions	132
4.7 Discussions	134
4.8 Conclusions and Recommendations	138
4.9 Acknowledgements:.....	139

4.10 References:	150
5. CONCLUSIONS	153
APPENDIX A: Evolution of the Experimental Apparatus	156
A.1 Apparatus:	156
A.2 Procedure for changing saturation:	161
A.3 High Air Entry disks:	162
A.4 Coarse Porous Stone:	165
A.5 Flow Pump:	166
A.6 Electrical Feed-throughs:	169
A.7 Electronic Pressure Regulator:	170
APPENDIX B: Experimental Methods	171
B.1 Sample Preparation:	171
B.1.1 Material Choice	171
B.1.2 Sample Preparation:	172
B.1.3 Prepare rubber jacket and mold:	172
B.1.4 Prepare soil:	173
B.1.5 Sample saturation strategy:	175
B.2 Flow pump operation:	176
B.3 Data Acquisition:	180
B.4 Acoustic Data Acquisition:	180
APPENDIX C: Data Analysis	183
C.1 Hydraulic Data Analysis:	183

C.1.1 Capillary Pressure Function:	183
C.1.2 Unsaturated Hydraulic Conductivity Function:	185
C.2 Acoustic Data Analysis:	185
C.2.1 Modeling Acoustic Waves:	185
C.2.2 Finding the capillary relaxation times using WAVE-UNSAT:	187
C.2.3 Prediction of the dynamic capillary pressure function:	190
COMPREHENSIVE BIBLIOGRAPHY:	191

LIST OF TABLES

Table 2-1: Properties of Bonny Silt	68
Table 2-2: Parameters used for the Van Genuchten models (Equations 1 - 3).....	69
Table 3-1: Variation in Quality Factor (Q) with window length.....	104
Table 3-2: Variation in Quality Factor (Q) with percent of cosine taper.....	105
Table 3-3: Properties used in numerical model	106

LIST OF FIGURES

Figure 2-1: Schematic of the apparatus	70
Figure 2-2: Photograph of the experimental setup.....	71
Figure 2-3: Grain size distribution of Bonny silt and Heterogeneous soil mixture	72
Figure 2-4: Kelly wavelet source with a center frequency of approximately 20 kHz	73
Figure 2-5: Example of modeled and experimental waveform matching.....	74
Figure 2-6: Soil water characteristic curves for (a) Bonny silt and (b) Heterogeneous soil mixture	75
Figure 2-7: Unsaturated hydraulic conductivity functions	76
Figure 2-8: (a) Compressional Wave Velocity, (b) Compressional Wave Attenuation vs. Moisture Content for Bonny silt and (c) Compressional Wave Velocity (d) Compressional Wave Attenuation vs. Moisture Content for Heterogeneous soil mixture.	77
Figure 2-9: (a) Shear Wave Velocity (b) Shear Wave Attenuation vs. Moisture Content for Bonny silt and (c) Shear Wave Velocity, (d) Shear Wave Attenuation vs. Moisture Content for Heterogeneous soil mixture.	78
Figure 2-10: (a) Compressional Wave Velocity, (b) Compressional Wave Attenuation vs. Capillary Pressure for Bonny Silt and (c) Compressional Wave Velocity, (d) Compressional Wave Attenuation vs. Capillary Pressure for Heterogeneous soil mixture.	79

Figure 2-11: (a) Shear Wave Velocity (b) Shear Wave Attenuation vs. Capillary Pressure for Bonny silt and (c) Shear Wave Velocity (d) Shear Wave Attenuation vs. Capillary Pressure for Heterogeneous soil mixture.	80
Figure 3-1: (a) Input signal Kelly wavelet with center frequency of 20kHz, (b) Example output signal.....	108
Figure 3-2: Points to consider as “first arrivals”.....	109
Figure 3-3: Example demonstration of the Spectral Ratios method.....	110
Figure 3-4: Example of cosine taper.....	111
Figure 3-5: A schematic of the transducer stack (not to scale).....	112
Figure 3-6: Measured and modeled waveform example.....	113
Figure 3-7: Acoustic wave velocities as a function of saturation found using the forward modeling technique and traditional “hand picking” methods.....	114
Figure 3-8: Standard Deviation in velocity measurements found using traditional “manual-picking” methods as a function of the attenuation of the wave analyzed.....	115
Figure 3-9: Compressional wave attenuation as a function of saturation found using the forward modeling technique and spectral ratios. Significant variation may exist in Q values obtained using the spectral ratio method.	116
Figure 3-10: Measured and modeled waveform.....	117
Figure 4-1: Schematic of the experimental apparatus.....	141
Figure 4-2: Grain size distribution for Bonny silt and heterogeneous soil mixture.....	142
Figure 4-3: Capillary pressure functions fitted with a Van Genuchten function.....	143

Figure 4-4: Unsaturated hydraulic conductivity functions found with inverse modeling	144
Figure 4-5: Comparisons of measured Compressional wave velocity and attenuation with predicted values for (a) Bonny silt and (b) Heterogeneous soil mixture	145
Figure 4-6: Capillary relaxation time versus saturation for (a) Bonny Silt and (b) Heterogeneous soil mixture	146
Figure 4-7: Predicted dynamic curves for (a) Bonny silt and (b) Heterogeneous soil mixture	147
Figure 4-8: Experimentally measured dynamic curves on heterogeneous soil mixture .	148
Figure 4-9: Measured and predicted constant flow dynamic curves on heterogeneous soil mixture	149
Figure A-1: Schematic of apparatus (early version).....	157
Figure A-2: Air distribution element in lower cap.....	158
Figure A-3: Schematic of improved apparatus	160
Figure A-4: First bottom high air entry disk design	163
Figure A-5: Final bottom high air entry disk design.....	165
Figure A-6: Elevation and plan view of final upper cap.....	166
Figure B-1: Flow pump data, Rate versus Time	179
Figure B-2: Flow pump data, Volume withdrawn versus Time	179
Figure C-1: Raw capillary pressure relationship data.....	184

LIST OF NOTATIONS

A	Amplitude
C	Soil water capacity
c_v	Consolidation coefficient
f	Frequency
G	Geometric factor
G_{soil}	Shear modulus of soil
h	Hydraulic head
$H(t)$	Heaviside function
h_m	Capillary pressure head
I	Gradient in hydraulic head
k	Saturated hydraulic conductivity
k	Wavenumber
$K(\theta)$	Unsaturated hydraulic conductivity
K_s	Saturated hydraulic conductivity
l, L	Tortuosity factor
L_s	Sample Length
m	Van Genuchten material parameter
n	Van Genuchten material parameter
n^f	Fluid volume fraction
P_{dyn}^c	Dynamic capillary pressure

P_{stat}^c	Static capillary pressures
p^f	Pressure in fluids
p^n	Pressure in non wetting phase
p^s	Pressure of solid phase
p^w	Pressure in the wetting phase
q	Specific flow
Q	Quality factor
S	Saturation of water
S_e	Effective degree of saturation
t	Time
u_a	Pore air pressure
u_w	Pore water pressure
v	Velocity
V_p	Compressional wave velocity
V_s	Shear wave velocity
x	distance
α	Attenuation coefficient
θ	Moisture content
Θ_f	Material parameter
θ_r	Residual moisture content
θ_s	Saturated moisture content
λ	Van Genuchten material parameter

ρ_{soil}	Density of soil
ζ_f	Material coefficient
τ	Material property
τ_c	Capillary relaxation time
τ_n	Characteristic relaxation time of non-wetting (air)
(τ_a)	phase
τ_w	Characteristic relaxation time of wetting phase
ω	Angular frequency

1. INTRODUCTION

1.1 Motivation

Groundwater hydrologists and environmental engineers are challenged with the task of characterizing the material and hydraulic properties of the subsurface with limited information generally collected from discrete points. Geophysical testing offers a suite of measurement techniques that allow for the non-destructive evaluation of potentially large areas in a continuous manner. Acoustic testing is one geophysical method used by many professions to characterize the subsurface. For example, the petroleum industry uses ultrasonic testing to characterize oil reserves, as well as enhance oil recovery, and geotechnical engineers use seismic surveys to evaluate the liquefaction potential of soils in earthquake prone areas.

Recently there has been an immense interest in the ability to relate soil properties, specifically hydraulic properties, to the acoustic response of soil (Guerin 2005). This ability could enhance high resolution non-destructive evaluation of the shallow subsurface, and would have applications in a variety of fields including groundwater and contaminant hydrogeology, oil recovery, soil dynamics, and the detection of buried artifacts. Seismic surveys have been used successfully to locate the water table (Haeni 1986), but give no information about the unsaturated zone above the water table. The unsaturated zone may be characterized by the acoustic properties instead of just the reflection of seismic waves (Bachrach and Nur 1998; Garambois et al. 2002).

Understanding the behavior of groundwater and contaminant flow in the unsaturated zone is a challenge in groundwater hydrology. Acoustic characterization of the unsaturated zone may be a tool which can help overcome this challenge.

1.2 Research Overview and Objectives

Unsaturated and multiphase flow modeling relies on the relationship between the capillary pressure and the level of saturation of the porous media. This relationship is known by many names such as the capillary pressure function, pressure-saturation relationship, water retention curve, and soil water characteristic curve. This is a hydraulic property of the porous media and the fluids that depends on many factors, including the pore size distribution of the media, the attraction of the fluids to the solids and the interfacial tension between the fluids. For unsaturated soils, the capillary pressure function is defined as the relationship between the differential pressure between the water and the air phase, i.e. the capillary pressure and the water saturation *at equilibrium*.

This relationship is obtained through methods that require (or assume that) static conditions have been achieved. Direct laboratory measurement methods include the hanging column method, pressure cell, pressure plate extractor, long column, suction table and controlled liquid volume methods (Dane and Topp 2002). These methods can be generally placed in two categories, suction methods (e.g. hanging column, long column) and axis translation methods (e.g. pressure cell, pressure plate extractor). Suction methods operate with the air phase pressure remaining at atmospheric and the

negative water pressures that result from capillary forces at partial saturation are measured. The range of these methods is limited by the cavitation pressure of water (-1 atm), yet it is possible for fine grained soils to achieve capillary pressures much lower than -1 atm. The axis translation technique avoids this limitation by elevating the air pressure to some value above atmospheric, thereby elevating the water pressure to that value minus the capillary forces (Fredlund and Rahardjo 1993). With the axis translation technique and the appropriate capillary barrier, it is possible to obtain the capillary pressure function for all materials, given a sufficient equilibration time.

All of the methods mentioned assume that the soil is at an equilibrium or static state before a point on the capillary pressure function is obtained. Two questions arise from this assumption, first has equilibrium been achieved, and second, should static properties be applied to model a dynamic phenomenon such as groundwater flow? Numerous studies have shown experimentally that the capillary pressure function is rate dependent (Chen et al. 2007; Constantz 1993; Davidson et al. 1966; Mohamed and Sharma 2007; Schultze et al. 1997; Topp et al. 1967; Vachaud et al. 1972; Wildenchild et al. 2002).

The capillary pressure function is also measured using indirect methods, such as one-step or multi-step outflow experiments. These experiments determine the static capillary pressure and the hydraulic conductivity functions using a transient test and inverse modeling of Richards' equation. A pressure change is applied to one side of the sample and the amount of water that outflows from the other side of the sample is measured, and

then predicted using Richards' equation. The same inconsistencies arise with these tests, which are performed in a transient state, but used to determine a static relationship. O'Carroll et al. (2005) showed that the prediction of outflow was inconsistent with the measured outflow unless a dynamic term that varies with saturation was used in the capillary pressure function.

In order to resolve these inconsistencies, it has been suggested to use a 'dynamic' capillary pressure function, which takes into account the dynamic nature of the relationship. The most prevalent existing model for the dynamic capillary pressure function was developed by Hassanizadeh and Gray (1993). The model proposes that the dynamic capillary pressure is equal to the static capillary pressure minus a constant (τ) multiplied by the rate of saturation change as shown in equation (1)

$$P_{dyn}^c = P_{stat}^c - \tau \frac{\partial S}{\partial t} \quad (1)$$

where P_{dyn}^c and P_{stat}^c are the dynamic and static capillary pressures, respectively, and S is the saturation.

This model is a thermodynamic theory of two phase flow based on a constitutive hypothesis that the Helmholtz free energy functions for the phases and interfaces depend on state variables such as mass, density, temperature, saturation, porosity and interfacial area density, and the solid phase strain tensor. The capillary pressure is defined as the change in the free energy of the system due to a change in the saturation. The theory suggests that the saturation will redistribute locally in order to restore equilibrium; the

coefficient (τ) can be interpreted as a measure of how fast this redistribution will take place. Tau is considered a material property that may also be dependent on the level of saturation (Hassanizadeh and Gray 1993). Tau has been back calculated from direct measurement of the dynamic capillary pressure function to range from 10^4 to 10^7 kg (m s)⁻¹, but a method to measure Tau directly has not been developed.

A new model of the dynamic capillary pressure function has been developed (Wei and Dewoolkar 2006b) which expands on Hassanizadeh and Gray's (1993) model to include hereditary effects and a method of quantifying the speed at which the local redistribution of saturation (or pressure) occurs. This speed is referred to as the capillary relaxation time, and can be measured in the laboratory using low frequency acoustic wave propagation theory as described below. The model is a linear viscoelastic model of nonequilibrium two phase flow. The partially saturated porous media are viewed as the superposition of three phases in continuum theory of mixtures. The model accounts for the effect of capillary relaxation based on the continuum theory of mixtures and describes energy dissipation due to fluid flow in terms of both macroscopic and local fluid flow, i.e. capillary relaxation (or local pressure redistribution).

Acoustics waves are used to determine the capillary relaxation time of the media, based on a wave propagation theory, which takes into account energy dissipation due to local flow (Wei and Muraleetharan 2002b). When a porous medium is disturbed by an external force such as an acoustic wave, the medium deforms in response to the passing stress

wave. This deformation may cause the pressure of the fluid to build up within the pores of the porous media. If the medium is saturated with multiple immiscible fluids, and depending on what type of fluid is occupying the region, different pressures will build up in each region. If these regions are located next to each other, a pressure gradient will exist across the boundary between the two regions. This pressure gradient will cause the fluid in one region to flow into the neighboring region. This “local flow” will dissipate the energy of the passing stress wave, causing attenuation and velocity dispersion of the wave.

The size of the regions (e.g. patches) and the wavelength of the acoustic wave will determine the existence and the effect of the local flow. If we consider that the two neighboring regions are occupied by water and air, as is the case in unsaturated soils, the acoustic wave will cause pressure to build in the water because of the deformation of the pores in the soil. If the period of the wave is long enough, there will be time for the pressure to equilibrate and the water to flow into the region containing air, before the next wave passes. But if the period of the wave is very short, there will not be time for the water to flow and equilibrate before the next wave passes and the pressure is built up again. This will result in the water acting as reinforcement to the matrix, and stiffening the porous media, instead of causing local flow. This also shows that a frequency dependent response to acoustic waves passed through unsaturated soils will be seen. The existence of local flow also depends on the distribution of fluids in the media. It is not seen as dramatically if the moisture is distributed uniformly, even at the same saturation

level (Cadoret 1995). When the moisture distribution is uniform over the length of the wave, the pressure distribution is also nearly uniform and local flow does not take place (Carcione, et. al 2003). Also, when a sample has uniformly distributed moisture content, the air phase is interconnected up to a high level of saturation. The relaxation of the air phase then is vanishingly small over the whole range of saturations.

The time that it takes for the patch of fluid (e.g. water or air) to equilibrate is known as the capillary relaxation time; this time can be extracted by analyzing the received waveforms (Wei and Muraleetharan 2002a). The capillary relaxation time includes information on the size of the patch of saturation and the dynamic behavior of the material as a whole. The capillary relaxation time is then included in the model of the dynamic capillary pressure function to quantify the dynamic behavior of the material.

This research attempts to experimentally verify the theories introduced. Acoustic and hydraulic properties of unsaturated soils have been simultaneously measured using a device developed as a part of this dissertation. The acoustic waves were analyzed and the capillary relaxation time for the soil determined for a range of saturations. Using this information along with the hydraulic properties of the soil and the model of the dynamic capillary pressure function, dynamic capillary pressure functions for a range of rates has been predicted. The results are compared to static capillary pressure relationship and the implications discussed.

1.3 Background

1.3.1 Flow in unsaturated soils

The basic theory of unsaturated flow in porous media begins with Darcy's law, which relates the flow (q) to the gradient in hydraulic head (i) in a saturated medium by a coefficient (k), the hydraulic conductivity. This derivation is simplified to one dimension.

$$q = -ki \quad (2)$$

To account for the unsaturated state of the porous medium Darcy's law is modified to relate the flow (q), to the gradient in the pressure head (∇h) by a coefficient (K) that is dependent on the degree of saturation, or the moisture content (θ).

$$q = -K(\theta)\nabla h \quad (3)$$

By combining the modified Darcy's equation with the continuity equation, which says that the change in moisture content is equal to the flux in flow, we obtain a form of Richards' equation (Richards 1931).

$$\frac{\partial \theta}{\partial t} = \nabla \cdot [K(\theta)\nabla h] \quad (4)$$

The equation of flow in unsaturated soils is expressed in many different forms, all of which can be referred to as Richards' equation. We can separate the first term into the following,

$$\frac{\partial \theta}{\partial t} = \frac{\partial \theta}{\partial h} \cdot \frac{\partial h}{\partial t} \quad (5)$$

By combining equations (4) and (5), and assuming one dimensional flow, Richards' equation can be written as,

$$\frac{\partial h}{\partial t} = C^{-1} \cdot \frac{\partial}{\partial z} \left(K(\theta) \frac{\partial h}{\partial z} \right) - \frac{\partial K}{\partial z} \quad (6)$$

where C is known as the soil water capacity and is defined as

$$C = \frac{\partial \theta}{\partial h}. \quad (7)$$

In order to use Richards' equation to model flow through unsaturated soils two properties must be measured in the laboratory; the soil water characteristic curve and the hydraulic conductivity function.

1.3.2 Experimental measurement of hydraulic properties

Generally, static unsaturated soil properties (e.g. the capillary pressure and the hydraulic conductivity functions) are obtained on small laboratory scale samples. The size of the sample can decrease the length of time needed to complete full characterization of the sample. For fine grained soils, such as clays, the time needed to complete an entire experiment can be prohibitive. Many methods exist for gathering this information, and recent focus has been placed on shortening the length of the experiment, and conducting both measurements simultaneously.

1.3.2.1 Static Capillary Pressure function

The capillary pressure function describes the relationship between capillary pressure and saturation. Measurement of the capillary pressure in a sample is taken at a static state,

when the saturation is constant and the capillary pressure has equilibrated. There are direct, indirect, and inverse methods used to determine this relationship. Direct laboratory methods consist of directly measuring the capillary pressure and the saturation at each point that the relationship is defined on. These methods include the hanging column method, pressure cell, pressure plate extractor, long column, suction table and controlled liquid volume methods (Dane and Topp 2002). Inverse methods use a transient flow experiment and inverse modeling to determine the relationships, they are known as one-step or multi-step outflow experiments. Indirect methods estimate these relationships using surrogate data that is more readily available or easier to collect, such as pore size distribution (Leij et al. 2002).

All of the direct methods consist of changing the saturation in a sample, and then measuring the resulting capillary pressure in the pore fluid, or the opposite of setting the capillary pressure in the pore fluid and measuring the change in saturation. Generally these experiments are performed on cylindrical remolded samples, but occasionally undisturbed samples are used. A hydrophilic porous plate with very small pores is used to keep the air phase and water phase separate during desaturation. The porous plate, which may be made of ceramic, nylon, metal, clay or diatomaceous earth, has pores that are small enough to prohibit the migration of air up to a certain air bubbling pressure determined by the size of the pores. This allows water to be withdrawn from the sample without withdrawing air. Direct methods can be generally placed in two categories, suction methods (e.g. hanging column, long column) and axis translation methods (e.g.

pressure cell, pressure plate extractor). Suction methods operate with the air phase pressure remaining at atmospheric and the negative water pressures that result from capillary forces at partial saturation are measured. The range of these methods is limited by the cavitation pressure of water (-1 atm), and it is possible for fine grained soils to achieve capillary pressures much lower than -1 atm. The axis translation technique avoids this limitation by elevating the air pressure to some value above atmospheric, thereby elevating the water pressure to that value minus the capillary forces (Fredlund and Rahardjo 1993; Hilf 1956). With the axis translation technique and the appropriate capillary barrier, it is possible to obtain the capillary pressure function for all materials, given a sufficient equilibration time. The entire relationship can be obtained by moving along the capillary pressure axis or along the saturation axis in both suction and axis translation methods. When the relationship is determined by moving along the capillary pressure axis, the capillary pressure is changed from one point to the next and the amount of water injected or withdrawn from the sample is measured. When the relationship is determined by moving along the saturation axis, a set amount of water is withdrawn or injected and the change in capillary pressure is measured.

Hydraulic soil properties can also be obtained through inverse modeling of transient flow experiments. Inverse methods are commonly referred to as one step or multi-step outflow experiments depending on the way the pressure at the top of the specimen is changed. Generally, a soil column is dried from a saturated state by applying an air pressure to the top of the sample and the outflow from the bottom of the sample is measured and

recorded over time. If the pressure at the top of the sample is changed in one large step very rapidly, the test is referred to as a one step outflow experiment; alternatively if the pressure is changed in a series of small steps, the test is referred to as a multi-step outflow experiment. Once the data has been collected from the transient flow experiment, including boundary conditions and initial conditions, a numerical flow model is developed to simulate the experiment and initial estimates of the hydraulic properties are made. Then an optimization algorithm is used to refine the estimates of the hydraulic properties until agreement between the numerical model and the experimental results is achieved. Inverse methods are believed to be faster than direct methods, and are able to quantify both the capillary pressure relationship and the hydraulic conductivity function simultaneously, but assumptions about the shape of these relationships need to be made prior to modeling the experiment. Two popular models of the capillary pressure function are mentioned in the next paragraph.

The experimental methods described above can be prohibitively expensive or time consuming for the application. If that is the case, one may consider using indirect methods. Indirect methods attempt to estimate unsaturated soil properties using other properties of the soil which is readily available or easily attainable. Two popular functions for the capillary pressure relationship exist that can be used either to fit laboratory data, or to estimate the relationship with these indirect methods. They are the Brooks and Corey (Brooks and Corey 1964) function:

$$S_e = \frac{\theta - \theta_r}{\theta_s - \theta_r} = \begin{cases} (\alpha |h_m|)^{-\lambda} & (\alpha |h_m| > 1) \\ 1 & (\alpha |h_m| \leq 1) \end{cases} \quad (8)$$

and the van Genuchten (1980) function:

$$S_e = \frac{\theta - \theta_r}{\theta_s - \theta_r} = \left[1 + (\alpha |h_m|^n) \right]^{-m} \quad (9)$$

where S_e is the effective degree of saturation, h_m is the capillary pressure head, θ_s and θ_r are the saturated and residual moisture contents, respectively, α is a parameter inversely related to the air entry value of the soil, and λ , m , and n are parameters that affect the shape of the function. Indirect methods range from simplistic to complex and are both semi-empirical and empirical. These methods are based on soil properties such as particle size distribution, pore size distribution, textural class, clay or sand fraction, porosity, or existing databases of properties.

1.3.2.2 Hydraulic conductivity as a function of saturation

For unsaturated soils the hydraulic conductivity is also known to vary with saturation. The highest hydraulic conductivity occurs when the soil is fully saturated and decreases as the saturation decreases. This relationship can be determined for each soil using direct methods in the field or laboratory, and inverse or indirect methods similar to those used to determine the capillary pressure function. Mathematical expressions exist to describe the unsaturated hydraulic conductivity function that utilize the same parameters used in the expressions to describe the capillary pressure function. Two of the more popular

expressions are described as follows. The Brooks and Corey unsaturated hydraulic conductivity function:

$$K = K_s S_e^{2/n+1+2} \quad (10)$$

and the Van Genuchten unsaturated hydraulic conductivity function:

$$K = K_s S_e^l \left[1 - \left(1 - S_e^{1/m} \right)^m \right]^2, \quad (11)$$

where l is defined as the tortuosity factor.

Field methods generally employ a double ring infiltrometer that allows for surface ponding of water and restricts flow to the vertical direction. The results of infiltration experiments, e.g. the infiltrated volume over time, can be used with inverse analysis of the one dimensional infiltration equation, based on Richards' equation, to obtain the hydraulic properties of the soil in the field (Clothier and Scotter 2002). Similar approaches may be used in the laboratory; overall, these approaches are simplistic and have limitations.

1.3.2.3 Dynamic capillary pressure function

Research has shown that the rate at which drainage takes place affects the capillary pressure function measured. That is, if sufficient time is not taken to reach equilibrium, the static soil water characteristic curve may not be obtained. In this case a “dynamic” capillary pressure function may be measured. When plotting the capillary pressure versus saturation, the curve shifts up and to the right as the rate of flow is increased, meaning

that for the same capillary pressure value, the moisture content was greater for higher rates of flow (Topp et al. 1967). Topp's findings have been confirmed on undisturbed soil samples (Schultze et al. 1997). Multi-step outflow and inflow experiments were performed showing that Richards' equation with a single static pressure saturation relationship does not accurately predict the outflow or inflow of water. The tensiometer readings responded quickly to a step in pressure, but the outflow or inflow of water continued for 24 hours or longer.

The opposite trend in the effect of rate on the capillary pressure function has been reported. Davidson et al. (1966) showed that rate dependent behavior did exist, but found that for the same capillary pressure value, the moisture content was lower for higher rates of flow. It was also noted that the effect was greater for wetting than drainage. Constantz (1993) confirmed Davidson's results, and attributed the rate dependence to variations in pore water salt concentrations which induced differences in pore water surface tension. More recently the original findings of Topp were confirmed by Wildenschild (2001). Chen et al. (2007) attempted to make rapid pseudo-static measurement of capillary pressure function. During the design of these dynamic pseudo static experiments, the researchers attempted a range of pressure change rates to find a constant rate that best matched the static relationship. This collection of research shows that the capillary pressure function is affected by the rate at which the saturation is changed, but little agreement or explanation exists.

1.3.3 Wave propagation in unsaturated soils

Biot was the first to describe low frequency elastic wave propagation in fluid saturated porous media (Biot 1956). The theory was further developed to describe acoustic wave propagation in porous media saturated by two fluids (Tuncay and Corapcioglu 1997). Although, this theory does not include the dynamic effect of capillary and neglects the dissipation caused by local flow in heterogeneous material with “patchy” saturation, which is shown to have an impact on unsaturated flow (Hassanizadeh et al. 2002). Wei and Muraleetharan (2006) included these dynamic effects into a model, which can be solved to characterize the time of local flow.

Foundation work on the mechanics of porous media is attributed to Biot. Biot’s theory was later generalized to account for non linear effects (Biot 1972; Prevost 1980; Zienkiewicz 1984), and more recently, Biot’s theory was generalized into the modern context of thermodynamics (Coussy et al. 1998). Biot’s theory and its generalizations take a macroscopic approach and fail to consider the microscopic structure of the porous media. It is also not clear if this theory can be used with plastic deformations of multiphase fluids. On a parallel front, Biot also completed the foundation work on wave propagation in porous media. This theory does a good job of describing the effects macroscopic flow, but fails to explain the effects of local flow on elastic wave propagation (Gist 1994; Winkler and Nur 1982). Stoll and Bryan (1969) extended Biot’s theory to saturated unconsolidated porous media and Brutsaert (1964) generalized Biot’s theory to porous media such as unsaturated soils.

More recently, improvements have been made to Biot's original theory to account for local flow using several approaches; most of these are considered local or "squirt" flow models. These models explain that the attenuation and velocity dispersion is due to flow occurring between gas and liquid filled areas of the same pore or crack. Theories have been developed that look at fluid flow in an individual crack (Mavko and Nur 1979; O'Connell and Budiansky 1977), fluid flow in a grain contact area (Murphy et al. 1986), and fluid flow inside crack like pores oriented perpendicular to the compressional wave characterized (Dvorkin and Nur 1993). Also, spatial heterogeneities such as fine layering and inclusions have been considered (Gurevich et al. 1994; Gurevich et al. 1997). Generally these theories consider microscopic flow and do not incorporate mesoscopic flow.

A second approach to account for mesoscopic or local flow considers the flow due to the disturbance of patches of saturation and its viscoelastic behavior. These models consider the mesoscopic distribution of fluids, and the attenuation and velocity dispersion is due to local flow created by pressure gradients induced between the fluids. White (1975) was the first to show theoretically that partial fluid saturation could cause significant attenuation and phase velocity dispersion, this theory was later improved by Dutta & Ode (1983) and Dutta & Seriff (1979). This was shown considering that the patches of saturation were in the form of concentric spheres and these theories were formed in the context of consolidated porous media, such as rocks. Experimental studies at the same

time showed a change in velocity due to partial saturation in unconsolidated sands (Domenico 1976) and rocks (Gregory 1976).

Later, Johnson (2001) formulated a theory that considered the patches of saturation with no restriction on geometry and this theory was used to deduce the size of patches of saturation (Tserkovnyak and Johnson 2002). Pride et al. (2003, 2004) use a dual porosity theory, where the properties are expressed as a function of the properties of individual constituents and the characteristic size of the embedding solid phase, but this theory could get very complicated with increasing heterogeneity. Muller and Gurevich (2004) showed that the previous three models (which are based on a periodic distribution of fluids) predict attenuation and velocity dispersion that is quite different than a model that is based on a random distribution of fluids.

There are a few experimental and numerical studies that show evidence of the effect of mesoscopic flow on the acoustic wave propagation. Lee (2004) showed experimentally and numerically a difference in the ratio of the compressional wave speed to the shear wave speed (V_p/V_s) depending on the distribution of gas in unconsolidated sediments. Cadoret et. al. (1995) showed experimentally differences in velocity and attenuation depending on moisture distribution, which were also verified with CT scans. Helle et al. (2003) predicted these experimental results numerically using Biot's theory. Carcione and Picotti (2006) showed numerically using White's model that mesoscopic losses are

the most probable attenuation mechanisms at seismic frequencies and are related to the microstructural characteristics of rock.

All of these theoretical models are based in micromechanics, meaning that the material properties depend on microscopic quantities, such as the size of the patches. These models consider the effects of local fluid redistribution, but the effects of local gas-pressure redistribution are not taken into account. The theory, which is focused on in this research (Wei and Muraleethanan 2002b), was formulated within the framework of the theory of Biot's poroelasticity. It is based on volume averaging of microscopic equations using the continuum theory of mixtures with interfaces. One key difference between this model and existing models is that it makes no assumptions about the local structure of the heterogeneity. Information on the details of the local heterogeneity is stored in the relaxation time of the dynamic compatibility condition. The capillary relaxation processes are governed by the local fluid flow occurring in the partially saturated porous media (Wei and Muraleethanan 2006).

Unsaturated porous media, by definition, is comprised of at least three phases of materials; a solid phase, a liquid phase and a gas phase. Continuum theory can be applied to each individual phase, but the properties of the mixture of the three phases as a whole are desired. Balance equations and constitutive relationships were developed by Wei and Muraleetharan (1999) for unsaturated soils under dynamic loading in isothermal conditions. In order to account for the effect of the multiple phases in the mixture, a

volume averaging approach based on Hassanizadeh and Gray's work (1979, 1989) and modified to include interfacial effects was used. The theory is briefly summarized in the next section, and the reader is referred to Wei and Muraleetharan (1999, 2007) for complete details of the formulation.

1.3.4 Elastic wave propagation – theory of mixtures with interfaces

When a stress wave passes through an unsaturated soil in which the moisture is heterogeneously distributed at the mesoscopic scale, local pore pressure gradients are generated and local flow takes place. The local flow induced by a stress wave dissipates wave energy, resulting in intrinsic wave attenuation and velocity dispersion (velocity depending upon frequency). Such acoustical signatures play a key role in determining the characteristics of local flow and dynamic capillarity.

Assume that the soils under consideration are *macroscopically* (i.e., at the wavelength scale) isotropic and homogeneous, with an average degree of saturation S_r . Consider an averaging volume of an unsaturated soil. When subjected to an external disturbance, the dynamic capillary pressures are given by (Wei and Muraleetharan 2007)

$$p^f - p^s = (p^f - p^s)_{eq} + \zeta_f \dot{n}^f, \quad (12)$$

where p^s is the pressure associated with the compression of solid grains (s); p^f is the pressure of a fluid, and $f = w$ (wetting fluid) or n (non-wetting fluid), in the case of unsaturated soil the wetting and non-wetting fluids would be water and air, respectively;

$(\)_{eq}$ represents the pressure difference at equilibrium; \dot{n}^f is the changing rate of the fluid volume fraction (n^f); and ζ_f is a material coefficient, which is a function of moisture content.

To analyze the acoustical behavior of unsaturated soils (strain $< 10^{-7}$), it is sufficient to consider the linear problem. The linear form of Eq. (12) is

$$\delta p^f - \delta p^s = \Theta_f (\delta n^f + \tau_f \delta \dot{n}^f), \quad (13)$$

where Θ_f ($f = w$ (water), a (air)) is a material parameter and equals the change of pressure difference ($p^f - p^s$) due to a unit change of volume fraction n^f ; $\tau_f = \zeta_f / \Theta_f$.

Parameters Θ_w and Θ_a can be determined using soil water capacity $C(\theta)$ (Wei and Muraleethanan 2006)

$$\Theta_w = (1 - S_r) / C, \quad \Theta_a = S_r / C. \quad (14)$$

Noting that $\dot{n}^w + \dot{n}^a \approx 0$, Eq. (13) can be used to derive

$$\delta(p^a - p^w) = (\delta\theta - \tau_c \delta\dot{\theta}) / C, \quad (15)$$

where

$$\tau_c = C\zeta = (1 - S_r)\tau_w + S_r\tau_a. \quad (16)$$

τ_f ($f = w, a$) is equal to the characteristic time of meso-scale flow of f -fluid resulting from local saturation heterogeneity. In general, τ_c is a function of the moisture content

(θ or S_r). It is clear that τ_c has two contributions, which are due to meso-scale water and air flow, respectively. In the range of low to moderate saturation, air phase is interconnected within the pore space. In this case, due to high mobility of air, $\tau_a = 0$ and the effect of meso-scale air flow is negligible. In high saturation, however, the effect of local air flow may become significant. In the latter case, the air phase is trapped as air bubbles, and local air flow occurs in the form of diffusion.

As usual in the acoustical analysis, the state parameters are assumed to have a time dependence of $\exp(-i\omega t)$, where $i^2 = -1$ and ω is the angular frequency. Eq. (13) yields

$$p^f - p^s = \tilde{\Theta}_f \Delta n^f \quad (17)$$

where $\tilde{\Theta}_f = \Theta_f(1 - i\omega\tau_f)$. Using this equation and the linear state equations of the solid and fluid phases, the macroscopic constitutive relationships describing the acoustical behavior of partially saturated porous media can be derived (Wei and Dewoolkar 2006). The velocity and attenuation of the acoustic wave is dependent on the capillary relaxation time, and other commonly measured material and hydraulic properties. By simultaneously solving Eq. (17), and the linear state equations of the solid and fluid phases with the measured material and hydraulic properties, the capillary relaxation time can be adjusted until convergence with the measured velocity and attenuation is reached.

1.3.5 Experimental measurement of acoustic properties

In order to implement the theory, the compressional wave velocity and attenuation of soil at a range of saturations is needed. In the past, a number of experimental acoustic investigations of porous media have been performed on unsaturated consolidated porous media, specifically rocks (Cadoret et al. 1995; Gist 1994; Goertz and Knight 1998; Klimentos and McCann 1990; Knight and Nolen-Hoeksema 1990; Murphy 1982; Paffenholz and Burkhardt 1989; Spencer 1979; Toksoz et al. 1979; Winkler and Nur 1982; Wulff and Mjaaland 2002). Acoustic studies of soils generally focus on measurement of the shear wave velocity, which is used to determine the shear modulus and is used in the study of the dynamic behavior of soils (e.g. Brignoli et al. 1996; Claria and Rinaldi 2007). Fewer experimental studies including compressional wave velocity measurements have been performed on unconsolidated porous media such as soils (Alramahi et al. 2008; Berge and Bonner 2002; Bonner et al. 2001; Flammer et al. 2001; Tsukamoto et al. 2002; Velea et al. 2000). One area of research on soils, the study of marine sediments has produced a number of laboratory and field studies that measure both velocity and attenuation of these saturated unconsolidated porous materials (Moran et al. 2007; Muthukrishniah et al. 1995; Stoll 1985; Turgut and Yamamoto 1990). Even fewer studies have included the attenuation in unsaturated soils (Leong et al. 2004; Liu et al. 2001; Lu et al. 2004; Oelze et al. 2002).

The apparatus developed as a part of this dissertation is capable of measuring compressional and shear waves at a range of saturations for a laboratory sized soil

sample. The hydraulic properties are also measured at the same time. The acoustic waves are created and measured using piezoceramic transducers and a pulse transmission technique. Full details on the apparatus are found in Chapter 2. Chapter 3 describes the forward modeling technique that was developed to extract the velocity and attenuation from the measured waveforms. The next section describes how the capillary relaxation time found from the acoustic properties can be used to find the dynamic capillary pressure function.

1.3.6 Dynamic capillary pressure function described with acoustic properties

It has been shown that the response of the moisture content is dependent on the rate of change of the capillary pressure. To simulate flow through heterogeneous material we must consider this non-equilibrium nature of the flow, specifically we are concerned with the rate dependent response and hereditary effects of the capillary pressure function. The hereditary effect of capillarity is a result of the viscous effects of the fluid that prevent the moisture content from responding instantaneously to a change in the capillary pressure.

In partially saturated porous media, the complexity is added due to the fact that the moisture content is non-uniformly distributed over the pore space (even if the porous medium is intrinsically homogeneous). When a fluid(s)-saturated heterogeneous porous medium is subjected to an external excitation, flow may take place at different spatial scales, resulting non-equilibrium flow conditions. As described in the section on wave propagation, the energy of the acoustic wave (in this case the compressional wave) is consumed by the local flow (or diffusion) that it causes. By analyzing the measured

waveform; we can characterize the time of local flow, which is equal to the capillary relaxation time.

A kinetic constitutive equation for the moisture content history has been proposed that takes hereditary and rate dependent effects into account by including the capillary relaxation time and the capillary pressure history as a function of time (Wei and Dewoolkar 2006b). The moisture content history $\theta(t)$ resulting from any history of capillary pressure $p_c(t)$ can be expressed as

$$\theta(t) = \theta(0) + K * p_c(t) \quad (18)$$

where $K(t, \theta)$ is given by

$$K(t, \theta) = C(\theta) \left[1 - \exp\left(-\frac{t}{\tau_c(\theta)}\right) \right] H(t) \quad (19)$$

and $K * p_c$ is the Stieltjes-type integral of functions $K(t, \theta)$ and $p_c(t)$, and defined by

$$K * p_c(t) = \int_0^t K(t - \tau, \theta) dp_c(\tau) + \sum_i K(t - t_i) [p_c(t_i^+) - p_c(t_i^-)], \quad (20)$$

where τ_c is the capillary relaxation time, $C(\theta)$ is a material property and $H(t)$ is the Heaviside function. The first term of the right hand side of equation (20) is included for smooth functions of $p_c(t)$, where the second term is included for step type functions of $p_c(t)$, with a discontinuity at t_i . An example of the former is a typical flow experiment, and the latter is necessary when “multistep outflow” experiment is performed.

By simultaneously and numerically solving the moisture content history equation (20), and Richards' equation (6), we can model unsaturated fluid flow taking into account the dynamic effects of capillarity.

1.3.7 Dynamic capillary pressure functions and implications

Some researchers have attempted to explain the dynamic effects by including a rate dependent term in the pressure saturation function. This term includes a material parameter that may have physical meaning, such as τ suggested by Hassanizadeh and Grey (2002), but is practically not measurable in the laboratory (Wei and Muraleetharan 2002a). Numerical models (dual porosity model) of a dynamic groundwater phenomenon (i. e. infiltration), using static material properties, have shown that the depth of infiltration maybe underestimated (Ross and Smettem 2000). The opposite conclusion has also been made through two studies using Hassanizadeh and Grey's theory. The first used a dynamic pore-scale network model of Richards' equation, showing that the dynamic effects can retard an infiltrating front into dry soil by about 50%, depending on the coefficients used (Hassanizadeh et al. 2002). The second study (Dahle et al. 2005), used numerical simulation of infiltration problems considering two phase flow, and also concluded that the dynamic effects can retard infiltrating fronts. These simulations were run with a fixed flow rate, resulting in more mass accumulating behind the front, and the front height was increased.

There is much work to be done in the area of non-equilibrium flow, understanding the causes and implications. This research attempts to verify existing theories that link the acoustic properties of a soil to its dynamic response.

1.4 Organization of Dissertation

This dissertation is divided into four chapters; (1) an introduction chapter, (2) a chapter describing the experimental apparatus used in this research, (3) a chapter on the methods used to analyze the acoustic waves, and (4) a final chapter using the wave propagation theory (Wei and Muraleetharan 2002b) to predict dynamic capillary pressure relationships. A summary for each chapter is provided below.

Chapter 2: Simultaneous laboratory measurement of acoustic and hydraulic properties of unsaturated soils

A complete set of acoustic properties, including compressional and shear wave velocities and attenuations and hydraulic properties (the soil water characteristic curve and the unsaturated hydraulic conductivity function) over a full range of saturation for a silt specimen is presented. The acoustic data, the soil water characteristic curve and the unsaturated hydraulic conductivity function were collected using a novel device developed at the University of Vermont. The acoustic data are consistent with data collected over a full range of saturations in rocks found in the literature. This

experimental data can be used to verify existing models that attempt to link acoustic and hydraulic properties of unconsolidated and unsaturated porous media.

Chapter 3: Interpretation of Compressional and Shear waves in laboratory unsaturated soils using a forward modeling technique

Determining the acoustic velocity and attenuation from low frequency waveforms collected in soils with piezoceramic transducers presents a challenge. The received waves may be weak and contaminated by noise or boundary effects. A number of methods have been suggested for determining the velocity by choosing the first arrival of the wave. These methods give variable results and have been criticized in the literature. Methods for determining the attenuation of a waveform have also been regarded as subjective and unstable. A forward modeling technique using a one-dimensional wave propagation model is presented. This technique was used to determine acoustic (compressional and shear wave) velocities and associated attenuations from waveforms collected in laboratory sized unsaturated soil specimens during a drainage experiment. The results of the forward modeling technique are compared with more traditional methods. It is shown that the forward modeling technique removes the subjectivity of the traditional methods and is capable of determining both the acoustic velocity and attenuation simultaneously. The validity of the one-dimensional model was evaluated by comparing the results with those from a two-dimensional model. The two-dimensional model provided a marginally improved simulation of received waveforms indicating that the one-dimensional model

was appropriate, especially because it is simple and computationally efficient in comparison to the two-dimensional model.

Chapter 4: Prediction of capillary relaxation time using measured velocity and attenuation with visco-poroelastic theory

Unsaturated and multiphase flow modeling relies on the relationship between the capillary pressure and the level of saturation of the porous media. It has been previously suggested that this relationship may be non-unique and rate dependent and a procedure for quantifying this dynamic relationship was developed by others. This research attempts to experimentally verify this procedure using data from acoustic characterization of unsaturated soil samples. The acoustic data collected shows variation in compressional wave velocity and attenuation with saturation, but the dynamic effects predicted with these acoustic measurements do not sufficiently explain the dynamic behavior seen in the laboratory. This is attributed to other causes of significant attenuation not accounted for in the wave propagation theory.

1.5 References

- Aramahi, B., Alshibli, K., Fratta, D., and Trautwein, S. J. (2008). "A Suction-Controlled Apparatus for the Measurement of P and S-Wave Velocity in Soils." *Geotechnical Testing Journal*, 31(1), 12-23.
- Bachrach, R., and Nur, A. (1998). "High-resolution shallow-seismic experiments in sand, Part 1: Water table, fluid flow and saturation." *Geophysics*, 63(4), 1225-1233.
- Berge, P. A., and Bonner, B. P. (2002). "Seismic velocities contain information about depth, lithology, fluid content and microstructure." *UCRL-JC-144792*, DOE Lawrence Livermore National Laboratory.
- Biot, M. A. (1956). "Theory of Propagation of Elastic Waves in a Fluid-Saturated Porous Solid I. Low Frequency Range." *The Journal of the Acoustical Society of America*, 28(2), 168-178.
- Biot, M. A. (1972). "Mechanics of finite deformation of porous solids." *Indiana University Mathematical Journal*, 21, 597-620.
- Bonner, B. P., Berge, P. A., and Wildenchild, D. (2001). "Compressional and Shear Wave Velocities for Artificial Granular Media Under Simulated Near Surface Conditions." *UCRL-JC-142935*, DOE Lawrence Livermore National Laboratory.
- Brignoli, E. G. M., Gotti, M., and Stokoe, K. H. (1996). "Measurement of Shear Waves in Laboratory Specimens by Means of Piezoelectric Transducers." *Geotechnical Testing Journal*, 19(4), 384-397.
- Brooks, R. H., and Corey, A. T. (1964). "Hydraulic properties of porous media." Colo. State Univ, Fort Collins, Colorado.

- Brutsaert, W. (1964). "The Propagation of Elastic Waves in Unconsolidated Unsaturated Granular Mediums." *Journal of Geophysical Research*, 69(2), 243-257.
- Cadoret, T., Marion, D., and Zinszner, B. (1995). "Influence of frequency and fluid distribution on elastic wave velocities in partially saturated limestones." *Journal of Geophysical Research*, 100(B6), 9789-9803.
- Carcione, J. M., and Picotti, S. (2006). "P-wave seismic attenuation by slow-wave diffusion: Effects of inhomogeneous rock properties." *Geophysics*, 71, 1-8.
- Chen, L., Miller, G. A., and Kibbey, T. C. (2007). "Rapid Pseudo-Static Measurement of Hysteretic Capillary Pressure-Saturation Relationships in Unconsolidated Porous Media " *Geotechnical Testing Journal*, 30(6), DOI: 10.1520/GTJ100850.
- Claria, J. J., and Rinaldi, V. A. (2007). "Shear Wave Velocity of a Compacted Clayey Silt." *Geotechnical Testing Journal*, 30(5), 1-9.
- Clothier, B., and Scotter, D. (2002). "Unsaturated Water Transmission Parameters Obtained from Infiltration." *Methods of Soil Analysis, Part 4, Physical Methods*, J. H. Dane and G. C. Topp, eds., SSSA, Madison, WI, 879-898.
- Constantz, J. (1993). "Confirmation of Rate-Dependent Behavior in Water Retention During Drainage in Nonswelling Porous Materials." *Water Resour. Res.*, 29(4), 1331-1334.
- Coussy, O., Dormieux, L., and Detournay, E. (1998). "From Mixture theory to Biot's approach for porous media." *International Journal of Solids and Structures*, 35(34-35), 4619-4635.

- Dahle, H. K., Celia, M. A., and Hassanizadeh, S. M. (2005). "Bundle-of-Tubes Model for Calculating Dynamic Effects in the Capillary-Pressure-Saturation Relationship." *Transport in Porous Media*, 58, 5-22.
- Dane, J. H., and Topp, G. C. (2002). *Methods of Soil Analysis Part 4 Physical Methods*, Soil Science Society of America, Inc. , Madison, WI.
- Davidson, J. M., Nielsen, D. R., and Biggar, J. W. (1966). "The dependence of soil water uptake and release upon the applied pressure increment." *Soil Science Society of America Journal*, 30, 298-303.
- Domenico, S. N. (1976). "Effect of brine-gas mixture on velocity in an unconsolidated gas reservoir." *Geophysics*, 41, 882-894.
- Dutta, N. C., and Odé, H. (1983). "Seismic reflections from a gas-water contact." *Geophysics*, 48, 148.
- Dutta, N. C., and Seriff, A. J. (1979). "On White's model of attenuation in rocks with partial gas saturation." *Geophysics*, 44, 1806.
- Dvorkin, J., and Nur, A. (1993). "Dynamic poroelasticity: A unified model with the squirt and the Biot mechanisms." *Geophysics*, 58(4), 524-533.
- Flammer, I., Blum, A., Leiser, A., and Germann, P. (2001). "Acoustic assessment of flow patterns in unsaturated soils." *Journal of Applied Geophysics*, 46, 115-128.
- Fredlund, D. G., and Rahardjo, H. (1993). *Soil Mechanics for Unsaturated Soils*, John Wiley & Sons, Inc.

- Garambois, S., Senechal, P., and Perroud, H. (2002). "On the use of combined geophysical methods to assess water content and water conductivity of near-surface formations." *Journal of Hydrology*, 259, 32-48.
- Gist, G. A. (1994). "Fluid effects on velocity and attenuation in sandstones." *Journal of Acoustic Society of America*, 96(2), 1158-1173.
- Goertz, D., and Knight, R. (1998). "Elastic wave velocities during evaporative drying." *Geophysics*, 63(1), 171-183.
- Gray, W. G., and Hassanizadeh, S. M. (1989). "Averaging theorems and averaged equations for transport of interface properties in multiphase systems." *International Journal of Multiphase Flow*, 15(1), 81-95.
- Gregory, A. R. (1976). "Fluid saturation effects on dynamic elastic properties of sedimentary rock." *Geophysics*, 41, 895-921.
- Guerin, R. (2005). "Borehole and surface-based hydrogeophysics." *Hydrogeology Journal*, 13, 251-254.
- Gurevich, B., Marschall, R., and Shapiro, S. A. (1994). "Effect of fluid flow on seismic reflections from a thin layer in a porous medium." *Journal of Seismic Exploration*, 3, 125-140.
- Gurevich, B., Zyrianov, V. B., and Lopatnikov, S. L. (1997). "Seismic attenuation in finely layered porous rocks: effects of fluid flow and scattering." *Geophysics*, 62(1-6).
- Haeni, F. P. (1986). "Application of seismic-refraction techniques to hydrologic studies." U.S. Geol. Sur. Open File Report 84-0746.

- Hassanizadeh, S. M., Celia, M. A., and Dahle, H. K. (2002). "Dynamic Effects in the Capillary Pressure-Saturation Relationship and its Impact on Unsaturated Flow." *Vadose Zone Journal*, 1, 38-57.
- Hassanizadeh, S. M., and Gray, W. G. (1979). "General Conservation Equations for multiphase systems: a & b." *Advances in Water Resources*, 2, 131-203.
- Hassanizadeh, S. M., and Gray, W. G. (1993). "Thermodynamic basis of capillary pressure in porous media." *Water Resour. Res.*, 29, 3389-3405.
- Helle, H. B., Pham, N. H., and Cacione, J. M. (2003). "Velocity and attenuation in partially saturated rocks: poroelastic numerical experiments." *Geophysical Prospecting*, 51, 551-566.
- Hilf, J. W. (1956). "An Investigation of Pore-water Pressure in Compacted Cohesive Soils, PhD dissertation." US Department of the Interior, Bureau of Reclamation, Design and Construction Division, Denver, Colorado.
- Johnson, D. L. (2001). "Theory of frequency dependent acoustics in patchy-saturated porous media." *Journal of the Acoustic Society of America*, 110(2), 682-694.
- Klimentos, T., and McCann, C. (1990). "Relationships among compressional wave attenuation, porosity, clay content and permeability in sandstones." *Geophysics*, 55(8), 998-1014.
- Knight, R., and Nolen-Hoeksema, R. (1990). "A Laboratory Study of the Dependence of Elastic Wave Velocities on Pore Scale Fluid Distribution." *Geophysical Research Letters*, 17(10), 1529-1532.

- Lee, M. (2004). "Elastic velocities of partially gas-saturated unconsolidated sediments." *Marine and Petroleum Geology*, 21(6), 641-650.
- Leij, F. J., Schaap, M. G., and Arya, L. R. (2002). "Indirect methods." *Methods of Soil Analysis, Part 4:3.6.3. SSSA Book Series 5*, J. H. Dane, Topp, C.G., ed., SSSA, Madison, WI.
- Leong, E.-C., Yeo, S.-H., and Rahardjo, H. (2004). "Measurement of wave velocities and attenuation using an ultrasonic test system." *Canadian Geotechnical Journal*, 41, 844-860.
- Liu, Z., Rector, J. W., Nihei, K. T., Tomutsa, L., Myer, L. R., and Nakagawa, S. (2001). "Extensional wave attenuation and velocity in partially saturated sand in the sonic frequency range." Paper LBNL-50301, Lawrence Berkeley National Laboratory.
- Lu, Z., Hickey, C. J., and Sabatier, J. M. (2004). "Effects of Compaction on the Acoustic Velocity in Soils." *Soil Science of America Journal*, 68, 7-16.
- Mavko, G., and Nur, A. (1979). "Wave attenuation in partially saturated rocks." *Geophysics*, 44(2), 161-178.
- Mohamed, M. H., and Sharma, R. S. (2007). "Role of Dynamic Flow in Relationships between Suction Head and Degree of Saturation." *Journal of Geotechnical and Geoenvironmental Engineering*, 133(3), 286-294.
- Moran, K., Altmann, V., O'Regan, M., and Ashmankas, C. (2007). "Acoustic Compressional Wave Velocity as a Predictor of Glacio-marine Sediment Grain Size " *Geotechnical Testing Journal*, 30(4), 1-7.

- Muller, T. M., and Gurevich, B. (2004). "One-dimensional random patchy saturation model for velocity and attenuation in porous rocks." *Geophysics*, 69(5), 1166-1172.
- Muraleetharan, K. K., and Wei, C. (1999). "Dynamic Behavior of Unsaturated Porous Media: Governing Equations using the Theory of Mixtures with Interfaces (TMI)." *International Journal of Analytical Methods in Geomechanics*, 23, 1579-1608.
- Murphy, W. F. (1982). "Effects of partial water saturation on attenuation in Massillon sandstone and Vycor porous glass." *Journal of Acoustic Society of America*, 71(6), 1458-1468.
- Murphy, W. F., Winkler, K. W., and Klienber, R. L. (1986). "Acoustic relaxation in sedimentary rocks: Dependence on grain contacts and fluid saturation." *Geophysics*, 51(3), 757-766.
- Muthukrishniah, K., Zachariah, R., Murthy, G. R. K., and Nair, P. V. (1995). "Relationship between geophysical and geotechnical properties of marine sediments using Biot-Stoll model." *Marine Georesources & Geotechnology* 13(3), 243-261.
- O'Carroll, D. M., Phelan, T. J., and Abriola, L. M. (2005). "Exploring dynamic effects in capillary pressure in multistep outflow experiments." *Water Resour. Res.*, 41(W11419, doi:10.1029/2005WR004010).
- O'Connell, R. J., and Budiansky, B. (1977). "Viscoelastic properties of fluid-saturated cracked solids." *Journal of Geophysical Research*, 82(36), 5719-5736.

- Oelze, M. L., O'Brien, W. D., and Darmody, R. G. (2002). "Measurement of Attenuation and Speed of Sound in Soils." *Soil Science Society of America Journal*, 66, 788-796.
- Paffenholz, J., and Burkhardt, H. (1989). "Absorption and Modulus Measurements in the Seismic Frequency and Strain Range on Partially Saturated Sedimentary Rocks." *Journal of Geophysical Research*, 94(B7), 9493-9507.
- Prevost, J. (1980). "Mechanics of Continuous Porous Media." *International Journal of Engineering Science*, 18(6).
- Pride, S. R., Berryman, J. G., and Harris, J. M. (2004). "Seismic attenuation due to wave-induced flow." *Journal of Geophysical Research*, 109(B1).
- Pride, S. R., Harris, J. M., and Johnson, D. L. (2003). "Permeability dependence of seismic amplitudes." *The Leading Edge*, 22, 518-525.
- Richards, L. A. (1931). "Capillary conduction of liquids in porous mediums." *Physics*, 1, 318-333.
- Ross, P. J., and Smettem, K. R. J. (2000). "A simple treatment of physical nonequilibrium water flow in soils." *Soil Society of America Journal*, 64, 1926-1930.
- Schultze, B., Ippisch, O., Huwe, B., and Durner, W. "Dynamic Nonequilibrium During Unsaturated Water Flow." *Characterization and Measurement of the Hydraulic Properties of Unsaturated Porous Media; Proc. Intern. Workshop., Riverside, CA, 22-24 October, 1997, Riverside, CA, 877-892.*
- Spencer, J. W. (1979). "Bulk and Shear Attenuation in Berea Sandstone: The Effects of Pore Fluids." *Journal of Geophysical Research*, 84(B13), 7521-7523.

- Stoll, R. D. (1985). "Marine Sediment Acoustics." *Journal of Acoustic Society of America*, 77, 1789-1799.
- Stoll, R. D., and Bryan, G. M. (1969). "Wave Attenuation in Saturated Sediments." *The Journal of the Acoustical Society of America*, 47(5 (Part 2)), 1440-1447.
- Toksoz, M. N., Johnston, D. H., and Timurr, A. (1979). "Attenuation of seismic waves in dry and saturated rocks: 1. Laboratory measurements." *Geophysics*, 44(4), 681-690.
- Topp, G. C., Klute, A., and Peters, D. B. (1967). "Comparison of Water Content-Pressure Head Data Obtained by Equilibrium, Steady-State, and Unsteady-State Methods." *Soil Science Society of America Journal*, 31, 312-314.
- Tserkovnyak, Y., and Johnson, D. L. (2002). "Can one hear the shape of a saturation patch?" *Geophysical Research Letters*, 29(7), 12.
- Tsukamoto, Y., Ishihara, K., Nakazawa, H., Kamada, K., and Huang, Y. (2002). "Resistance of partly saturated sand to liquefaction with reference to longitudinal and shear wave velocities." *Soils and Foundations*, 42(6), 93-104.
- Tuncay, K., and Corapcioglu, M. Y. (1997). "Wave Propagation in Poroelastic Media Saturated by Two Fluids." *Journal of Applied Mechanics*, 64, 313-320.
- Turgut, A., and Yamamoto, T. (1990). "Measurement of acoustic wave velocity and attenuation in marine sediments." *Journal of Acoustic Society of America*, 87(6), 2376-2383.

- Vachaud, G., Vauclin, M., and Wakil, M. (1972). "A study of the uniqueness of the soil moisture characteristic during desorption by vertical drainage." *Soil Science Society of America Journal*, 36, 531-532.
- van Genuchten, M. T. (1980). "A Closed-form Equation for Predicting the Hydraulic Conductivity of Unsaturated Soils." *Soil Science Society of America Journal*, 44, 892-898.
- Velea, D., Shields, F. D., and Sabatier, J. M. (2000). "Elastic Wave Velocities in Partially Saturated Ottawa Sand: Experimental Results and Modeling." *Soil Science Society of America Journal*, 4, 1226-1234.
- Wei, C., and Dewoolkar, M. "A Continuum Theory of Nonequilibrium Two-Phase Flow through Porous Media with Capillary Relaxation." *Advances in Unsaturated Soil, Seepage, and Environmental Geotechnics, Proceedings of Sessions of GeoShanghai, Shanghai, 6-8 June 2006, Shanghai*, 246-254.
- Wei, C., and Dewoolkar, M. (2006b). "Rate-Dependent Behavior of Soil Moisture Retention Characteristics." In Progress.
- Wei, C., and Muraleethanan, K. K. (2006). "Acoustic characterization of fluid-saturated porous media with local heterogeneities: Theory and application." *International Journal of Solids and Structures*, 43, 982-1008.
- Wei, C., and Muraleetharan, K. K. (2002a). "A continuum theory of porous media saturated by multiple immiscible fluids: II. Lagrangian description and variation structure." *International Journal of Engineering Science*, 40, 1835-1854.

- Wei, C., and Muraleetharan, K. K. (2002b). "A continuum theory of porous media saturated by multiple immiscible fluids: I. Linear Poroelasticity." *International Journal of Engineering Science*, 40, 1807-1833.
- Wei, C., and Muraleetharan, K. K. (2007). "Linear viscoelastic behavior of porous media with non-uniform saturation." *International Journal of Engineering Science*, 45, 698-715.
- White, J. E. (1975). "Computed seismic speeds and attenuation in rocks with partial gas saturation." *Geophysics*, 40, 224-232.
- Wildenchild, D., Hopmans, J. W., and Simunek, J. (2001). "Flow rate dependence of Soil Hydraulic Characteristics." *Soil Science of America Journal*, 65, 35-48.
- Wildenchild, D., Hopmans, J. W., Vaz, C. M. P., Rivers, M. L., Rikard, D., and Christensen, B. S. B. (2002). "Using X-ray computed tomography in hydrology: systems, resolutions, and limitations." *Journal of Hydrology*, 267, 285-297.
- Winkler, K. W., and Nur, A. (1982). "Seismic attenuation: Effects of pore fluids and frictional sliding." *Geophysics*, 47, 1-15.
- Wulff, A., and Mjaaland, S. (2002). "Seismic monitoring of fluid fronts: An experimental study." *Geophysics*, 67(1), 221-229.
- Zienkiewicz, O. C. a. S., T. (1984). "Dynamic behavior of saturated porous media: the generalized Biot formulation and its numerical solution." *Int. J. Numer. Anal. Methods Geomech.*, 8, 71-96.

2. SIMULTANEOUS LABORATORY MEASUREMENT OF ACOUSTIC AND HYDAULIC PROPERTIES OF UNSATURATED SOILS

Lindsay A. George, Mandar M. Dewoolkar and Dobroslav Znidarcic

L. A. George and M. M. Dewoolkar, School of Engineering, Univ. of Vermont, 33 Colchester Ave., Burlington, VT 05401; D. Znidarcic, Dept. of Civil, Env. And Arch. Engineering, University of Colorado, Engineering Center ECOT 441, UCB 428, Boulder, CO 80309. Received 3 October 2008. * Corresponding author (lgeorge@cems.uvm.edu).

Submitted for publication in Vadose Zone Journal on October 4, 2008.

2.1 ABSTRACT

A complete set of acoustic properties, including compressional and shear wave velocities and attenuations and hydraulic properties (the soil water characteristic curve and the unsaturated hydraulic conductivity function) over a full range of saturation for two soil specimens is presented. The acoustic data, the soil water characteristic curve and the unsaturated hydraulic conductivity function were collected using a novel device developed at the University of Vermont. The acoustic data are consistent with data collected over a full range of saturations in rocks found in the literature. This experimental data can be used to verify existing models that attempt to link acoustic and hydraulic properties of unconsolidated and unsaturated porous media.

2.2 INTRODUCTION

There is an immense interest in the ability to relate soil properties, specifically hydraulic properties, to the acoustic response of soil (Guerin 2005). This ability could enhance high resolution non-destructive evaluation of the shallow subsurface, and would have applications in a variety of fields including groundwater and contaminant hydrogeology, oil recovery, soil dynamics, and the detection of buried artifacts. For example, seismic surveys have been used successfully to locate the water table (Haeni 1986), but give no information about the unsaturated zone above the water table. The unsaturated zone, also referred to as the vadose zone, may be characterized by the acoustic properties instead of just the reflection of seismic waves (Bachrach and Nur 1998; Garambois et al. 2002). Sonic and ultrasonic waves have been used to enhance oil recovery by initiating motion and increasing the permeability of an aquifer, but the effect of weak waves on porous media is not fully understood, calling for more laboratory investigations that may help quantify and predict the involved mechanisms (Beresnev and Johnson 1994).

The acoustic response of porous materials that are saturated with a single fluid are relatively straight forward, but the acoustic response of porous media saturated by two fluids is much more complex. Models have been developed that predict the acoustic response of unsaturated soils, with the goal of relating soil properties to the acoustic velocity and attenuation. For example, the fundamental theoretical work explaining acoustic wave propagation through porous media was formulated by Biot (1955, 1956). Biot's theory provides a general framework for modeling low frequency elastic wave

propagation through porous media saturated with a compressible, viscous fluid. Expanding Biot's theory to porous media saturated by two fluids introduces some challenges. Several approaches have been taken to describe the partial saturation, including the distribution of moisture and the interfaces between phases. A review, conducted by Toms et al. (2006), groups these approaches into three broad categories, each attributing the cause of significant attenuation to different physical mechanisms; (1) "squirt" flow models, (2) mesoscale or "patchy" heterogeneity models, and (3) effective pore fluid models. "Squirt" flow models assume that significant attenuation is caused by flow occurring in a pore or fracture (Mavko and Nur 1979; Murphy et al. 1986), while mesoscale heterogeneity models assume that the attenuation is caused by local flow created by pressure gradients between "patches" of fluids (Johnson 2001; Pride et al. 2004; White 1975). Effective pore fluid approaches look at the effects of viscous and thermal damping on attenuation (Bedford and Stern 1982). This variety of models shows there is debate on what theoretical and physical mechanism creates attenuation and dispersion of acoustic waves in unsaturated porous media, speaking to the need for more laboratory data.

A number of experimental acoustic investigations of porous media have been performed on unsaturated consolidated porous media, specifically rocks (Cadoret et al. 1995; Gist 1994; Goertz and Knight 1998; Klimentos and McCann 1990; Knight and Nolen-Hoeksema 1990; Murphy 1982; Paffenholz and Burkhardt 1989; Spencer 1979; Toksoz et al 1979; Winkler and Nur 1982; Wulff and Mjaaland 2002). Acoustic studies of soils

generally focus on measurement of the shear wave velocity, which is used to determine the shear modulus and is used in the study of the dynamic behavior of soils (e. g. Brignoli et al. 1996; Claria and Rinaldi 2007). Fewer experimental studies including compressional wave velocity measurements have been performed on unconsolidated porous media such as soils (Alramahi et al 2008; Berge and Bonner 2002; Bonner et al. 2001; Flammer et al 2001; Tsukamoto et al. 2002; Velea et al. 2000). One area of research on soils, the study of marine sediments has produced a number of laboratory and field studies that measure both velocity and attenuation of these saturated unconsolidated porous materials (Moran et al. 2007; Muthukrishniah et al. 1995; Stoll 1985; Turgut and Yamamoto 1990). Even fewer studies have included the attenuation in unsaturated soils (Leong et al. 2004; Liu et al. 2001; Lu et al. 2004; Oelze et al. 2002).

The soil water characteristic curve (SWCC) and the unsaturated hydraulic conductivity function (UHCF) are generally required to describe the hydrological and mechanical behavior of unsaturated soils. The SWCC is a relationship between the level of saturation in a soil sample and the capillary pressure at equilibrium, and the UHCF describes how the hydraulic conductivity varies with saturation, or capillary pressure. Capillary pressure is defined as the difference between the pore air pressure and the pore water pressure. The pores in soil can be represented as capillary tubes, and the soil as a whole can be thought of as a bundle of different sized capillary tubes. As the soil desaturates, the largest capillaries are emptied first followed by smaller capillaries with higher capillary pressures. As the saturation of the soil decreases, the capillary pressure

increases. A relationship can be determined for each soil for a given structure between the saturation and the capillary pressure at an equilibrium state. This relationship has been estimated and measured using a number of direct and indirect techniques. Direct techniques include laboratory and field methods, while indirect methods attempt to estimate unsaturated soil properties using other properties of the soil that are readily available or easily attainable. Indirect methods range from simplistic to complex and are both empirically based (Ghosh 1976; Wösten and van Genuchten 1998) and physically based (Arya and Paris 1981). These methods are based on soil properties such as particle size distribution, pore size distribution, textural class, clay or sand fraction, porosity, or existing databases of properties.

This paper presents an apparatus and test procedures capable of determining the acoustic properties of an unsaturated soil over a full range of saturations, while also measuring the soil water characteristic curve and the hydraulic conductivity function. Measurements of compressional and shear wave velocities, as well as the associated attenuations, have been conducted over a range of saturations at low frequency through silt samples. These measurements may help to validate existing models, or at least increase our understanding of wave propagation and mechanisms of attenuation in unsaturated soils and how to relate the hydraulic properties of soils to these acoustic properties. This would have practical applications in the fields of agricultural engineering, soil science, hydrogeology and unsaturated soil mechanics.

In the following, the experimental setup is described first, followed by a short description of the soils and three sections describing the three properties that were measured in this experiment; the soil water characteristic curve, the unsaturated hydraulic conductivity function, and the acoustic properties. Each section provides a short introduction of the property and describes the procedure used to measure the property. All of the data is presented in the results section; this includes the soil water characteristic curves, the unsaturated hydraulic conductivity functions and the acoustic properties over saturation. A brief discussion section concludes the paper.

2.3 EXPERIMENTAL SETUP

A schematic of the experimental setup is depicted in Figure 2-1 and a photograph of the setup is shown in Figure 2-2. The soil sample is housed in a confining cell and is jacketed by a semi-flexible Viton® rubber membrane. The sample is in contact with a high air entry ceramic disc on the bottom and a coarse porous stone on the top. High air entry ceramic discs have pores which are capable of transferring water, but are small enough to prevent air from passing up to a specified pressure limit. In this case, 1 bar high flow ceramic disks were used, meaning air at a pressure of less than 1 bar above water pressure cannot pass through the disk. Because of this feature water can be removed from the bottom of the sample without removing air, and the saturation of the sample is known from the volume of water removed. Water is removed from the sample using a flow pump (GeoComp FlowTrac), which has the capability of withdrawing at a constant rate or maintaining the pressure in the pore fluid. The confining cell is filled with air instead of water to protect the electronic components within the cell. A differential pressure

transducer (Omega PX26) is used to measure the capillary pressure, it is placed between the upper air pressure line and the lower water pressure line.

The laboratory device is capable of housing a cylindrical soil sample 100 mm in diameter and up to 125 mm in height. This large sample size is necessary to allow low frequency acoustic waves to travel through the media for a distance larger than its wavelength without interference from the boundaries. The acoustic transmitter and receiver are housed in the Viton[®] rubber jacket which was made flexible enough to conform to the sample under confinement, but also rigid enough to support the transducers. The transducers were placed on the side of the sample so they would not interfere with the end caps, allowing for one-dimensional flow through the sample. The device is also capable of utilizing a rigid walled sample when the acoustic measurements are not taken from the sides. The acoustic equipment (Autolab System) developed by New England Research, Inc. (NER) of White River Junction, Vermont, includes flat piezo-ceramic transducers, a waveform function generator (Agilent Model 33220A), an oscilloscope (Tektronics Model TDS3012B) and the data acquisition system, as seen in Figure 2-2.

2.4 MATERIAL AND METHODS

2.4.1 Soil Samples

Soil from the Bonny Dam Site in eastern Colorado was selected for this experimental design. The properties of the Bonny Silt are listed in Table 2-1. The silt classifies as CL-ML according to the Unified Soil Classification System (USCS). The sample was compacted at 10% moisture content inside of the membrane supported by a two-part split

mold using static compaction. The initial dry density of the sample under confinement was 1.6 g/cc.

A second soil type was prepared in the laboratory and is referred to as the Heterogeneous soil mixture. The sample was prepared by mixing sand, silt and clay sized particles to achieve a locally heterogeneous distribution of pore sizes. The clay was broken up into small pieces that passed through the ¼” sieve, the silt was also broken up from a dry state, and then both were mixed with the sand to achieve a patchy distribution of silt and clay within the overall sandy mixture. The mixture consists of approximately 55% by weight sand, 27% silt, and 18% clay sized particles. The overall grain size distribution for both soil types are shown in Figure 2-3.

2.4.2 Soil Water Characteristic Curve

The SWCC is determined using a suction control method with axis translation. During a suction control method, the saturation in the sample is changed by controlling the level of suction at one end of the sample, and the amount of outflow is monitored over time. The basic concept behind the axis translation technique is to translate the range of capillary pressures ($u_a - u_w$) by elevating both the pore air pressure (u_a) and the pore water pressure (u_w). This technique allows for levels of capillary pressure higher than atmospheric without reaching negative water pressures. If the pressure of the water is maintained below -100kPa, the potential for cavitation exists, which may allow unmeasured air to enter the system. This method was chosen because of the large range of capillary

pressures possible with the axis translation technique. Other methods may also be employed using this apparatus, such as controlled volume methods (Olsen et al. 1994).

The pore air pressure is maintained at a specific pressure determined by the anticipated capillary pressures of the media being tested. The level of suction is controlled by a flow pump connected to a reservoir at the bottom of the sample. The flow pump is set to maintain a desired capillary pressure and the volume of water that is withdrawn to maintain that capillary pressure is recorded. To ensure that the sample is always drying during this portion of the test, the pressure is maintained at the desired level until equilibrium is achieved. The flow pump has a built in function that maintains the pressure of the water in the flow pump by withdrawing or injecting the appropriate amount of water. The capillary pressure is then also maintained, since the air pressure is constant. Equilibrium is achieved when the rate at which the flow pump has to either inject or withdraw water is sufficiently low, and a point on the SWCC is obtained. The saturation is determined by calculating the volume of water in the sample, and the capillary pressure is measured by the differential pressure transducers connected between the pore air and the lower pore water reservoir.

The measured drainage points were fitted with a van Genuchten model (van Genuchten 1980) of the soil water characteristic curve described in Equations 1 and 2. The van Genuchten parameters are then used in the following section to determine the unsaturated hydraulic conductivity function.

$$S_e = \left[1 + (\alpha |h_m|^n) \right]^{-m} \quad (1)$$

where,

$$S_e = \frac{\theta - \theta_r}{\theta_s - \theta_r}, \quad (2)$$

and, θ_r is the irreducible water content, θ_s is the saturated water content, h is the capillary pressure, α , m , n are fitting parameters. The parameters found for each soil type are listed in Table 2-2.

The sample size in this apparatus is much larger than those traditionally used for measurement of the characteristic curve and a few challenges arise when using a large sample. Samples used in Tempe cells are typically approximately 50 mm in diameter and 4-5 mm in height. Generally it is assumed that the saturation variation along the height of the sample is negligible and the saturation of the entire sample can be taken as an average calculated using the amount of water withdrawn. Since the samples used in this study are approximately 100 mm in height, there could be an appreciable amount of variation in saturation over the height of the sample due to the effect of gravity. The amount of variation depends on the pore size distribution of the sample and the capillary pressure at the bottom of the sample. Bonny silt was chosen for this experiment to minimize this variation so that the acoustic measurements are more representative of one level of saturation. The level of saturation at mid height of the sample is calculated considering the variation in pressure that occurs over the sample and the SWCC.

The air pressure was measured at the top of the sample and the water pressure was measured at the bottom of the sample, but the capillary pressure at a point within the sample is desired. Since the height of the sample is relatively large, one cannot assume that the value of capillary pressure one measures is actually the capillary pressure at a point within the sample (Liu and Dane 1995). Therefore, Liu and Dane (1995) developed a method to determine the SWCC at a point given pressure measurements at different points on the sample and the program TrueCell (Liu and Dane 1995) is available to implement the method. Liu and Dane showed that there may be an appreciable difference between the measured capillary pressure and the capillary pressure at a point depending on sample height, relative fluid densities, and position of measurements.

2.4.3 Unsaturated Hydraulic Conductivity Function

The hydraulic conductivity of a soil sample is the highest when the pores are saturated with water, this allows for the highest transmission of water through the sample. When the soil becomes unsaturated the ability for it to transmit water is decreased, until the capillary pressures in the soil are so great that the transmission of water is almost impossible and the hydraulic conductivity is at a minimum. The relationship between the hydraulic conductivity and the saturation is referred to as the Unsaturated Hydraulic Conductivity Function (UHCF) and is used to describe flow through unsaturated soils. The UHCF is generally not measured directly. Usually data is collected during an

infiltration or drainage experiment, either in the field or the laboratory, and inverse modeling techniques are employed to determine the relationship.

The hydraulic data collected throughout this experiment is similar to the data collected in a multi-step outflow experiment, that is, the cumulative outflow volume and the capillary pressure over time. This information can be used with an unsaturated flow model and an optimization procedure to inversely model the UHCF. HYDRUS-1 version 4.0 (Šimůnek 2008) was used to simulate this experiment and the built-in optimization procedure was used to determine the hydraulic conductivity function parameters. A van Genuchten model (van Genuchten 1980) was chosen to describe the hydraulic properties and is described by Equation 3

$$K(\theta) = K_s S_e^L \left[1 - (1 - S_e^{1/m})^m \right]^2. \quad (3)$$

where, S_e is given by Equation 2, K_s is the saturated hydraulic conductivity and L is the tortuosity factor.

2.4.4 Acoustic Properties

Compressional wave velocity is the speed at which a compressional wave travels through a particular material and is determined by the arrival time of the wave at the receiver. Attenuation is related to the dissipation of wave energy, which may be caused by motion of the fluid relative to the frame and the relative motion of contiguous particles (Stoll 1969). Attenuation is described by the inverse of the quality factor (Q^{-1}). In this study, piezo-ceramic sheet material (PZT) is used to produce and receive the acoustic waves,

which are transmitted through the soil. Piezo-ceramic material converts electrical energy into mechanical deformation. When an electrical field is placed across the sheet it responds by expanding its thickness in the longitudinal direction and contracting its length in the transverse direction of polarization. Compressional wave transducers and shear wave transducers are polarized in opposite planes in order to produce the appropriate wave. The movement of these sheets is very small (on the order of tens of nanometers). Bender elements are made of the same material, but consist of two sheets that are polarized in opposite directions and oriented like a beam, when one sheet expands the other contracts and causes a bending motion. Bender elements were not chosen for this apparatus because of the large deformations they produce (on the order of hundreds to thousands of microns).

The transducers used in this apparatus consist of a stack of five cylindrical layers. A curved titanium head, approximately 8 mm thick at the center, is in contact with the soil sample. The polarized PZT layers are attached to the titanium head, consisting of two layers, closest to the sample is the S –wave polarized PZT (0.8 mm), and second is the P-wave polarized pzt (2 mm). A third piece of PZT (6 mm) and a secondary piece of lead zirconite (13 mm) is placed outside of the polarized crystals to act as an absorptive backing to reduce reflections inside of the transducer. Canada Balsam, a non-water soluble acoustic couplant, is used between the titanium head and the soil sample to ensure mechanical coupling between the two materials, and to prevent an interface that may result in reflection of the acoustic waves. A Kelly wavelet (see Figure 2-4) was chosen as

a source wave for the experiments. The AutoLab system is equipped with automated switching controls that switch between exciting the shear and compressional waves.

The acoustic properties can be measured at any time throughout the experiment. Compressional and shear waveforms for a range of frequencies were taken at intervals and represent varying degrees of saturation. Waveforms were collected while the sample was equilibrating for each pressure step and when equilibrium was reached. The response of the unsaturated media is thought to be frequency dependent; therefore, the acoustic waves were collected over a range of frequencies. The frequency of interest is in the vicinity of 10 kHz. The compressional and shear waves were produced with the piezo-ceramic transducer stack, which is excited by the waveform function generator. The wave is received by the opposite stack, displayed on an oscilloscope and the data acquisition system collects the raw data. The acoustic properties of interest are the compressional wave velocity and attenuation, which are determined from the compressional waveform. The shear wave velocity and attenuation can be determined from the shear waveform and be used to determine the shear modulus of the soil sample.

Because of the small strains produced, the highly attenuating soil, and the complex geometry of the sample, determining the velocity and attenuation of the soil over the entire range of saturations is a difficult task. Traditionally, velocities are determined by hand picking the first arrival of the wave, and attenuations are found by comparing the frequency spectra of two waves using a method known as Spectral Ratios (Toksoz et al

1979). An alternative forward modeling technique was utilized in this research to obtain both the velocity and attenuation of the waveform as follows.

The compressional and shear wave velocity and attenuation were determined using a one dimensional wave propagation model that assumes a constant band limited Q. The model was developed by New England Research, Inc. It models a one-dimensional stack of elastic media with complex, frequency-dependent elastic parameters. The imaginary portion of the elastic parameters is assumed to arise from a band-limited constant-Q rheology. The model also handles piezoelectric effects. This process is superior to traditional spectral ratio methods in that it provides information on both velocity and attenuation, while providing a more robust test of model assumptions by fitting the actual waveform rather than just its power spectrum (Smith 1993). It is also a more robust estimator of velocity, since it includes the effects of dispersion in modifying the arrival of the waveform. This allows one to objectively track changes in arrival time of a waveform that does not have a clearly defined arrival.

The experimental waveform was matched to the model waveforms by adjusting the velocity and attenuation of the modeled soil sample. A reasonable match was obtained over the first peak, including arrival, amplitude and period. Examples of the modeled and experimental waveforms are shown in Figure 2-5.

2.5 RESULTS

The sets of acoustic and hydraulic results were collected in experiments that lasted approximately one month each, and are presented here as examples. The length of the experiment is determined by both the soil type and the height of the soil sample. The soil water characteristic curve and the unsaturated hydraulic conductivity function are shown in Figures 2-6 and 2-7, respectively. The parameters used in the van Genuchten relationship described in equations (1) through (3) are listed in Table 2-2.

Figures 2-8 through 2-11 present the compressional and shear wave velocity and attenuation over a full range of saturations and capillary pressures produced with a Kelly wavelet source with a center frequency of 20 kHz. The trends shown in both the compressional wave velocity and attenuation are consistent with previously measured data on sandstone and limestone using the resonant bar technique (Cadoret et al. 1995; Murphy 1982). These trends are also consistent with those predicted by theoretical models (Lo et al. 2007; Wei and Dewoolkar 2006).

2.6 DISCUSSION

The soil water characteristic curves shown in Figure 2-6 was measured as described in previous sections. After implementing the method of Liu and Dane (1995) presented earlier, it is clear that the soil types and configuration of pore pressure transducers does not have a significant effect on the measured SWCC. The SWCC measured is equal to the SWCC at a physical point.

The unsaturated hydraulic conductivity functions shown in Figure 2-7 were found through inverse modeling of the cumulative outflow using HYDRUS-1. Both the saturated hydraulic conductivity and the tortuosity factor (L) were optimized.

Figures 2-8 (a) and (c) show the relationship between compressional wave velocity and moisture content, and Figures 2-8 (b) and (d) show the relationship between the compressional wave attenuation and moisture content. Compressional wave velocity is shown to be a maximum at full saturation; this is due to the decreased compressibility of the soil matrix in the absence of air (Murphy 1984). The velocity quickly decreases when air is introduced into the sample, and then slightly recovers at lower moisture contents. This increase may be due to the increased stiffness of the soil matrix offered by increased capillary pressures. The compressional wave attenuation shows a peak at near full saturation and a minimum at low saturation.

Both of the sets of data show a difference in both compressional wave velocity and attenuation between those points taken during wetting and those taken during drying. This phenomenon has been seen in rock samples and has been attributed to the difference in the distribution of moisture achieved when a sample is dried from a fully saturated state compared to when the sample has been wetted to the same saturation (Cadoret et al. 1995). When a sample is dried from a fully saturated state, the distribution of moisture

tends to be “patchy”, compared to when the sample is wetted, the distribution tends to be more uniform.

An inverse relationship between shear wave velocity and moisture content is shown in Figures 2-9 (a) and (c). As the moisture content decreases, the shear wave velocity increases. This is consistent with the effect of density and the increase in shear modulus due to increasing effective stress. The shear wave velocity at low frequency can be represented by Equation 4:

$$V_s = \sqrt{\frac{G_{soil}}{\rho_{soil}}} \quad (4)$$

where G_{soil} is the shear modulus of the soil and depends on the skeletal shear stiffness of the soil, and ρ_{soil} is the bulk mass density of the soil. As the saturation decreases, so does the bulk mass density of the material. Also as saturation decreases, suction increases, increasing the effective pressure on the sample and increasing the shear modulus of the soil.

Figures 2-9 (b) and (d) show that there is not a significant change in shear wave attenuation due to changes in moisture content. Shear attenuation is expected to be at a minimum in dry rock, greater in unsaturated rock and at a maximum in saturated rock. Shear attenuation is also expected to decrease with increasing effective stress in rocks (Winkler and Nur 1979). These expected trends combined should result in decreasing

attenuation with decreasing saturation depending on the levels of effective stress. These data show no significant increase or decrease in shear wave attenuation due to changes in moisture content or capillary pressure.

Equilibrium between the capillary pressure and saturation in the sample was achieved after each change in saturation. The acoustic measurements taken at those equilibrium points are plotted in Figures 2-10 and 2-11 and show the variation of acoustic velocity and attenuation with capillary pressure. The same trends are observed in the plots versus moisture content.

2.7 CONCLUSIONS

The development of a new type of laboratory device capable of making simultaneous measurements of acoustic signatures and hydraulic properties on relatively large soil specimens is presented. The acoustic properties include the compressional and shear wave speeds and attenuations. A complete set of these measurements over a full range of saturations is presented. The results are consistent with previously published data collected on unsaturated rocks. The soil water characteristic curves and the unsaturated hydraulic conductivity functions are also measured and presented.

2.8 ACKNOWLEDGEMENTS

The study presented here was supported by Vermont Experimental Program to Stimulate Competitive Research (VT EPSCoR), (grant EPS 0236976) and the Vermont Space Grant

Consortium through funding from NASA (grant NNG05GH16H). The authors are grateful to Dr. George Pinder for his time and advice, Floyd Vilmont and Kurt Anthony of the University of Vermont for assistance in the apparatus development and Gregory Boitnott, of New England Research, Inc. for collaboration on acoustic data collection and analysis.

2.9 REFERENCES

- Aramahi, B., Alshibli, K., Fratta, D., and Trautwein, S. J. (2008). "A Suction-Controlled Apparatus for the Measurement of P and S-Wave Velocity in Soils." *Geotechnical Testing Journal*, 31(1), 12-23.
- Arya, L. M., and Paris, J. F. (1981). "A physico-empirical model to predict the soil moisture characteristic from particle size distribution and bulk density data." *Soil Science Society of America Journal*, 45, 1023-1030.
- Bachrach, R., and Nur, A. (1998). "High-resolution shallow-seismic experiments in sand, Part 1: Water table, fluid flow and saturation." *Geophysics*, 63(4), 1225-1233.
- Bedford, A., and Stern, M. (1982). "A model for wave propagation in gassy sediments." *Journal of Acoustic Society of America*, 73, 409-417.
- Beresnev, I. A., and Johnson, P. A. (1994). "Elastic-wave simulation of oil production: a review of methods and results." *Geophysics*, 59(6), 1000-1017.
- Berge, P. A., and Bonner, B. P. (2002). "Seismic velocities contain information about depth, lithology, fluid content and microstructure." *UCRL-JC-144792*, DOE Lawrence Livermore National Laboratory.

- Biot, M. A. (1955). "Theory of Propagation of Elastic Waves in a Fluid-Saturated Porous Solid. II. Higher Frequency Range." *The Journal of the Acoustical Society of America*, 28(2), 179-191.
- Biot, M. A. (1956). "Theory of Propagation of Elastic Waves in a Fluid-Saturated Porous Solid I. Low Frequency Range." *The Journal of the Acoustical Society of America*, 28(2), 168-178.
- Bonner, B. P., Berge, P. A., and Wildenchild, D. (2001). "Compressional and Shear Wave Velocities for Artificial Granular Media Under Simulated Near Surface Conditions." *UCRL-JC-142935*, DOE Lawrence Livermore National Laboratory.
- Brignoli, E. G. M., Gotti, M., and Stokoe, K. H. (1996). "Measurement of Shear Waves in Laboratory Specimens by Means of Piezoelectric Transducers." *Geotechnical Testing Journal*, 19(4), 384-397.
- Cadoret, T., Marion, D., and Zinszner, B. (1995). "Influence of frequency and fluid distribution on elastic wave velocities in partially saturated limestones." *Journal of Geophysical Research*, 100(B6), 9789-9803.
- Claria, J. J., and Rinaldi, V. A. (2007). "Shear Wave Velocity of a Compacted Clayey Silt." *Geotechnical Testing Journal*, 30(5), 1-9.
- Flammer, I., Blum, A., Leiser, A., and Germann, P. (2001). "Acoustic assessment of flow patterns in unsaturated soils." *Journal of Applied Geophysics*, 46, 115-128.
- Garambois, S., Senechal, P., and Perroud, H. (2002). "On the use of combined geophysical methods to assess water content and water conductivity of near-surface formations." *Journal of Hydrology*, 259, 32-48.

- Ghosh, R. K. (1976). "Model of the soil moisture characteristic." *Journal of the Indian Society of Soil Science*, 24, 353-355.
- Gist, G. A. (1994). "Fluid effects on velocity and attenuation in sandstones." *Journal of Acoustic Society of America*, 96(2), 1158-1173.
- Goertz, D., and Knight, R. (1998). "Elastic wave velocities during evaporative drying." *Geophysics*, 63(1), 171-183.
- Guerin, R. (2005). "Borehole and surface-based hydrogeophysics." *Hydrogeology Journal*, 13, 251-254.
- Haeni, F. P. (1986). "Application of seismic-refraction techniques to hydrologic studies." U.S. Geol. Sur. Open File Report 84-0746.
- Johnson, D. L. (2001). "Theory of frequency dependent acoustics in patchy-saturated porous media." *Journal of the Acoustic Society of America*, 110(2), 682-694.
- Klimentos, T., and McCann, C. (1990). "Relationships among compressional wave attenuation, porosity, clay content and permeability in sandstones." *Geophysics*, 55(8), 998-1014.
- Knight, R., and Nolen-Hoeksema, R. (1990). "A Laboratory Study of the Dependence of Elastic Wave Velocities on Pore Scale Fluid Distribution." *Geophysical Research Letters*, 17(10), 1529-1532.
- Leong, E.-C., Yeo, S.-H., and Rahardjo, H. (2004). "Measurement of wave velocities and attenuation using an ultrasonic test system." *Canadian Geotechnical Journal*, 41, 844-860.

- Liu, H. H., and Dane, J. H. (1995). "Improved Computational Procedure for Retention Relations of Immiscible Fluids Using Pressure Cells." *Soil Science Society of America Journal*, 59, 1520-1524.
- Liu, Z., Rector, J. W., Nihei, K. T., Tomutsa, L., Myer, L. R., and Nakagawa, S. (2001). "Extensional wave attenuation and velocity in partially saturated sand in the sonic frequency range." *Paper LBNL-50301*, Lawrence Berkeley National Laboratory.
- Lo, W., Yeah, C., and Tsai, C. (2007). "Effect of soil texture on the propagation and attenuation of acoustic waves at unsaturated conditions." *Journal of Hydrology*, 338, 273-284.
- Lu, Z., Hickey, C. J., and Sabatier, J. M. (2004). "Effects of Compaction on the Acoustic Velocity in Soils." *Soil Science of America Journal*, 68, 7-16.
- Malone, M. K. (1987). "The Influence of Groundwater on Slope Stability," M. S. Thesis, University of Colorado, Boulder.
- Mavko, G., and Nur, A. (1979). "Wave attenuation in partially saturated rocks." *Geophysics*, 44(2), 161-178.
- Moran, K., Altmann, V., O'Regan, M., and Ashmankas, C. (2007). "Acoustic Compressional Wave Velocity as a Predictor of Glacio-marine Sediment Grain Size" *Geotechnical Testing Journal*, 30(4), 1-7.
- Murphy, W. F. (1982). "Effects of partial water saturation on attenuation in Massillon sandstone and Vycor porous glass." *Journal of Acoustic Society of America*, 71(6), 1458-1468.

- Murphy, W. F. (1984). "Acoustic Measures of Partial Gas Saturation in Tight Sandstones." *Journal of Geophysical Research*, 89(B13), 11,549-11,559.
- Murphy, W. F., Winkler, K. W., and Klienbergl, R. L. (1986). "Acoustic relaxation in sedimentary rocks: Dependence on grain contacts and fluid saturation." *Geophysics*, 51(3), 757-766.
- Muthukrishniah, K., Zachariah, R., Murthy, G. R. K., and Nair, P. V. (1995). "Relationship between geophysical and geotechnical properties of marine sediments using Biot-Stoll model." *Marine Georesources & Geotechnology* 13(3), 243-261.
- Oelze, M. L., O'Brien, W. D., and Darmody, R. G. (2002). "Measurement of Attenuation and Speed of Sound in Soils." *Soil Science Society of America Journal*, 66, 788-796.
- Olsen, H. W., Willden, A. T., Kiusalaas, N. J., Nelson, K. R., and Poeter, E. P. (1994). "Volume-Controlled Hydrologic Property Measurements in Triaxial Systems." *Hydraulic Conductivity and Waste Contaminant Transport in Soil*, ASTM STP 1142, D. E. Daniel and S. J. Trautwein, eds., American Society for Testing and Materials, Philadelphia, 482-504.
- Paffenholz, J., and Burkhardt, H. (1989). "Absorption and Modulus Measurements in the Seismic Frequency and Strain Range on Partially Saturated Sedimentary Rocks." *Journal of Geo-physical Research*, 94(B7), 9493-9507.
- Pride, S. R., Berryman, J. G., and Harris, J. M. (2004). "Seismic attenuation due to wave-induced flow." *Journal of Geophysical Research*, 109(B1).
- Šimůnek, J., M. Šejna, H. Saito, M. Sakai, and M. Th. van Genuchten. (2008). "The HYDRUS-1D Software Package for Simulating the Movement of Water, Heat, and

- Multiple Solutes in Variably Saturated Media, Version 4.0, HYDRUS Software Series 3." Department of Environmental Sciences, University of California Riverside, Riverside, California, USA.
- Smith, M. L. (1993). *Ultrasonic Waveform Matching, NER Application Note AN93-1, AutoLab Users Manual*, New England Research, Inc.
- Spencer, J. W. (1979). "Bulk and Shear Attenuation in Berea Sandstone: The Effects of Pore Fluids." *Journal of Geophysical Research*, 84(B13), 7521-7523.
- Stoll, R. D. (1985). "Marine Sediment Acoustics." *Journal of Acoustic Society of America*, 77, 1789-1799.
- Toksoz, M. N., Johnston, D. H., and Timurr, A. (1979). "Attenuation of seismic waves in dry and saturated rocks: 1. Laboratory measurements." *Geophysics*, 44(4), 681-690.
- Toms, J., Muller, T. M., Ciz, R., and Gurevich, B. (2006). "Comparative review of theoretical models for elastic wave attenuation and dispersion in partially saturated rocks." *Soil Dynamics and Earthquake Engineering*, 26, 548-565.
- Tsukamoto, Y., Ishihara, K., Nakazawa, H., Kamada, K., and Huang, Y. (2002). "Resistance of partly saturated sand to liquefaction with reference to longitudinal and shear wave velocities." *Soils and Foundations*, 42(6), 93-104.
- Turgut, A., and Yamamoto, T. (1990). "Measurement of acoustic wave velocity and attenuation in marine sediments." *Journal of Acoustic Society of America*, 87(6), 2376-2383.

- van Genuchten, M. T., (1980). "A closed-form equation for predicting the hydraulic conductivity of unsaturated soils." *Soil Science Society of America Journal*. 44(5), 892-898.
- Velea, D., Shields, F. D., and Sabatier, J. M. (2000). "Elastic Wave Velocities in Partially Saturated Ottawa Sand: Experimental Results and Modeling." *Soil Science Society of America Journal*, 4, 1226-1234.
- Wei, C., and Dewoolkar, M. "A Continuum Theory of Nonequilibrium Two-Phase Flow through Porous Media with Capillary Relaxation." *Advances in Unsaturated Soil, Seepage, and Environmental Geotechnics, Proceedings of Sessions of GeoShanghai, Shanghai, 6-8 June 2006*, Shanghai, 246-254.
- White, J. E. (1975). "Computed seismic speeds and attenuation in rocks with partial gas saturation." *Geophysics*, 40, 224-232.
- Winkler, K., and Nur, A. (1979). "Pore Fluids and Seismic Attenuation in Rocks." *Geophysical Research Letters*, 6(1), 1-4.
- Winkler, K. W., and Nur, A. (1982). "Seismic attenuation: Effects of pore fluids and frictional sliding." *Geophysics*, 47, 1-15.
- Wösten, J. H. M., and Genuchten, M. T. v. (1988). "Using texture and other soil properties to predict the unsaturated soil hydraulic functions." *Soil Science of America Journal*, 52, 1762-1770.
- Wulff, A., and Mjaaland, S. (2002). "Seismic monitoring of fluid fronts: An experimental study." *Geophysics*, 67(1), 221-229.

Figure Captions

Figure 2-1: Schematic of the apparatus

Figure 2-2: Photograph of the experimental setup

Figure 2-3: Grain size distribution of Bonny silt and Heterogeneous soil mixture

Figure 2-4: Kelly wavelet source with a center frequency of approximately 20 kHz

Figure 2-5: Example of modeled and experimental waveform matching

Figure 2-6: Soil water characteristic curves for (a) Bonny silt and (b) Heterogeneous soil mixture

Figure 2-7: Unsaturated hydraulic conductivity functions

Figure 2-8: (a) Compressional Wave Velocity, (b) Compressional Wave Attenuation vs. Moisture Content for Bonny silt and (c) Compressional Wave Velocity (d)

Compressional Wave Attenuation vs. Moisture Content for Heterogeneous soil mixture

Figure 2-9: (a) Shear Wave Velocity (b) Shear Wave Attenuation vs. Moisture Content for Bonny silt and (c) Shear Wave Velocity, (d) Shear Wave Attenuation vs. Moisture Content for Heterogeneous soil mixture

Figure 2-10: (a) Compressional Wave Velocity, (b) Compressional Wave Attenuation vs. Capillary Pressure for Bonny Silt and (c) Compressional Wave Velocity, (d)

Compressional Wave Attenuation vs. Capillary Pressure for Heterogeneous soil mixture

Figure 2-11: (a) Shear Wave Velocity (b) Shear Wave Attenuation vs. Capillary Pressure for Bonny silt and (c) Shear Wave Velocity (d) Shear Wave Attenuation vs. Capillary

Pressure for Heterogeneous soil mixture

Table 2-1: Properties of Bonny Silt

Property	Value
Liquid Limit	25 %
Plastic Limit	21 %
Clay Fraction	6 %
USCS Classification	CL-ML

Table 2-2: Parameters used for the Van Genuchten models (Equations 1 - 3)

Bonny silt	Value
Residual Moisture Content (θ_r)	0.214
Saturated Moisture Content (θ_s)	0.405
Alpha (α)	0.00515
Exponent (n)	3.576
Saturated Hydraulic Conductivity	1.23×10^{-7} m/s
Tortuosity Factor (L)	3.32×10^{-3}
Heterogeneous soil mixture	Value
Residual Moisture Content (θ_r)	0.176
Saturated Moisture Content (θ_s)	0.290
Alpha (α)	0.00624
Exponent (n)	1.996
Saturated Hydraulic Conductivity	4.25×10^{-9} m/s
Tortuosity Factor (L)	8.29×10^{-6}

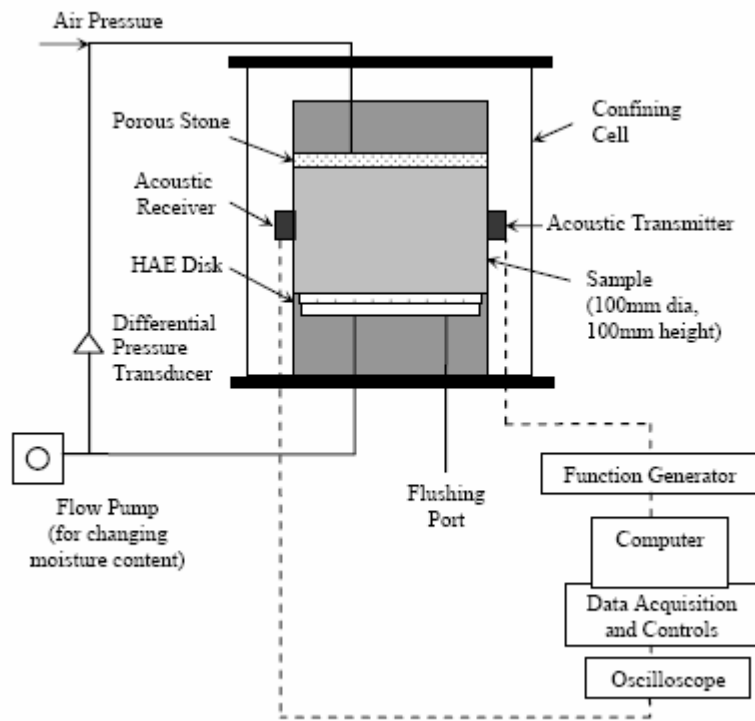


Figure 2-1: Schematic of the apparatus

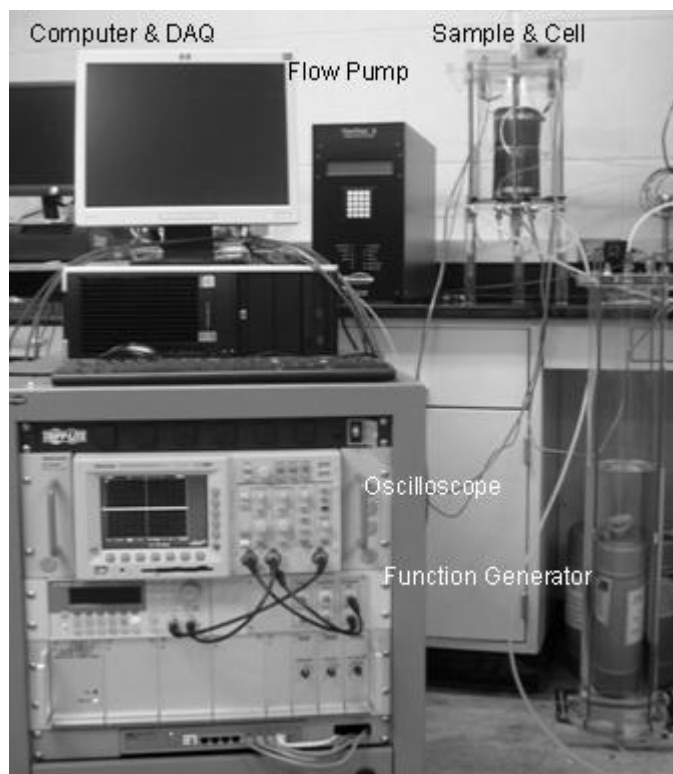


Figure 2-2: Photograph of the experimental setup

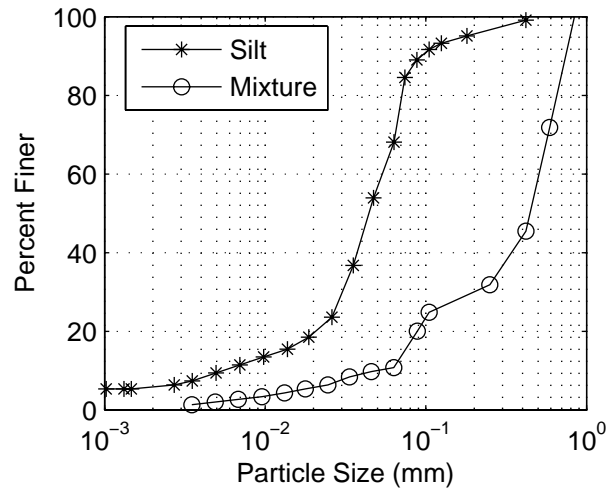


Figure 2-3: Grain size distribution of Bonny silt and Heterogeneous soil mixture

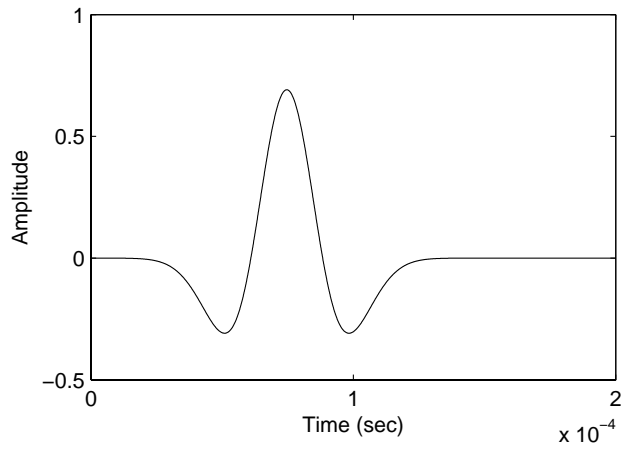


Figure 2-4: Kelly wavelet source with a center frequency of approximately 20 kHz

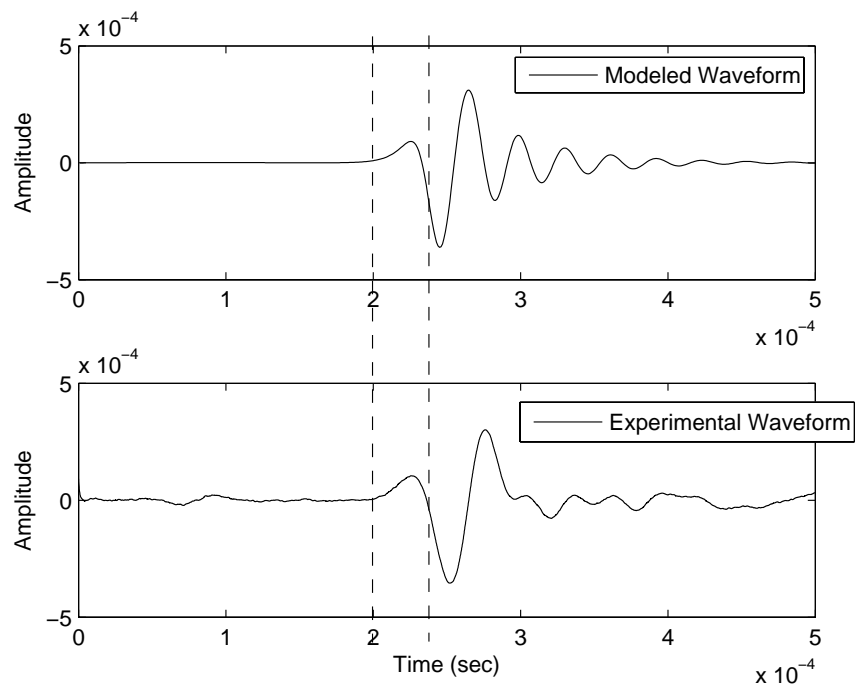
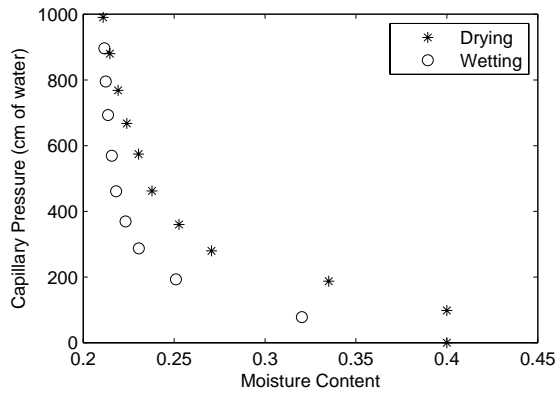
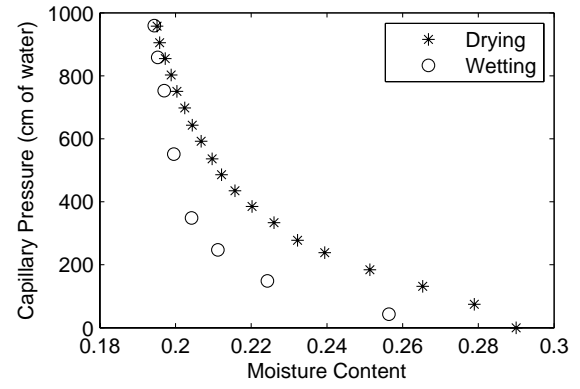


Figure 2-5: Example of modeled and experimental waveform matching



(a) Bonny silt



(b) Heterogeneous soil mixture

Figure 2-6: Soil water characteristic curves for (a) Bonny silt and (b) Heterogeneous soil mixture

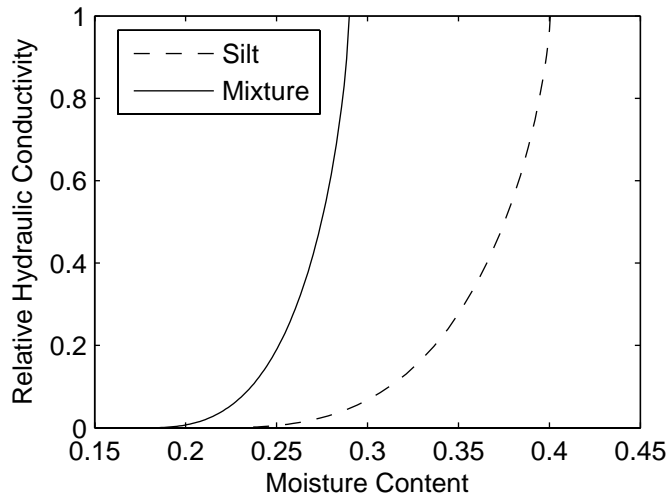
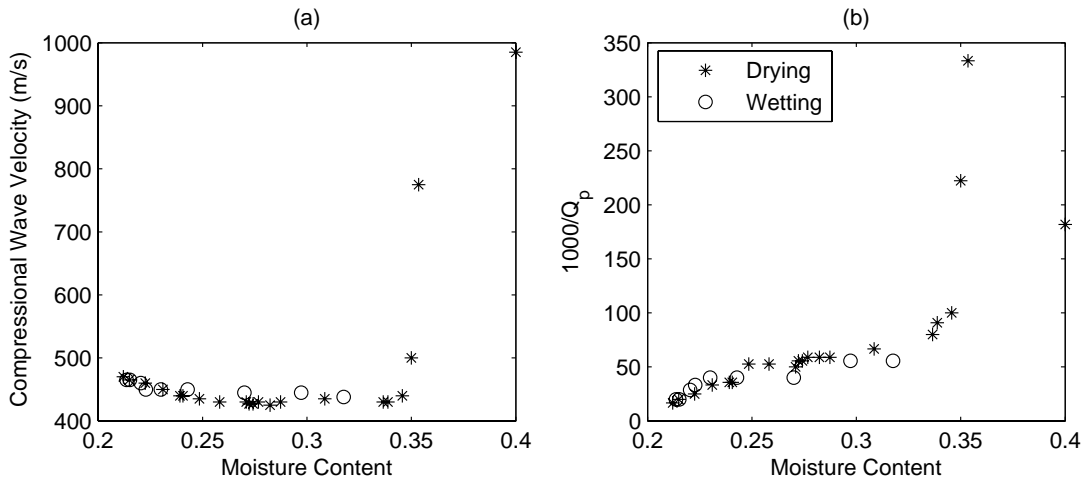
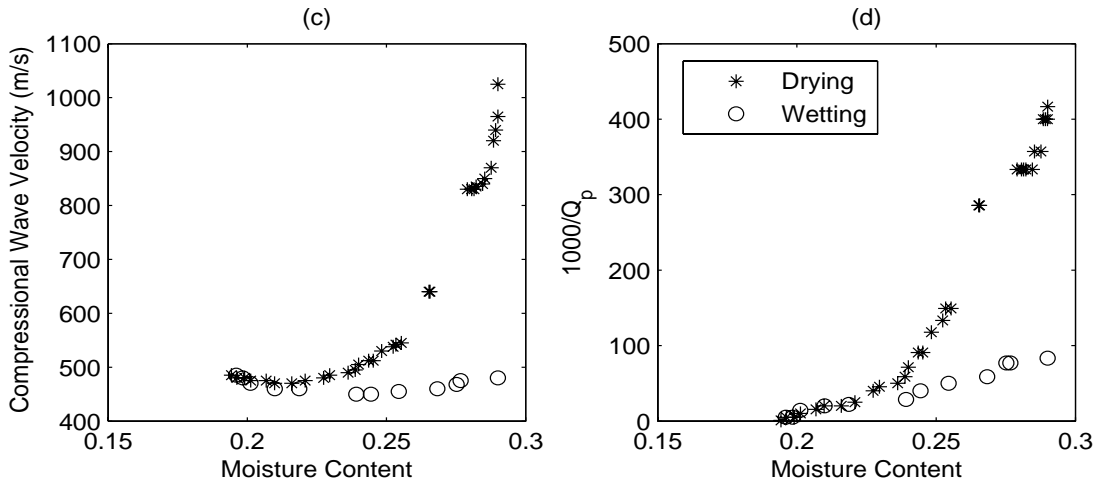


Figure 2-7: Unsaturated hydraulic conductivity functions

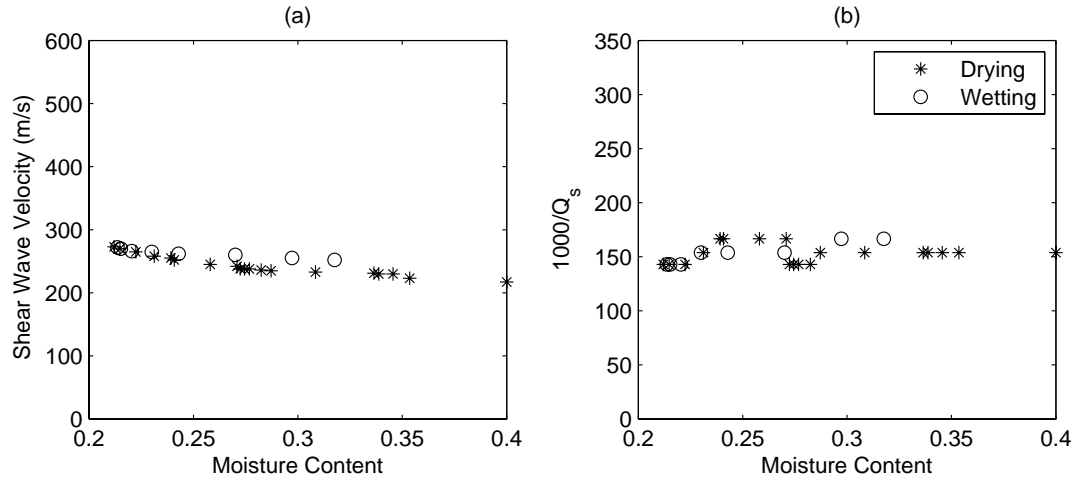


(a) and (b) Bonny Silt

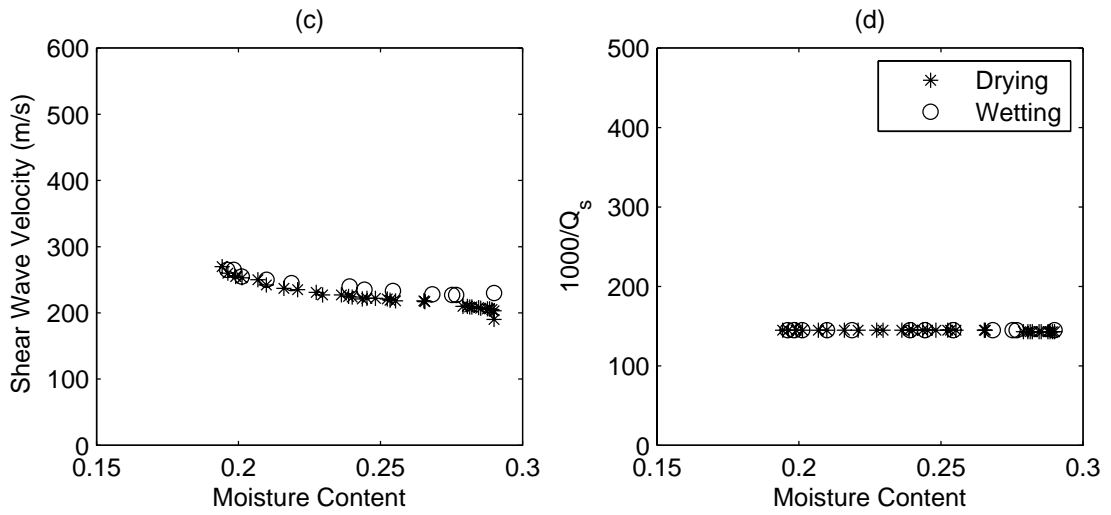


(c) and (d) Heterogeneous soil mixture

Figure 2-8: (a) Compressional Wave Velocity, (b) Compressional Wave Attenuation vs. Moisture Content for Bonny silt and (c) Compressional Wave Velocity (d) Compressional Wave Attenuation vs. Moisture Content for Heterogeneous soil mixture.

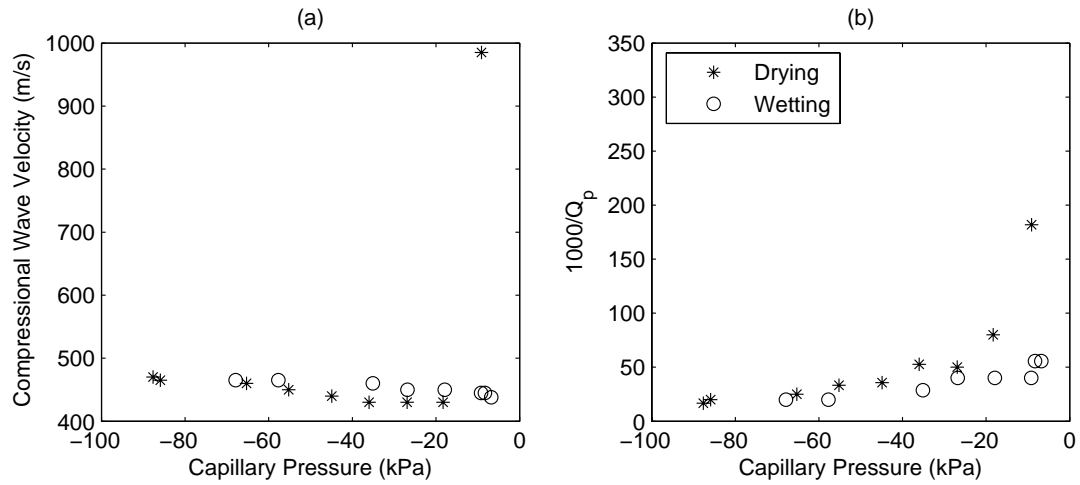


(a) and (b) Bonny Silt

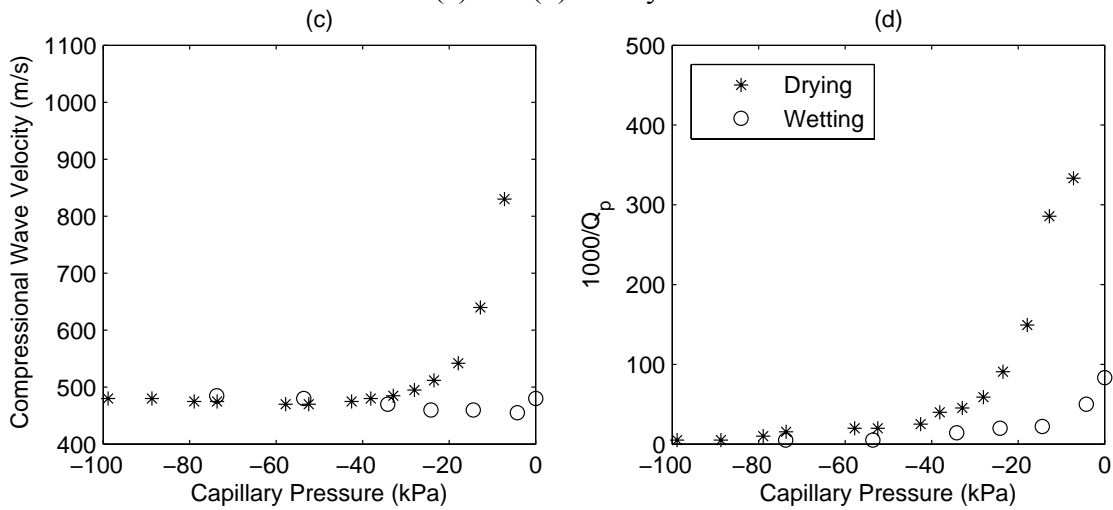


(c) and (d) Heterogeneous soil mixture

Figure 2-9: (a) Shear Wave Velocity (b) Shear Wave Attenuation vs. Moisture Content for Bonny silt and (c) Shear Wave Velocity, (d) Shear Wave Attenuation vs. Moisture Content for Heterogeneous soil mixture.

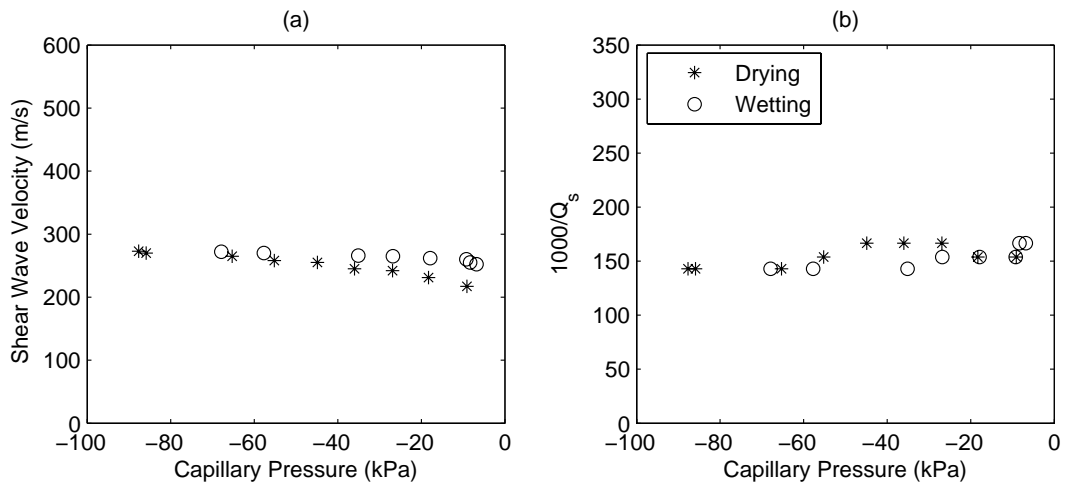


(a) and (b) Bonny Silt

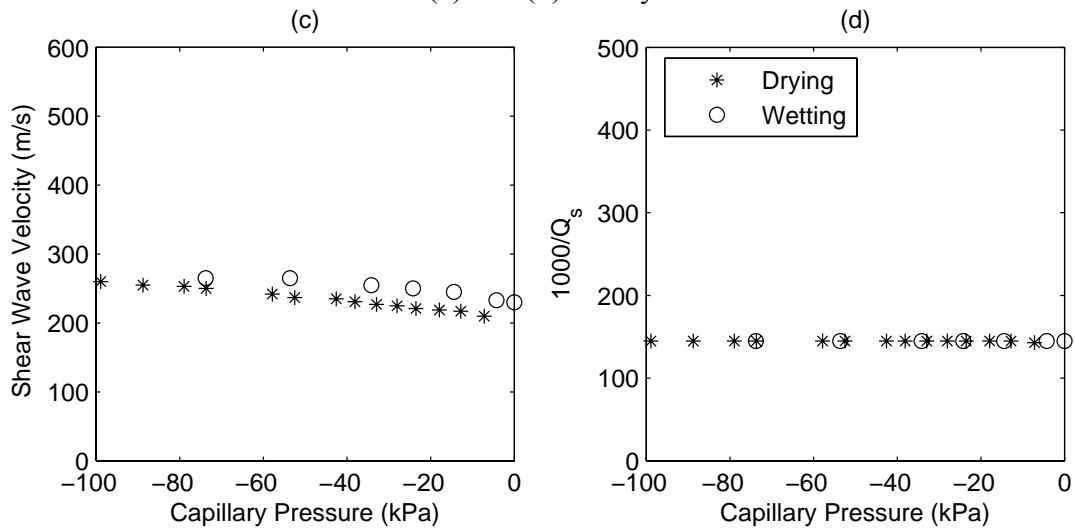


(c) and (d) Heterogeneous soil mixture

Figure 2-10: (a) Compressional Wave Velocity, (b) Compressional Wave Attenuation vs. Capillary Pressure for Bonny Silt and (c) Compressional Wave Velocity, (d) Compressional Wave Attenuation vs. Capillary Pressure for Heterogeneous soil mixture.



(a) and (b) Bonny Silt



(c) and (d) Heterogeneous soil mixture

Figure 2-11: (a) Shear Wave Velocity (b) Shear Wave Attenuation vs. Capillary Pressure for Bonny silt and (c) Shear Wave Velocity (d) Shear Wave Attenuation vs. Capillary Pressure for Heterogeneous soil mixture.

3. INTERPRETATION OF COMPRESSIONAL AND SHEAR WAVES IN LABORATORY UNSATURATED SOIL SPECIMENS USING A FORWARD MODELING TECHNIQUE

Lindsay A. George¹ and Mandar M. Dewoolkar¹

¹School of Engineering, Univ. of Vermont, 33 Colchester Ave., Burlington, VT 05401.

Submitted for publication to Geotechnical Testing Journal on November 10, 2008.

Abstract:

Determining the acoustic velocity and attenuation from low frequency waveforms collected in soils with piezoceramic transducers presents a challenge. The received waves may be weak and contaminated by noise or boundary effects. A number of methods have been suggested for determining the velocity by choosing the first arrival of the wave. These methods give variable results and have been criticized in the literature. Methods for determining the attenuation of a waveform have also been regarded as subjective and unstable. A forward modeling technique using a one-dimensional wave propagation model is presented. This technique was used to determine acoustic (compressional and shear wave) velocities and associated attenuations from waveforms collected in laboratory sized unsaturated soil specimens during a drainage experiment. The results of the forward modeling technique are compared with more traditional methods. It is shown that the forward modeling technique removes the subjectivity of the traditional methods

and is capable of determining both the acoustic velocity and attenuation simultaneously. The validity of the one-dimensional model was evaluated by comparing the results with those from a two-dimensional model. The two-dimensional model provided a marginally improved simulation of received waveforms indicating that the one-dimensional model was adequate, especially because it is simple and computationally efficient in comparison to the two-dimensional model.

Keywords:

Acoustic Velocity, Acoustic Attenuation, Compressional Waves, Shear Waves, Laboratory Acoustics, Spectral Ratios, First Arrival, low frequency acoustics, forward modeling, one dimensional wave propagation model.

3.1 Introduction

Acoustical characterization of geomaterials has become a popular method of nondestructive evaluation in the field as well as in the laboratory. In recent years, bender elements and flat piezoceramic transducers have found increasing use in characterizing soils as laboratory sized specimens at the element level, as well as in physical models. These transducers are often used to generate low-strain shear waves, and sometimes to generate compressional waves in soil specimens to determine their moduli. Attenuation of these waves is also desired, however, often less frequently than the velocities.

It is challenging to determine the acoustic velocity and attenuation from the collected low frequency waveforms that may be contaminated by noise or boundary effects; and therefore, it is a topic of some debate. A number of methods have been suggested for choosing the first arrival of the wave, which is used to determine the acoustic velocity (Blewett et al. 1999; Jovicic et al. 1996; Mohsin and Airey 2003; Viggiani and Atkinson 1995). These methods have been criticized (Arulnathan et al. 1998; Lee and Santamarina 2005), generally due to near field effects that may arise when collecting low frequency acoustic waves on small soil samples. Traditionally the attenuation of a waveform collected using a pulse transmission technique is determined by comparing the frequency spectra of a reference wave with known attenuation to the wave of interest using a method known as Spectral Ratios (Toksoz et al. 1979). This method has also received criticism for its instability, unreliability and subjectivity (Pan 1998; Sams and Goldberg

1990). It has been suggested that several methods should be utilized in determining both the velocity and attenuation to obtain reliable results (Badri and Mooney 1987). Forward modeling techniques have been suggested as a reliable, yet potentially time consuming alternative to the above methods (Arroyo et al. 2006; Cheng and Toksoz 1981; Lee and Santamarina 2005; Sams and Goldberg 1990).

In this paper, a forward modeling technique is used with a one dimensional linearly elastic wave propagation model to analyze compressional and shear waveforms collected through partially saturated soils at a frequency of 20 kHz. The waves were collected in the radial direction through a cylindrical laboratory sample with a diameter and height of approximately 10 cm. The sample was confined under pressure in a rubber Viton[®] semi-flexible membrane with the acoustic transmitter and receiver attached to it. The sample was initially saturated and acoustic measurements were taken at intervals during drainage of the sample.

First, traditional techniques of determining both velocity and attenuation will be introduced, and then the results using these methods to analyze the experimental waveforms will be compared to those obtained using forward modeling. Also, the validity of the one dimensional model is evaluated by comparing its results against a two dimensional wave propagation model.

3.2 Background

3.2.1 Analysis Methods for Determining Velocity

The velocity of an acoustic wave is defined by the travel distance divided by the travel time. The travel distance is a relatively straightforward calculation given an appropriate experimental set up. The travel time on the other hand is more difficult to determine. Examples of a source wave and received wave are shown in Figure 3-1. In the geotechnical engineering field, more attention has been paid to determining the velocity of the shear wave, generally using bender elements. The techniques developed for the analysis of shear waves can be directly used to analyze compressional waves.

A common method of determining the travel time is to manually pick the first arrival of the wave to determine the velocity (Jovicic et al. 1996). Manually picking the first arrival of the wave can be subjective, given high noise to signal ratios or waves distorted by near field effects, but it is the most commonly used method of determining acoustic velocity in the geotechnical engineering field (Alramahi et al. 2008; Brignoli et al. 1996; Lu et al. 2004; Tsukamoto et al. 2002). Deciding which point to choose as a first arrival has been questioned (Lee and Santamarina 2005). Figure 3-2 shows the four points (a-d) which have been suggested as first arrivals; the first deflection (a), the first maxima (b), the first zero crossing (c) or the first major peak (d). When choosing a first arrival point, the travel time is calculated by also choosing the corresponding point on the source function. The time between the two corresponding points is considered the travel time between the source and the receiver. The choice of points to use as a first arrival can depend on the

shape of the source function. The travel time must also be adjusted to account for any material between the source and the receiver that is not the sample. The apparatus that was used to collect this data included titanium heads placed between the transducers and the sample. The acoustic velocity and the thickness of the titanium is known, therefore the travel time through the titanium can be calculated and subtracted from the travel time through the entire set up to obtain the travel time through the soil sample.

Arulnathan et al (1998) showed that the above methods of determining travel time were unreliable since the first arrival of the wave may be masked by near field effects. Brignoli et al (1996) also showed that near field effects need to be considered and the design of the experimental apparatus, as well as the source function and frequency need to be investigated closely before using a manual picking method. Other methods have been suggested, but are not utilized as frequently as manual first arrival picking methods. Alternative methods include analyzing the frequency domain of the waveform to determine the travel time (Blewett et al. 1999; Viggiani and Atkinson 1995) and using the peak of the cross – correlation between the entire source and received waveform (Mohsin and Airey 2003) to determine the arrival time.

3.2.2 Analysis Methods for Determining Attenuation

The attenuation of compressional waves through soils is an area of growing interest. The mechanisms of compressional wave attenuation in unconsolidated porous media are not

well understood. Researchers believe that they may be able to link the material, mechanical, and hydraulic properties of soils to these mechanisms, such as local flow created by heterogeneities (Wei and Dewoolkar 2006).

Attenuation is defined as “the reduction in amplitude and intensity of a signal with respect to distance traveled through a medium. Attenuation can also be understood to be the opposite of amplification.” (Zagzebski 1996) Attenuation is typically reported in values of the attenuation coefficient (α) or the inverse of the quality factor (Q^{-1}), and measured in terms of the quality factor (Q).

The Spectral ratios method appears to be the most popular method for determining attenuation from measured waveforms. The Fourier amplitude of waveforms collected through two different samples of identical geometry using the same source and receiver are compared in this method. By using two waveforms collected on the same geometry and with the same equipment, the influence of spreading and reflections on the attenuation due to geometry and equipment is eliminated. One sample, the reference sample, is a material of known Q , preferably of very low attenuation or infinite Q , and the other sample is the sample of interest. Q can be determined from the slope of the line fitted to the natural log of the ratio of the Fourier amplitudes of the two samples versus frequency. The method is based on the following equations as explained by Toksoz et al (Toksoz et al. 1979).

The amplitude of the reference (subscript 1) and the sample wave (subscript 2) can be expressed as

$$A_1(f) = G_1(x)e^{-\alpha_1(f)x}e^{i(2\pi ft - k_1x)} \quad (1)$$

$$A_2(f) = G_2(x)e^{-\alpha_2(f)x}e^{i(2\pi ft - k_2x)} \quad (2)$$

where A = amplitude, f = frequency, x = distance, k = wave number, v = velocity, $G(x)$ is a geometric factor specific to the apparatus, and $\alpha(f)$ = the frequency dependent attenuation coefficient, which is assumed to be related to frequency linearly, and can be written as,

$$\alpha(f) = \gamma \cdot f, \quad (3)$$

where γ is related to the quality factor Q as

$$Q = \frac{\pi}{\gamma \cdot v}. \quad (4)$$

If the reference and the sample waveform are collected using the same apparatus, the geometric factors are frequency-independent scale factors. If the ratio is taken between the two Fourier amplitudes, the following equation results

$$\frac{A_1}{A_2} = \frac{G_1}{G_2} e^{-(\gamma_1 - \gamma_2)fx}, \quad (5)$$

where x = sample length. The above equation can also be written as

$$\ln\left(\frac{A_1}{A_2}\right) = (\gamma_2 - \gamma_1)xf + \ln\left(\frac{G_1}{G_2}\right). \quad (6)$$

Using equation (6), $(\gamma_2 - \gamma_1)$ can be found from the slope of the natural logarithm of the ratio of the amplitudes versus frequency. If the attenuation of the reference sample is known, the attenuation of the sample of interest can be found using equation (4).

This method is based on two key assumptions. The attenuation coefficient (α) is assumed to be a linear function of frequency (Knopoff 1964), and the geometric factors, which include spreading and reflections, for each sample have the same frequency dependence. Sams and Goldberg (1990) show evidence that these two assumptions may not be true, and suggest that forward modeling is a superior technique. It is also necessary to window the linear portion of the relationship, which can introduce uncertainty (Sams and Goldberg 1990).

The Spectral ratios method requires that a reference waveform has been obtained using the same equipment that is used to collect the sample waveforms. This reference waveform is collected through a material of known attenuation with an acoustic impedance similar to that of the measured sample. The acoustic impedance is a measure of the materials resistance to pass acoustic waves, and is defined as the product of the acoustic velocity and density. Aluminum is generally used as a reference for rocks because the impedance is 8.170×10^5 gm/cm²-s and it has a Q factor of about 150,000 (Zamanek and Rudnick 1961). Saturated soil has an approximate impedance of 1 to 3×10^5 gm/cm²-s (Hamilton 1970), and an appropriate reference material would have a similar impedance and infinite attenuation. Materials with such a low impedance include

wood (specifically softwoods, such as pine), paraffin or some rubbers. These types of materials are known to have damping effects on acoustics; in other words, they have low Q values. Another option is to use a material of known attenuation, not necessarily infinite Q. Therefore, for this analysis, the reference sample has been chosen to be the most unsaturated sample, which had the highest modeled Q value equal to 20. It is assumed that the modeled Q is the actual or known Q value.

Subjectivity enters the spectral ratios method in three areas; windowing, tapering and choosing the linear portion of the attenuation versus frequency plot. The waveform is windowed so that contamination from lower velocity arrivals is eliminated. The start and length of the window for both the reference and the sample waveform are chosen. One may also choose to use to taper the data contained in the window. The choice of tapering function and the percentage of the data tapered is also a decision that needs to be made which can affect the results. As mentioned previously, one assumption of spectral ratios is that a linear relationship exists between the attenuation coefficient and frequency. This is only true for a range of frequencies; this range must also be chosen.

The following example has been prepared to demonstrate the spectral ratios method and how this subjectivity can affect the determination of the quality factor (Q). The portion of each waveform which has been windowed is shown in Figures 3-3 (a) and (b) within the rectangles. Figure 3-3 (c) is the corresponding Fourier amplitude of the windowed waveforms, the reference waveform is dashed and the sample waveform is dotted. Figure

3(d) shows the logarithm of the ratio of the amplitudes versus frequency. The chosen frequency range of the linear portion is also shown within the rectangle in Figure 3(d). The linear regression of the chosen portion is shown in Figure 3(e). A 10 % cosine taper, as shown in Figure 3-4, was chosen as a taper function of the windowed waveforms for this example. The value of Q which was obtained with this set of parameters was 3.56.

Table 3-1 presents the possible variation in Q if the window length is varied for the example considered in Figure 3-3. The start time of the window was kept constant. The first row in Table 1 represents the window length shown in Figures 3(a) and (c), which is 1,902 to 2,961 microseconds for the reference waveform, and 1,395 to 2,155 microseconds for the sample waveform. The window of each waveform was then lengthened by 50 – 250 microseconds. The second column of Table 3-1 lists results obtained when the frequency range of the linear portion of the attenuation versus frequency plot is fixed, and corresponds to the window shown in Figure 3(d). The third column in Table 3-1 lists the Q values obtained by visually choosing the frequency range of the linear portion of the attenuation versus frequency plot for each trial. This illustrates that the determination of Q depends both on the user's decision of the frequency range and the window length.

Table 3-2 presents the variation in Q obtained by changing the percent taper of a cosine taper function. Again, the frequency range of the linear portion of the attenuation versus frequency plot is fixed in the second column and visually chosen for each trial in the third

column. Each row represents a percentage of the window which is tapered, from 10% to 50%. Table 3-2 illustrates that the value of Q is influenced by both the taper function, and again, the user's decision of the frequency range.

Overall, this example shows that a value of attenuation calculated with the spectral ratios method depends on the chosen windowing length, window tapering and the frequency range of linear regression. For the example considered the calculated value of Q is 3.56, but could range from 2.44 to 5.20 depending on the window length, etc., as illustrated in Tables 3-1 and 3-2. Attenuation is generally reported as an inverse of the quality factor, depending on the range of values it is also multiplied by a factor. In this case the attenuations are reported as $100/Q$. This amount of variability is equivalent to up to 67% in the value of $100/Q$.

3.2.3 Forward Modeling Technique

Forward modeling techniques are generally used in the field of geophysics for analyzing surface and borehole waves, where problem geometries are typically complex (Cheng and Toksoz 1981). Recently, the application of forward modeling has been extended to laboratory sized samples. For example, Lee and Santamarina (Lee and Santamarina 2005) suggested a signal matching technique, which utilizes an analytical solution of wave motion within an elastic medium. Arroyo et al. (2006) used a three dimensional, finite

difference model to simulate shear wave propagation through a cylindrical soil sample with bender elements to explain distortion of the measured wave due to sample size.

For this study the computer program, Taffy, was used to simulate the compressional and shear waveforms for the purpose of the forward modeling technique. Taffy was developed by New England Research, Inc, which has generously consented to release the source code to the public domain. The program models the media as a one dimensional stack of elastic materials. The transducer stacks used to collect the waves consist of an absorptive backing, three layers of piezo-ceramic (PZT) material, and a titanium head which is in contact with the soil sample. The numerical model included the appropriate thickness of all of these layers in the simulation. The material properties used for each of these materials are listed in Table 3-3, and a schematic of the transducer stack is depicted in Figure 3-5. The properties for the backing, PZT and titanium are standard, and the density of the soil was measured. The source and receiver stacks consist of the same layers.

Taffy computes the linear elastic time-response of the one-dimensional stack of homogeneous, viscoelastic layers. It can account for the generation of elastic waves by any combination of piezoelectric elements or direct stress discontinuities in the stack. It detects and reports vibrations in the stack using any combination of stress, displacement, and piezoelectric sensors in the stack.

Taffy is built around a direct propagator-matrix solution for the elastic equations of motion for a particular frequency in which the stacked homogeneous layers are allowed to have complex elastic parameters. The current code computes the elastic parameters in each layer from a standard geophysical model for a band-limited, constant-Q material in the high-Q limit (Aki and Richards 1980). Table 3-3 shows the range of frequencies for which Q is considered constant, “f low” is the lower limit, “f high” is the upper limit and “f ref” is the target frequency.

To implement the forward modeling technique, a library of waveforms was created within the expected range of velocities and attenuations using Taffy. A MATLAB program was written which searches through the library of possible waveforms and minimizes the root-mean-square-error between the measured and modeled waveforms over a specified time range. In this study we were able to obtain a good match between the modeled and measured waveform over the first quarter cycle, which is considered sufficient to quantify the velocity and attenuation of the sample. An example is shown in Figure 3-6, in which the modeled waveform that minimizes the error is plotted against the measured waveform and is visually inspected to confirm that a good match has been obtained. The velocity and attenuation of the modeled waveform that best matches the measured waveform is then considered the velocity and attenuation of the experimental waveform.

In the following, the forward modeling technique is compared to the methods presented earlier for determining the velocity and attenuation of a measured waveform. The first arrival of the waves was chosen by picking features (a-d) of the waveform shown in Figure 3-2. This first arrival was compared to the arrival time of the similar feature on the source wave to determine the travel time. The Kelly wavelet was chosen as a source function for this work because of its numerical stability in modeling, this does make choosing arrivals a bit more difficult, since the arrival of the source wave is not well defined. The attenuation of the experimental waveforms was also determined using the spectral ratios methods. The reference waveform was chosen as the least attenuated or highest Q sample of the set. In this case, the least attenuated sample has a Q of 20, as determined by the forward modeling technique; this was included in equations (4) and (6) to determine the Q of the sample using spectral ratios.

3.3 Results

Figures 3-7 (a) and (b) compare the compressional and shear wave velocities obtained by manually picking the first arrival of the wave to those obtained by using the one dimensional forward modeling. The data were collected during a drainage experiment of a silt specimen. The velocity values obtained by manually picking each point (a) – (d) are plotted separately in Figure 3-7. To determine the travel time, the time between similar features of the source wave and the received wave was found for each of the four points shown in Figure 3-2, and the travel time through the titanium heads was subtracted to

find the travel time through the soil only. There is generally good agreement between the two methods in terms of the trend of velocity versus saturation. In this case, manual picking tends to overestimate both the compressional and shear wave velocities. This is probably due to the emergent nature of the Kelly wavelet, and the choice of the “zero time”. The compressional wave data has the greatest variation in velocities, and the larger variations appear at higher saturations. This also coincides with the more attenuated waves.

Figure 3-8 shows the standard deviation in manually picked velocities and the attenuation of the wave. The velocities determined by manually picking appear to be more varied at higher attenuations. This is probably due to the velocity dispersion created by attenuation. The wave tends to spread as it is attenuated, spreading the first and second peak of the waveform, creating a larger difference in the velocities obtained by picking the first arrival and the second peak, points (a) and (d), respectively.

The variability in the shear wave velocities are lower than that seen in the compressional wave velocities. This can be seen in Figure 3-8, where the standard deviation in velocity is plotted versus the attenuation. The standard deviation of the four velocity picking methods is lower than any of the standard deviations in compressional wave velocity for all of the waves analyzed. Figure 3-8 also shows that the attenuations of all analyzed shear waves are almost equal ($100/Q = 11.1$ to 12.3).

The attenuation of each wave is determined using spectral ratios and compared to those attenuations obtained with the forward modeling. Figure 3-9 presents these data. It was shown previously that depending on the parameters chosen in determining Q using spectral ratios, an error of approximately 67% could be imposed on the value of $100/Q$. The Q values presented in Figure 3-8 represent values obtained by using the spectral ratios method in the manner in which it is commonly used. That is, the windows shown in the example (Figure 3-3) are chosen by the user for each waveform analyzed. A 10% cosine taper was also chosen for this analysis.

3.4 Verification with the two-dimensional model

A two dimensional finite difference model originally intended for simulating borehole wave propagation in an anisotropic, viscoelastic formation (Cheng et al. 1995) was used to examine if the one-dimensional model, Taffy, was sufficiently accurate to represent the involved geometry. The two-dimensional model represents the problem with a horizontal slice through the transducer stack of infinite height. The model includes the transducer stacks, the soil and the rubber jacket used to confine the sample. The confining fluid is also considered in the model. The two-dimensional model was built using the same material properties as in the one dimensional model, with the addition of the known properties for the rubber jacket and the air confinement of the sample.

The two-dimensional model approximates the first order time derivative using a second order finite difference operator, and the first order space derivatives are approximated using a fourth order finite difference operator (Cheng et al. 1995). The wave equations are written with 9 elastic constants to allow for orthorhombic anisotropy in the media. The wave equation is formulated in velocity and stress, and discretized on a staggered grid (Krasovec 2004). Inclusion of attenuation in the model follows the procedure developed by Emmerich and Korn (1987). The viscoelastic modulus is approximated with a low-order rational function of frequency in order to incorporate attenuation in the time-domain computations of wave propagation. Relaxation frequencies are chosen to be logarithmically equidistant in the frequency band of interest, and the weight factors are determined by simple numerical curve fitting to an arbitrary Q law.

The results of the one-dimensional and two-dimensional models are compared to a measured waveform in Figure 3-10, as an example. A good match exists between the one-dimensional model and the experimental results over the first quarter cycle of the waveform, that is, up to the first peak. The two-dimensional model is able to capture more than a half cycle of the measured waveform. The same modeling parameters were used in the one and two-dimensional model, and a slightly better match was obtained by adding a dimension. The one-dimensional model with attenuation is run in approximately five seconds on a Pentium 4 2.8 GHz processor, as compared to the run time of the two-dimensional model with attenuation that is approximately ten hours on the same computer. Therefore, the one-dimensional model is able to capture the properties of the

material used in this study satisfactorily. The two-dimensional model does not increase the accuracy of the velocity or attenuation prediction but requires significantly more computational time.

3.5 Conclusions

A forward modeling technique was used to interpret compressional and shear waveforms collected on a silt sample during a drainage experiment. The acoustic wave velocities and attenuations found using this method were compared to the values obtained using more traditional methods, i.e. “manually-picking” arrival times for velocity and spectral ratios for attenuation. A one dimensional model was used in this forward modeling technique and it was shown that this model reduced computational time and provided essentially same results as a two dimensional model. The one dimensional model was able to capture the wave behavior over the first quarter cycle of the received wave. This means that the model was able to capture the arrival and the amplitude of the first peak, which is considered sufficient to quantify the velocity and attenuation of the sample. This forward modeling technique provides less subjective results than the traditional methods, and is able to find both the velocity and attenuation of the wave simultaneously.

3.6 Acknowledgements

The study presented here was supported by Vermont Experimental Program to Stimulate Competitive Research (VT EPSCoR), (grant EPS 0236976) and the Vermont Space Grant Consortium through funding from NASA (grant NNG05GH16H). The authors are grateful to Dr. Gregory Boitnott and Martin Smith, of New England Research, Inc. for collaboration on acoustic data collection and analysis.

3.7 References

- Aki, K., and Richards, P. G. (1980). *Quantitative Seismology Theory and Methods*, W. H. Freeman and Company, San Francisco.
- Aramahi, B., Alshibli, K., Fratta, D., and Trautwein, S. J. (2008). "A Suction-Controlled Apparatus for the Measurement of P and S-Wave Velocity in Soils." *Geotechnical Testing Journal*, 31(1), 12-23.
- Arroyo, M., Wood, D. M., Greening, P. D., Medina, L., and Rio, J. (2006). "Effects of sample size on bender-based axial G_0 measurements." *Geotechnique*, 56(1), 39-52.
- Arulnathan, R., Boulanger, R. W., and Riemer, M. F. (1998). "Analysis of bender element tests." *Geotechnical Testing Journal*, 21(2), 120-131.
- Badri, M., and Mooney, H. M. (1987). "Q measurements from compressional seismic waves in unconsolidated sediments." *Geophysics*, 52(6), 772-784.
- Blewett, J., Blewett, I. J., and Woodward, P. K. (1999). "Measurement of shear-wave velocity using phase-sensitive detection techniques." *Canadian Geotechnical Journal*, 36, 934-939.
- Brignoli, E. G. M., Gotti, M., and Stokoe, K. H. (1996). "Measurement of Shear Waves in Laboratory Specimens by Means of Piezoelectric Transducers." *Geotechnical Testing Journal*, 19(4), 384-397.
- Cheng, C. H., and Toksoz, M. N. (1981). "Elastic wave propagation in a fluid-filled borehole and synthetic acoustic logs." *Geophysics*, 46(7), 1042-1053.

- Cheng, N., Cheng, C. H., and Toksoz, M. N. (1995). "Borehole wave propagation in three dimensions." *Journal of Acoustic Society of America*, 97(6), 3483-3493.
- Emmerich, H. a. K., M. . (1987). "Incorporation of attenuation into time-domain computations of seismic wave fields." *Geophysics*, 52(9), 1252-1264.
- Hamilton, E. L. (1970). "Reflection coefficients and bottom losses at normal incidence computed from pacific sediment properties." *Geophysics*, 35(6), 995-1004.
- Jovicic, V., Coop, M. R., and Simic, M. (1996). "Objective criteria for determining Gmax from bender element tests." *Geotechnique*, 46(2), 357-362.
- Knopoff, L. (1964). "Q." *Reviews of Geophysics*, 2(4), 625-660.
- Krasovec, M. K., D. R. Burns, M. E. Willis, S. Chi, and M. N. Toksöz (2004). "3-D Finite Difference Modeling for Borehole and Reservoir Application." In MIT-ERL Reservoir Delineation Consortium Report.
- Lee, J., and Santamarina, J. C. (2005). "Bender Elements: Performance and Signal Interpretation " *Journal of Geotechnical and Geoenvironmental Engineering*, 131(9), 1063-1069.
- Lu, Z., Hickey, C. J., and Sabatier, J. M. (2004). "Effects of Compaction on the Acoustic Velocity in Soils." *Soil Science of America Journal*, 68, 7-16.
- Mohsin, M. K., and Airey, D. W. "Automating Gmax measurements in triaxial apparatus." *Lyon '03 International symposium on deformation behavior of Geomaterials*.
- Pan, C. (1998). "Spectral ringing suppression and optimal windowing for attenuation and Q measurements." *Geophysics*, 63(2), 632-636.

- Sams, M., and Goldberg, D. "Short Note: The validity of Q estimates from borehole data using spectral ratios." *Geophysics*, 97-101.
- Toksoz, M. N., Johnston, D. H., and Timurr, A. (1979). "Attenuation of seismic waves in dry and saturated rocks: 1. Laboratory measurements." *Geophysics*, 44(4), 681-690.
- Tsukamoto, Y., Ishihara, K., Nakazawa, H., Kamada, K., and Huang, Y. (2002). "Resistance of partly saturated sand to liquefaction with reference to longitudinal and shear wave velocities." *Soils and Foundations*, 42(6), 93-104.
- Viggiani, G., and Atkinson, J. H. (1995). "Interpretation of bender element tests." *Geotechnique*, 45(1), 149-154.
- Wei, C., and Dewoolkar, M. "A Continuum Theory of Nonequilibrium Two-Phase Flow through Porous Media with Capillary Relaxation." *Advances in Unsaturated Soil, Seepage, and Environmental Geotechnics, Proceedings of Sessions of GeoShanghai, Shanghai, 6-8 June 2006*, Shanghai, 246-254.
- Zagzebski, J. A. (1996). *Essentials of Ultrasound Physics*, Mosby Inc.
- Zamanek, J., and Rudnick, J. (1961). "Attenuation and dispersion of elastic waves in a cylindrical bar." *Journal of Acoustic Society of America*, 33, 1283-1288.

Table 3-1: Variation in Quality Factor (Q) with window length

Window length	Quality Factor (Q)	
	Fixed ² linear range	Chosen ³ linear range
Picked ¹	3.56	3.43
Picked ¹ + 50	3.63	3.22
Picked ¹ + 100	4.33	3.31
Picked ¹ + 150	5.20	2.95
Picked ¹ + 200	5.14	2.52
Picked ¹ + 250	4.88	2.44

¹ Picked window length = 1,902 to 2,961 microseconds for the reference waveform, and 1,395 to 2,155 microseconds for the sample waveform.

² The fixed linear frequency range is 7,328 to 36,639 Hz

³ The chosen linear frequency range is visually chosen by the user

Table 3-2: Variation in Quality Factor (Q) with percent of cosine taper

Percent taper ¹	Quality Factor (Q)	
	Fixed ² linear range	Chosen ³ linear range
0	3.47	3.20
0.1	3.56	3.33
0.2	3.74	3.23
0.3	4.05	3.36
0.4	4.47	3.16
0.5	4.75	2.78

1 The percentage of the window which is tapered with a cosine function (see Figure 4).

2 The fixed linear frequency range is 7,328 to 36,639 Hz

3 The chosen linear frequency range is visually chosen by the user

Table 3-3: Properties used in numerical model

	Density (kg/m^3)	Velocity (m/s)	Attenuation (Q)	f-ref ¹ (Hz)	f-low ¹ (Hz)	f-high ¹ (Hz)
Backing	10,100	1,374	4.6	1.00E+05	100	1.00E+06
PZT	7,710	3,950	75	1.00E+05	100	1.00E+06
Titanium	4,500	6,070	500	1.00E+05	100	1.00E+06
Soil Sample	1,800	*	*	1.00E+05	100	1.00E+06

* Velocity and attenuation of soil sample are changed to match the modeled wave with the measured wave.

¹ Frequency range for which Q is considered constant, f-ref is the target frequency, and f-low and f-high are the low and high frequency limits, respectively.

Figure Captions:

Figure 3-1: (a) Input signal Kelly wavelet with center frequency of 20kHz, (b) Example output signal

Figure 3-2: Points to consider as “first arrivals”

Figure 3-3: Example demonstration of the Spectral Ratios method

Figure 3-4: Example of cosine taper

Figure 3-5: A schematic of the transducer stack (not to scale)

Figure 3-6: Measured and modeled waveform example

Figure 3-7: Acoustic Wave Velocities as a function of saturation found using the forward modeling technique and traditional “hand picking” methods

Figure 3-8: Standard Deviation in velocity measurements found using traditional “manual-picking” methods as a function of the attenuation of the wave analyzed

Figure 3-9: Compressional wave attenuation as a function of saturation found using the forward modeling technique and spectral ratios. Significant variation may exist in Q values obtained using the spectral ratio method.

Figure 3-10: Measured and modeled waveforms

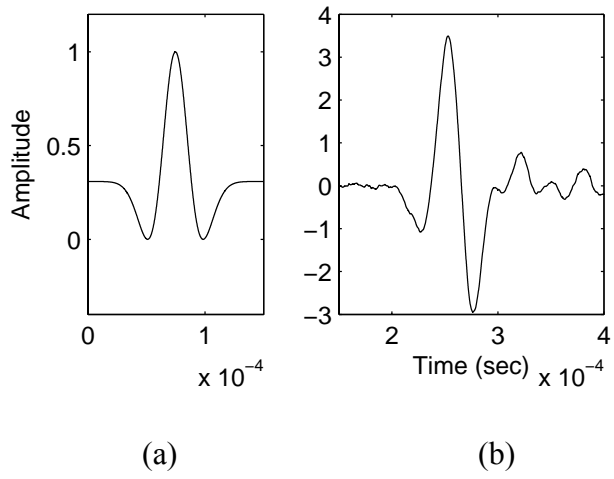


Figure 3-1: (a) Input signal Kelly wavelet with center frequency of 20kHz, (b) Example output signal

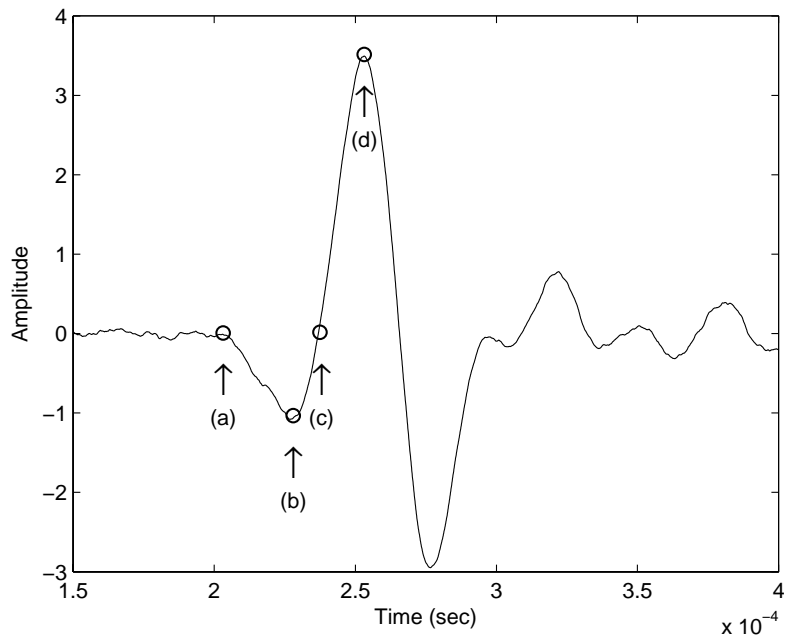


Figure 3-2: Points to consider as “first arrivals”

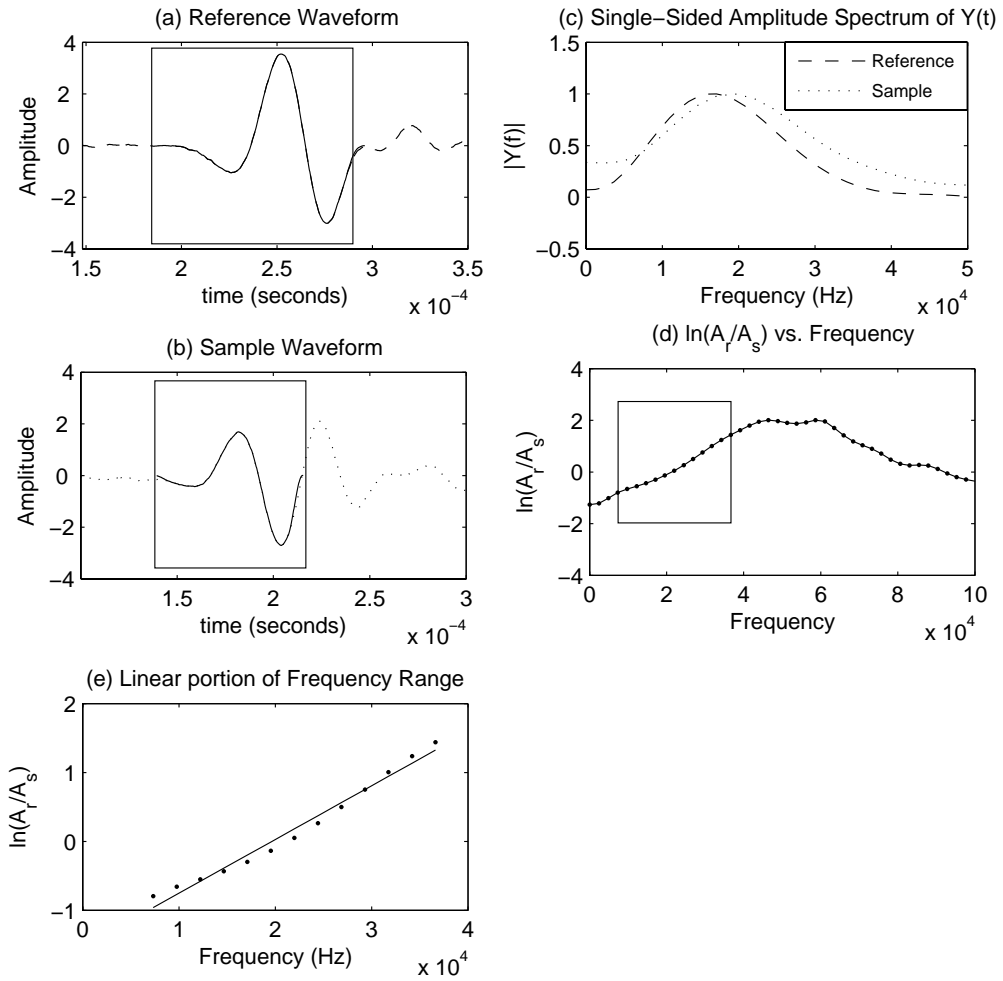


Figure 3-3: Example demonstration of the Spectral Ratios method

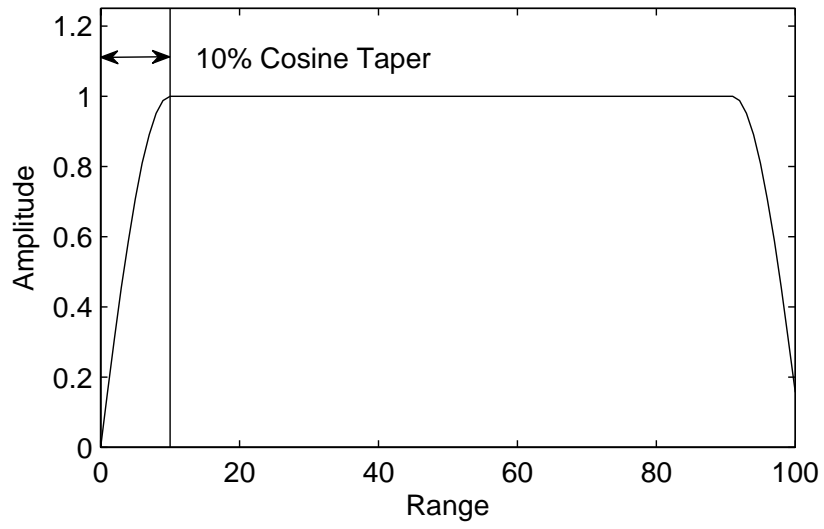


Figure 3-4: Example of cosine taper

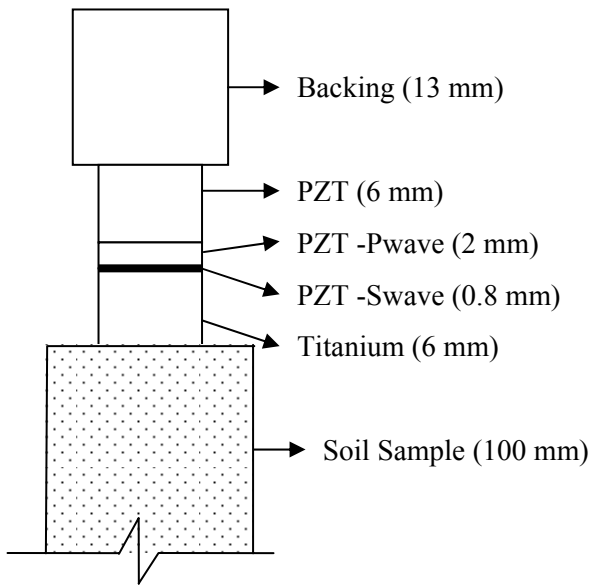


Figure 3-5: A schematic of the transducer stack (not to scale)

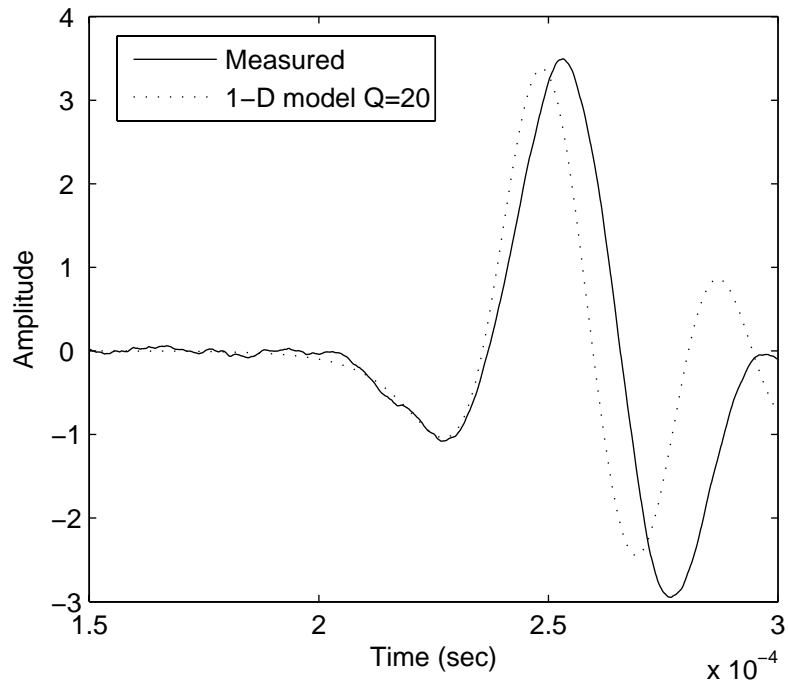
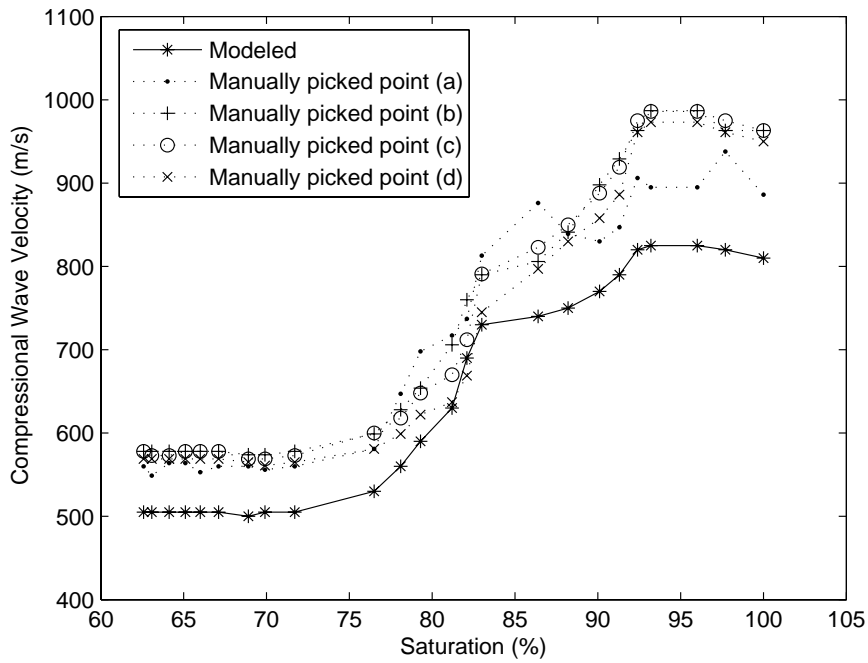
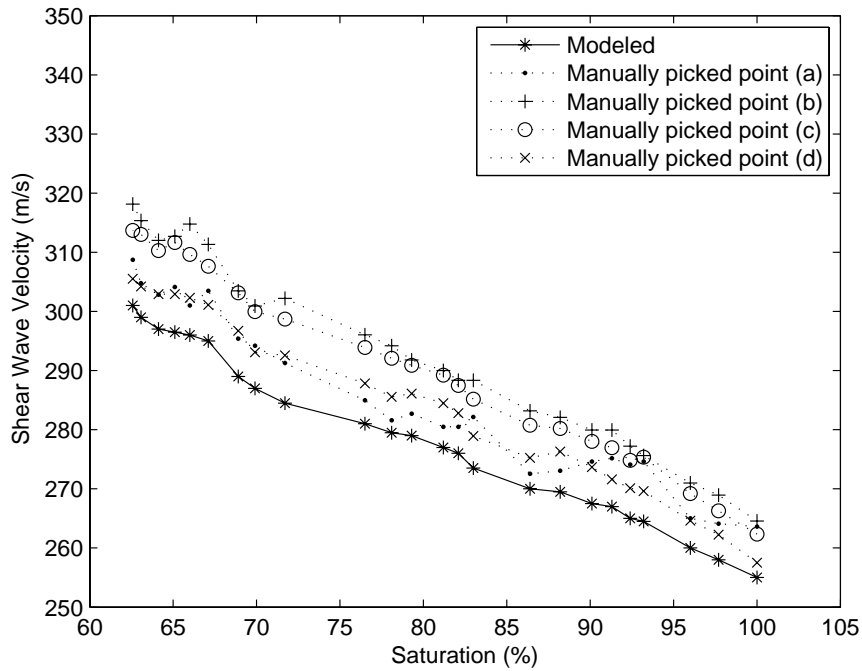


Figure 3-6: Measured and modeled waveform example



(a) Compressional wave velocities



(b) Shear wave velocities

Figure 3-7: Acoustic wave velocities as a function of saturation found using the forward modeling technique and traditional “hand picking” methods

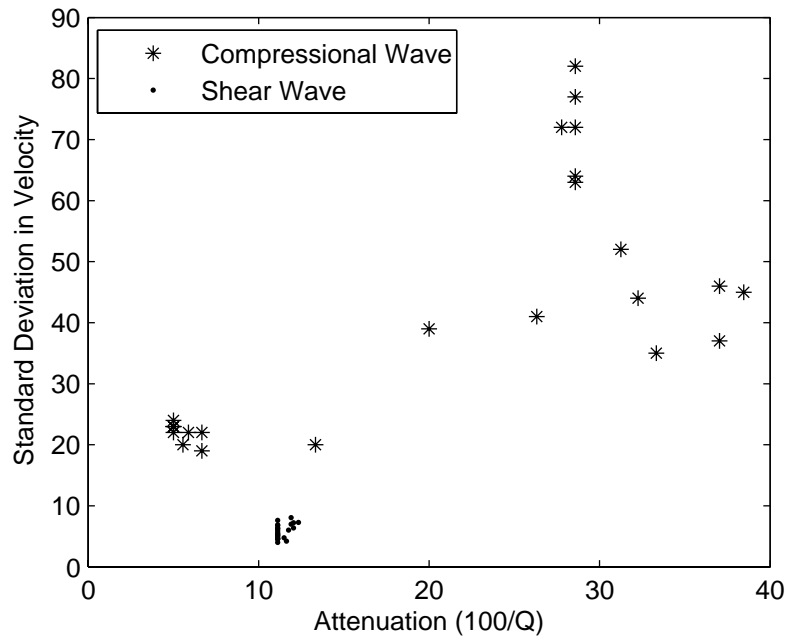


Figure 3-8: Standard Deviation in velocity measurements found using traditional “manual-picking” methods as a function of the attenuation of the wave analyzed

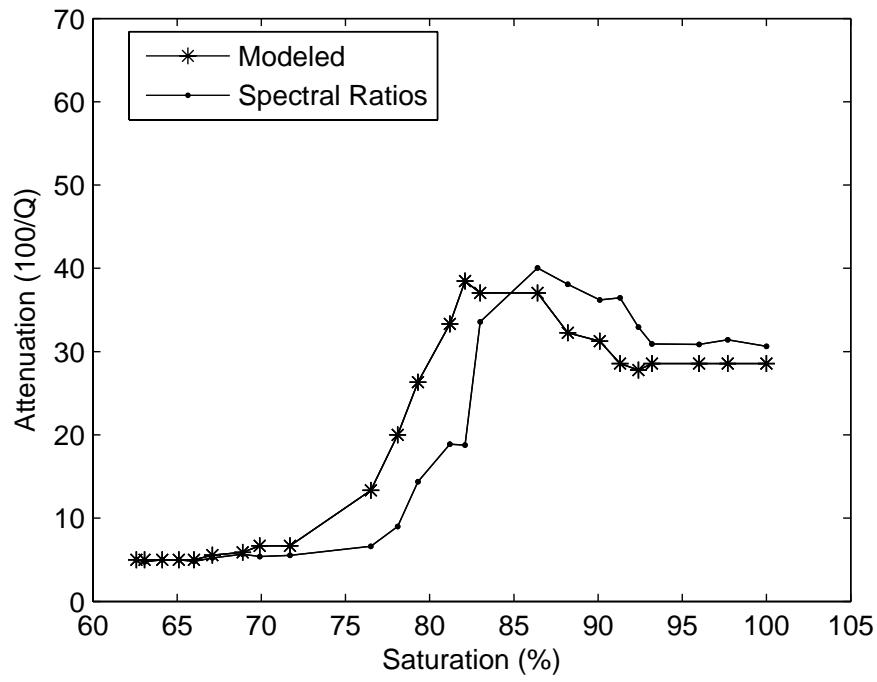


Figure 3-9: Compressional wave attenuation as a function of saturation found using the forward modeling technique and spectral ratios. Significant variation may exist in Q values obtained using the spectral ratio method.

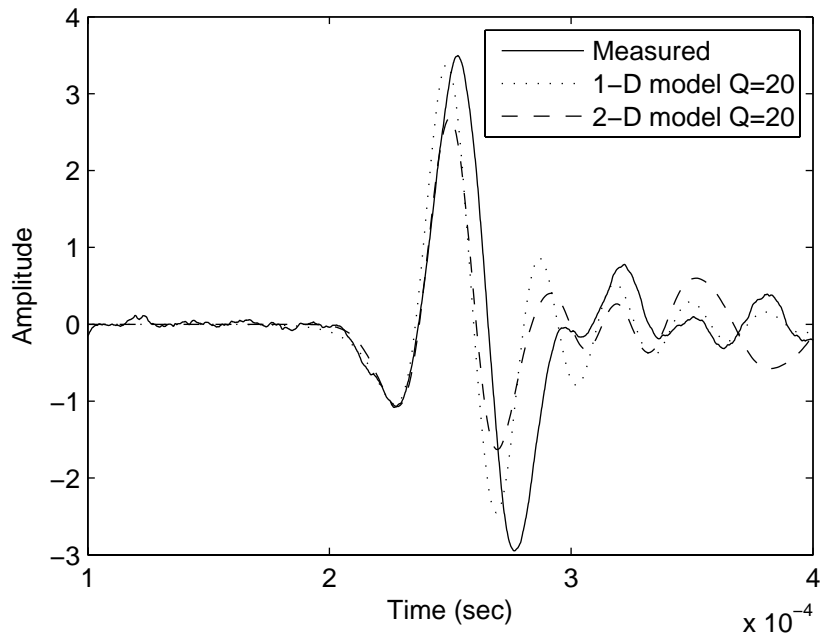


Figure 3-10: Measured and modeled waveform

4. PREDICTION OF CAPILLARY RELAXATION TIME OF UNSATURATED SOILS USING MEASURED ACOUSTIC VELOCITY AND ATTENUATION WITH VISCO-POROELASTIC THEORY

Abstract: Unsaturated and multiphase flow modeling relies on the relationship between the capillary pressure and the level of saturation of the porous media. It has been previously suggested that this relationship may be non-unique and rate dependent and a procedure for quantifying this dynamic relationship was developed by others. This research attempts to experimentally verify this procedure using data from acoustic characterization of unsaturated soil samples. The acoustic data collected shows variation in compressional wave velocity and attenuation with saturation, but the dynamic effects predicted with these acoustic measurements do not sufficiently explain the dynamic behavior seen in the laboratory. This is attributed to other causes of significant attenuation not accounted for in the wave propagation theory that was evaluated.

Keywords: Non-Equilibrium Flow, Dynamic capillary pressure function, capillary relaxation, acoustic properties, unsaturated soils

4.1 Introduction

Unsaturated and multiphase flow modeling relies on the relationship between the capillary pressure and the level of saturation of the porous media. This relationship is known by many names such as the capillary pressure function, pressure-saturation relationship, water retention curve, and soil water characteristic curve. The relationship will be referred to as the capillary pressure function here in. The capillary pressure function is a hydraulic property of the porous media and the fluids. It depends on many factors, including the pore size distribution of the media, the attraction of the fluids to the solids and the interfacial tension between the fluids. For unsaturated soils, the capillary pressure function is defined as the relationship between the differential pressure between the water and the air phase, i.e. the capillary pressure and the water saturation *at equilibrium*.

The capillary pressure function can be measured using direct or indirect methods; direct methods can be divided into two general categories, suction control and axis translation methods. All of the direct methods commonly used to experimentally determine the capillary pressure function assume that the soil is at an equilibrium or static state before a point on the function is obtained. Two questions arise from this assumption; first, has equilibrium been achieved, and second, should static properties be applied to model a dynamic phenomenon such as groundwater flow? Numerous studies have shown experimentally that the capillary pressure function is indeed rate dependent (Chen et al.

2007; Constantz 1993; Davidson et al. 1966; Mohamed and Sharma 2007; Schultze et al. 1997; Topp et al. 1967; Vachaud et al. 1972; Wildenchild et al. 2002).

The capillary pressure function can also be measured using indirect methods, such as one-step or multi-step outflow experiments. These experiments determine the static capillary pressure and the hydraulic conductivity functions using a transient test and inverse modeling of Richards' equation. The same inconsistencies arise with these tests which are performed in a transient state, but used to determine a static relationship. O'Carroll et al. showed that the prediction of outflow amounts was inconsistent with the measured amounts unless a dynamic term which varies with saturation was used in the capillary pressure function (O'Carroll et al. 2005).

In order to resolve these inconsistencies, it has been suggested to use a 'dynamic' capillary pressure function which takes into account the dynamic nature of the relationship. The most prevalent existing model for the dynamic capillary pressure function was developed by Hassanizadeh and Gray (1993). The model proposes that the dynamic capillary pressure is equal to the static capillary pressure minus a constant (τ) multiplied by the rate of saturation change. This model is a thermodynamic theory of two phase flow based on a constitutive hypothesis that the Helmholtz free energy functions for the phases and interfaces depend on state variables such as mass, density, temperature, saturation, porosity and interfacial area density, and the solid phase strain tensor. The capillary pressure is defined as the change in the free energy of the system

due to a change in the saturation. The theory suggests that the saturation will redistribute locally in order to restore equilibrium; the coefficient (τ) can be interpreted as a measure of how fast this redistribution will take place. τ is considered a material property which may also be dependent on the level of saturation (Hassanizadeh and Gray 1993). τ has been back calculated from direct measurement of the dynamic capillary pressure function to range from 10^4 to 10^7 kg (m s)⁻¹, but a method to measure τ directly was not developed.

A new model of the dynamic capillary pressure function has recently been developed which expands on Hassanizadeh and Gray's (1993) model to include hereditary effects and a method of quantifying the speed at which the local redistribution of saturation (or pressure) occurs (Wei and Dewoolkar 2006). This speed is quantified by the capillary relaxation time, or the time needed for redistribution to occur, and is measured in the laboratory using low frequency acoustic wave propagation theory as described below. The model is a linear viscoelastic model of nonequilibrium two phase flow. The model accounts for the effect of capillary relaxation based on the continuum theory of mixtures and describes energy dissipation due to fluid flow in terms of both macroscopic and local fluid flow, i.e. capillary relaxation (or local pressure redistribution). Partially saturated porous medium is viewed as the superposition of three phases in continuum theory of mixtures (Wei and Dewoolkar 2006).

Acoustics waves are used to determine the capillary relaxation time of the media, based on a wave propagation theory which takes into account energy dissipation due to local flow (Wei and Muraleetharan 2007). Local flow results from the local heterogeneous distribution of pore fluids (say water). Soils which have been drained from saturated are shown to generally exhibit a heterogeneous distribution of water, or patchy saturation, even if the distribution of pore space is relatively homogenous (Cadoret et al. 1995; Knight and Nolen-Hoeksema 1990). When porous medium is disturbed by an external force such as an acoustic wave, the medium deforms in response to the passing stress wave. This deformation may cause the pressure of the fluid to build up within the pores of the porous media. If the medium is saturated with multiple immiscible fluids this pressure will depend on what type of fluid is occupying the region, or patches of saturation, and the size of the pores within the region. Variations of pressure will exist between fluids and within fluid regions depending on the deformation of the pores within the region. This variation in pressure will result in a pressure gradient across the boundary between the two regions, or within the region. This pressure gradient will cause local fluid flow. This flow may occur across fluid boundaries, or within the fluid itself, possibly causing the boundary to change. This local flow will dissipate the energy of the passing stress wave, causing attenuation and velocity dispersion of the wave.

The size of the regions (e.g. saturation patches) and the wavelength of the acoustic wave will determine the existence and the effect of the local flow on the acoustic measurements. If we consider that the two neighboring regions are occupied by water and

air, as is the case in unsaturated soils, the acoustic wave will cause pressure to build in the water because of the deformation of the pores in the soil. If the period of the wave is long enough, there will be time for the pressure to equilibrate and the water to flow into the region containing air, before the next wave passes. But if the period of the wave is very short, there will not be time for the water to flow and equilibrate before the next wave passes and the pressure is built up again. This will result in the water acting as reinforcement to the matrix, and stiffening the porous media, instead of causing local flow. This also shows that we will see a frequency dependent response to acoustic waves passed through unsaturated soils.

The existence of local flow also depends on the distribution of fluids in the media. It is not seen as dramatically if the moisture is distributed uniformly, even at the same saturation level (Cadoret 1995). When the moisture distribution is uniform over the length of the wave, the pressure distribution is also nearly uniform and local flow does not take place (Carcione, et. al 2003). Also, when a sample has uniformly distributed moisture content, the air phase is interconnected up to a high level of saturation. The relaxation of the air phase then is vanishingly small over the whole range of saturations.

The time that it takes for the patch of fluid (e. g. water or air) to equilibrate is known as the capillary relaxation time; this time can be extracted by analyzing the received waveforms (Wei and Muraleetharan 2007). The capillary relaxation time includes information on the size of the patch of saturation and the dynamic behavior of the

material as a whole. The capillary relaxation time is then included in the model of the dynamic capillary pressure function to quantify the dynamic behavior of the material.

In this paper, an attempt to experimentally verify the theories is presented. Acoustic and hydraulic properties of unsaturated soils were simultaneously measured using a device developed at the University of Vermont. The acoustic waves were analyzed and the capillary relaxation time determined for a range of saturations. Using this information along with the hydraulic properties of the soil and the model of the dynamic capillary pressure function, dynamic capillary pressure functions for a range of rates were predicted. Dynamic pressure functions are then experimentally produced; the results are compared and discussed.

4.2 Theoretical Background

This section briefly summarizes the theoretical background of both the newly developed dynamic capillary pressure function (Wei and Dewoolkar 2006) and wave propagation theory through partially saturated soil which attributes attenuation to local flow (Wei and Muraleetharan 2007). For details of the formulations, readers are referred to Wei and Dewoolkar (2007) and Wei and Muraleetharan (2007).

4.2.1 Dynamic capillary pressure function

Assume that the soils under consideration are *macroscopically* (i.e., at the wavelength scale) isotropic and homogeneous, with an average degree of saturation S_r . Consider an

averaging volume of an unsaturated soil. When subjected to an external disturbance, the dynamic capillary pressures are given by (Wei and Muraleetharan 2007)

$$p^f - p^s = (p^f - p^s)_{eq} + \zeta_f \dot{n}^f, \quad (1)$$

where p^s is the pressure associated with the compression of solid grains (s); p^f is the pressure of a fluid, and $f = w$ (wetting fluid) or n (non-wetting fluid), in the case of unsaturated soil the wetting and non-wetting fluids would be water and air, respectively; $(\)_{eq}$ represents the pressure difference at equilibrium; \dot{n}^f is the changing rate of the fluid volume fraction (n^f); and ζ_f is a material coefficient, which is a function of moisture content.

As far as the flow problem is concerned, it is reasonable to assume that the porosity change is negligible, i.e., $\dot{n}^w + \dot{n}^n \approx 0$. From Eq. (1), it follows that

$$p^n - p^w = (p^n - p^w)_{eq} - \zeta \dot{n}^w, \quad (2)$$

where the material coefficient, $\zeta = \zeta_w + \zeta_n$; the first term in the right-hand side is the *static* matric suction, and it is a function of n^w (equals the specific moisture content θ), i.e.

$$(p^n - p^w)_{eq} = h(\theta), \quad (3)$$

where $h(\theta)$ is the capillary pressure function that can be determined in the laboratory. Eq. (2) is the same as the one derived by Hassanizadeh and Gray (1993). It can be rewritten as

$$p^n - p^w = h(\theta) - \zeta \dot{\theta}. \quad (4)$$

This equation can be cast into the following incremental form

$$\delta(p^n - p^w) = \Theta \delta\theta - \zeta \delta\dot{\theta}, \quad (5)$$

where Θ is a function of θ , and can be related to the soil water capacity $C(\theta)$ by

$$\Theta(\theta) = \frac{dh(\theta)}{d\theta} = \frac{1}{C(\theta)}. \quad (6)$$

Suppose that capillary pressure is suddenly changed by a small amount, i.e., $\delta p_c(t) = \Delta p_c H(t)$, where $H(t)$ is the Heaviside function and Δp_c is a small quantity, due to the viscous effects, the instant change in moisture content is zero, i.e. $\delta\theta(0) = 0$.

Now, Eq. (5) can be solved to yield

$$\delta\theta(t) = \Delta p_c C \left[1 - \exp\left(-\frac{t}{\tau_c}\right) \right] H(t), \quad (7)$$

where $\tau_c (= \zeta C)$ is a function of moisture content. Due to the linear nature of Eq. (5), the moisture content history $\theta(t)$ resulting from any history of capillary pressure $p_c(t)$ can be expressed as

$$\theta(t) = \theta_0 + K * p_c(t), \quad (8)$$

where $K(t, \theta)$ is given by

$$K(t, \theta) = C(\theta) \left[1 - \exp\left(-\frac{t}{\tau_c(\theta)}\right) \right] H(t), \quad (9)$$

and $K * p_c$ is the Stieltjes-type integral of functions $K(t, \theta)$ and $p_c(t)$, and defined by

$$K * p_c(t) = \int_0^t K(t - \tau, \theta) dp_c(\tau) + \sum_i K(t - t_i) [p_c(t_i^+) - p_c(t_i^-)]. \quad (10)$$

Here, function $p_c(t)$ is assumed to have possible discontinuity at $t = t_i$.

The dynamic capillary pressure function given by Eq. (8) includes the rate dependent and hereditary effects of capillarity, and it plays a key role in describing nonequilibrium flow in unsaturated porous media. The only parameter yet to be evaluated is parameter τ_c , the capillary relaxation time. As shown in the next section, τ_c can be determined using acoustical data. Given proper boundary and initial conditions, equation. (8) and the macroscopic equations governing two-phase flow (e.g., the Richards equation) can be solved numerically to describe nonequilibrium flow in unsaturated porous media.

4.2.2 Wave propagation including the effects of local flow

When a stress wave passes through an unsaturated soil in which the moisture is heterogeneously distributed at the mesoscopic scale, local pore pressure gradients are generated and local flow takes place. The local flow induced by a stress wave dissipates wave energy, resulting in intrinsic wave attenuation and velocity dispersion (velocity depending upon frequency). Such acoustical signatures play a key role in determining the characteristics of local flow and dynamic capillarity.

To analyze the acoustical behavior of unsaturated soils (strain $< 10^{-7}$), it is sufficient to consider the linear problem. The linear form of Eq. (1) is

$$\delta p^f - \delta p^s = \Theta_f (\delta n^f + \tau_f \delta \dot{n}^f), \quad (11)$$

where Θ_f ($f = w$ (water), a (air)) is a material parameter and equals the change of pressure difference ($p^f - p^s$) due to a unit change of volume fraction n^f ; $\tau_f = \zeta_f / \Theta_f$.

Parameters Θ_w and Θ_a can be determined using soil water capacity $C(\theta)$ (Wei and Muraleethanan 2006)

$$\Theta_w = (1 - S_r) / C, \quad \Theta_a = S_r / C. \quad (12)$$

Noting that $\dot{n}^w + \dot{n}^a \approx 0$, Eq. (11) can be used to derive

$$\delta(p^a - p^w) = (\delta\theta - \tau_c \delta\dot{\theta}) / C, \quad (13)$$

where

$$\tau_c = C\zeta = (1 - S_r)\tau_w + S_r\tau_a. \quad (14)$$

Equation (13) is just another form of Eq. (5). τ_f ($f = w, a$) is equal to the characteristic time of meso-scale flow of f -fluid resulting from local saturation heterogeneity. In general, τ_c is a function of the moisture content (θ or S_r). It is clear that τ_c has two contributions, which are due to meso-scale water and air flow, respectively. In the range of low to moderate saturation, air phase is interconnected within the pore space. In this case, due to high mobility of air, $\tau_a = 0$ and the effect of meso-scale air flow is negligible. In high saturation, however, the effect of local air flow may become

significant. In the latter case, the air phase is trapped as air bubbles, and local air flow occurs in the form of diffusion.

As usual in the acoustical analysis, the state parameters are assumed to have a time dependence of $\exp(-i\omega t)$, where $i^2 = -1$ and ω is the angular frequency. Eq. (11) yields

$$p^f - p^s = \tilde{\Theta}_f \Delta n^f \quad (15)$$

where $\tilde{\Theta}_f = \Theta_f(1 - i\omega\tau_f)$. Using this equation and the linear state equations of the solid and fluid phases, the macroscopic constitutive relationships describing the acoustical behavior of partially saturated porous media can be derived (Wei and Dewoolkar 2006). The velocity and attenuation of the acoustic wave is dependent on the capillary relaxation time, and other commonly measured material and hydraulic properties. By simultaneously solving Eq. (15), and the linear state equations of the solid and fluid phases with the measured material and hydraulic properties, the capillary relaxation time can be adjusted until convergence with the measured velocity and attenuation is reached.

4.3 Methods to measure static properties

The acoustic and hydraulic properties are experimentally measured simultaneously on a soil sample using a novel apparatus developed at the University of Vermont. The methods used to collect the static hydraulic and acoustic properties are briefly described in this section; a more detailed description of the apparatus and methods used in this

experiment is given by George et al. (In Review). A schematic of the apparatus is provided in Figure 4-1.

The capillary pressure function is determined using a suction control method with axis translation. The level of suction at the bottom of the sample is controlled with a flow pump and is increased in increments once equilibrium has been achieved. The flow pump monitors the amount of water withdrawn or injected to maintain the level of suction in the pore fluid. Once the rate at which the flow pump has to withdraw or inject is sufficiently small, equilibrium has been achieved and a point on the static capillary pressure function is obtained. The amount of air pressure applied in the axis translation technique is determined by the expected range of capillary pressures, and the capacity of the high air entry disk used.

The Unsaturated Hydraulic Conductivity Function (UHCF) is the relationship between the hydraulic conductivity and the saturation, and is used to describe flow through unsaturated soils. The UHCF is generally not measured directly instead inverse modeling techniques of transient experiments are employed to determine the relationship. The hydraulic data collected throughout this experiment is similar to the data collected in a multi-step outflow experiment, that is, the cumulative outflow volume and the capillary pressure over time. HYDRUS-1 version 4.0 (Šimůnek 2008) was used to simulate this experiment and the built-in optimization procedure was used to determine the hydraulic conductivity function parameters.

The acoustic properties of interest in this study include the compressional and shear wave velocity and attenuation. Wave velocity is the speed at which an acoustic wave travels through a particular material and is determined by the arrival time of the wave at the receiver. Attenuation is related to the dissipation of wave energy which may be caused by motion of the fluid relative to the frame and the relative motion of contiguous particles (Stoll 1969). Attenuation is described by the inverse of the quality factor (Q^{-1}). In this study, piezo-ceramic sheet material (PZT) was used to produce and receive the acoustic waves which were transmitted through the soil. A Kelly wavelet was chosen as a source wave for the experiments. The AutoLab system is equipped with automated switching controls which switch between exciting the shear and compressional waves.

Because of the small strains produced, the highly attenuating soil, and the complex geometry of the sample, determining the velocity and attenuation of the soil over the entire range of saturations is a difficult task. Traditionally, velocities are determined by hand picking the first arrival of the wave, and attenuations are found by comparing the frequency spectra of two waves using a method known as Spectral Ratios (Toksoz et al. 1979). An alternative forward modeling techniques was utilized in this research to obtain both the velocity and attenuation of the waveform (George and Dewoolkar In Review).

4.4 Methods to measure the dynamic properties

After the static capillary pressure function, UHCF and acoustic properties have been measured; the dynamic capillary pressure function can be predicted and experimentally

measured on the same soil sample. The method used to experimentally measure the dynamic capillary pressure function is as follows. The original sample used for the testing described above was resaturated by flooding assisted by a vacuum drawn from the top of the specimen. Once the specimen was fully saturated, indicated by the compressional wave velocity, the dynamic experiment was started. The apparatus was capable of performing two types of dynamic experiments. The first was conducted in steps and the second was conducted at a constant flow rate. For the dynamic curve measured with steps, the water pressure at the bottom of the sample was changed in the same manner as the static test. Instead of waiting for equilibrium, each pressure was maintained for four hours. For the dynamic curve measured with a constant flow rate, water was withdrawn from the bottom of the sample at a constant flow rate of 0.04 cc/min until the capillary pressure reached the capacity of the high air entry disk. The capillary pressure which resulted from this constant flow rate was recorded and then used to predict the dynamic curve using the relationships given by equations (8) through (10).

4.5 Experimental Results and Predictions

Acoustic and hydraulic properties were measured for two soil types. The first soil type was a silt sample collected from the Bonny Dam site in eastern Colorado, and the second soil type was prepared by mixing sand, silt and clay sized particles to achieve a locally heterogeneous distribution of pore sizes. The clay was broken up into small pieces that passed through the 1/4" sieve, the silt was also broken up from a dry state, and then both were mixed with the sand to achieve a patchy distribution of silt and clay within the overall sandy mixture. The mixture consists of approximately 55% by weight sand, 27%

silt, and 18% clay sized particles. The overall grain size distribution for both soil types are shown in Figure 4-2, the static capillary pressure functions and unsaturated hydraulic conductivity functions are shown in Figures 4-3 and 4, respectively. Figures 4-5 (a) and (b) show the measured velocity and attenuation versus saturation for both soil types. Also Figure 4-5 shows the velocity and attenuation predicted using the wave propagation theory (equations 11-15) which considers attenuation created from local flow. Figure 4-6 (a) and (b) present the capillary relaxation times which were found to best predict the velocity and attenuation in Figures 4-5 (a) and (b). Finally, Figures 4-7 (a) and (b) show the dynamic capillary pressure functions given by equation (8) which are predicted with the capillary relaxation times from Figure 4-6 for both soil types.

Starting with Figure 4-6, it can be seen that the capillary relaxation of the gas phase (τ_n) is near zero, or zero for saturations below approximately 85% for both soil types. This is consistent with the notion that the air phase is generally disconnected above saturations of 85%, when the air phase is connected its pressure is dissipated quickly and the relaxation time of the air phase is negligible, due to high mobility. The magnitude of the capillary relaxation time is also noteworthy. The range of capillary relaxation times found for both soil types is between 10^{-3} and 10^{-5} seconds, this is a very short time for equilibration to occur.

The implications of these low capillary relaxation times can be seen in the prediction of the dynamic capillary pressure functions shown in Figure 4-7. Since the capillary

relaxation times are so low, the effect of local flow on the dynamic pressure saturation relationship is very minimal, resulting in needing a relatively high rate (0.1 cm/s) of capillary change to predict a non unique pressure saturation relationship. This is equivalent to completing a drainage experiment on these soil samples in 2.8 hours each, without building up significant capillary pressures. The drainage experiment which was performed allowing for equilibrium to be achieved lasted over 20 days for each soil. The rate which has been predicted is not reasonable; and reasons behind it will be discussed in the next section.

As explained in Section 4.4, two types of dynamic curves were measured in the laboratory on the locally heterogeneous mixture sample. The results, along with the static capillary pressure function can be seen in Figure 4-8. The constant flow dynamic curve was predicted using the dynamic capillary pressure function given by equation (8), using the actual pressure history from the dynamic experiment. The theory predicts a dynamic curve which is very similar to the static curve, as shown in Figure 4-9. The measured dynamic curve is very different from that predicted.

4.7 Discussions

The compressional wave attenuation values ($1000/Q$) found for both of the soil samples tested here were very high as compared with attenuation values found from compressional waves propagated through rock samples (Cadoret et al. 1995; Murphy 1982). The values of attenuation were closer to values obtained on saturated sand and

glass beads (Molyneux and Schmitt 2000). This shows that the compressional waves traveling through partially saturated unconsolidated porous media were more attenuated than compressional waves traveling through partially saturated rocks, implying that there are mechanisms which cause attenuation in unconsolidated porous media that do not exist in consolidated porous media.

The actual mechanisms that dissipate wave energy and cause attenuation are poorly understood (Bourbie et al. 1987). Attenuation is generally divided into two categories; intrinsic and extrinsic. Intrinsic attenuation is directly related to the porous media and extrinsic attenuation results from the geometry, scattering, etc. Suggestions for sources of intrinsic attenuation include breakage of chemical bonds, capillary forces, thermo relaxation, local flow and intergranular friction, which can depend on the presence of water which could lubricate the interface between solid particles, among others (Bourbie et al. 1987). It has also been suggested that significant intrinsic scattering exists in unsaturated soils due to the high contrast between the acoustic impedance of the materials i.e. air, water and solid particles (Flammer et al. 2001). The theory (Wei and Muraleetharan 2007) assumes that macroscopic fluid flow and capillary relaxation are the dominant mechanism of intrinsic attenuation and all other mechanisms are negligible. This may be a reasonable assumption in consolidated porous media, which show modest scattering and absorption (Flammer et al. 2001). Extrinsic attenuation due to geometric factors is accounted for in the forward modeling analysis technique (and spectral ratios method) for determining the attenuation of the measured waveform.

The relaxation times are based on the attenuation and velocity of the material. The relaxation times are very low as a result of the very high values of attenuation seen. If all of the attenuation is not attributed to fluid flow and capillary relaxation, the theory may be predicting an artificially small capillary relaxation time. The relatively small relaxation times are suggesting that the dynamic effects are not pronounced, which is not supported by the experimental data (see Figures 4-8 and 9).

It was mentioned earlier that the measured velocity and attenuation are frequency dependent. If the frequency of the source wave is too high the pressures built up in the fluids may not have time to relax and dissipate wave energy. This would result in stiffening the soil matrix and not capillary relaxation. All of the data presented here was collected using a Kelly wavelet with a center frequency of 20 kHz. This results in a characteristic time of loading of 5×10^{-5} seconds, and a wavelength at 800-500 m/s of 0.04 - 0.025 meters (4.0 - 2.5 cm). This wavelength is appropriate since a wavelength smaller than the travel path between source and receiver (10 cm), but larger than the expected size of the patches is desired. Although, using a lower frequency source wave may reduce the effects of scatter and give a better measure of attenuation due to local flow, the size of the sample used in this study was a restricting factor.

The small relaxation times also imply that the sizes of the patches of saturation are also small. Using the procedure suggested by Wei and Muraleetharan (2007) to find the size

of a patch of gas at high saturation, and the capillary relaxation times found through this experiment, the predicted size of a gas pocket in the Bonny silt at approximately 90% saturation would be approximately 4 mm. This prediction is reasonable.

The dynamic effect appearing in measurements (Figures 4-8 and 9) could also be induced by the flow due to the pressure difference between the two ends of the sample. It is to be noted that the dynamic SWCC is measured for the sample as a whole. This means that the whole sample is viewed as a point (or an element), which has a single suction and saturation. Therefore, when a suction increment (or decrement) is applied, the degree of saturation will vary with time and finally attain a determined value. In this case, the relaxation time due to macro-scale flow is given by

$$\tau_c = \frac{L_s^2}{c_v} \sim \frac{0.05^2 m^2}{10^{-6} m^2 / s} \sim 2000s \quad (16)$$

where L_s is the sample length; c_v is the pressure diffusivity due to Darcy's flow, i.e., the consolidation coefficient, and a reasonable value of c_v for silts and fine sands is $10^{-6} m^2/s$.

Recall that the frequency of excitation wave is around 20 KHz and the wavelength is around 2-5 cm. This range of frequency definitely can not detect the dissipative mechanism due to Darcy's flow. As noted above, the dissipation in the sample may be not only due to local flow, but also due to other mechanisms including Darcy's flow.

4.8 Conclusions and Recommendations

The data presented here suggests that attributing all attenuation seen to local flow ignoring all other mechanisms of attenuation is inappropriate for unconsolidated porous media. The model of wave propagation proposed by Wei and Muraleetharan (2007) could be improved to include attenuation from other sources if it is applied to unconsolidated porous media. This is a difficult task due to the complex interactions of the soil grains and the lack of understanding of other mechanisms of attenuation. The model should also include the effects of Darcy's macroscopic flow on the dynamic capillary pressure function. If the height of the sample was very short (on the order of 2-3 cm) the assumption could be made that the measurements being taken are representative of a point, and the effect of macroscopic flow could be neglected. Since the acoustic measurements require a large sample height, the effect of Darcy's flow should be included in the analysis.

It is difficult to make conclusions concerning the validity of the dynamic capillary pressure model. This model requires a measure of attenuation based on local flow only from which the capillary relaxation time can be found. If it was possible to measure the attenuation due to local flow only, the validity of this model could be tested. It may be possible to use much lower frequency waves (~5 to 10 kHz) on a larger sample (~50 cm in diameter) to reduce the effects of scatter and increase the effects of local flow on the wave propagation. It may be possible to use acoustics to obtain an accurate measure of capillary relaxation in consolidated porous media, as has been shown previously (Wei

and Dewoolkar 2006). This dynamic capillary pressure model could then be applied with the acoustic data to predict the dynamic effects in consolidated media, such as rocks. This is not of great interest to geotechnical and environmental engineer, but it may be of interest to the petroleum industry.

4.9 Acknowledgements:

The study presented here was supported by Vermont Experimental Program to Stimulate Competitive Research (VT EPSCoR), (grant EPS 0236976) and the Vermont Space Grant Consortium through funding from NASA (grant NNG05GH16H). The authors are grateful to Dr. George Pinder for his time and advice, Floyd Vilmont and Kurt Anthony of the University of Vermont for assistance in the apparatus development and Dr. Gregory Boitnott and Martin Smith, of New England Research, Inc. for collaboration on acoustic data collection and analysis.

Figure Captions:

Figure 4-1: Schematic of the experimental apparatus

Figure 4-2: Grain size distribution for Bonny silt and heterogeneous soil mixture

Figure 4-3: Capillary pressure functions fitted with a Van Genuchten function

Figure 4-4: Unsaturated hydraulic conductivity functions found with inverse modeling

Figure 4-5: Comparisons of measured Compressional wave velocity and attenuation with predicted values for (a) Bonny silt and (b) Heterogeneous soil mixture

Figure 4-6: Capillary relaxation time versus saturation for (a) Bonny Silt and (b) Heterogeneous soil mixture

Figure 4-7: Predicted dynamic curves for (a) Bonny silt and (b) Heterogeneous soil mixture

Figure 4-8: Experimentally measured dynamic curves on heterogeneous soil mixture

Figure 4-9: Measured and predicted constant flow dynamic curves on heterogeneous soil mixture

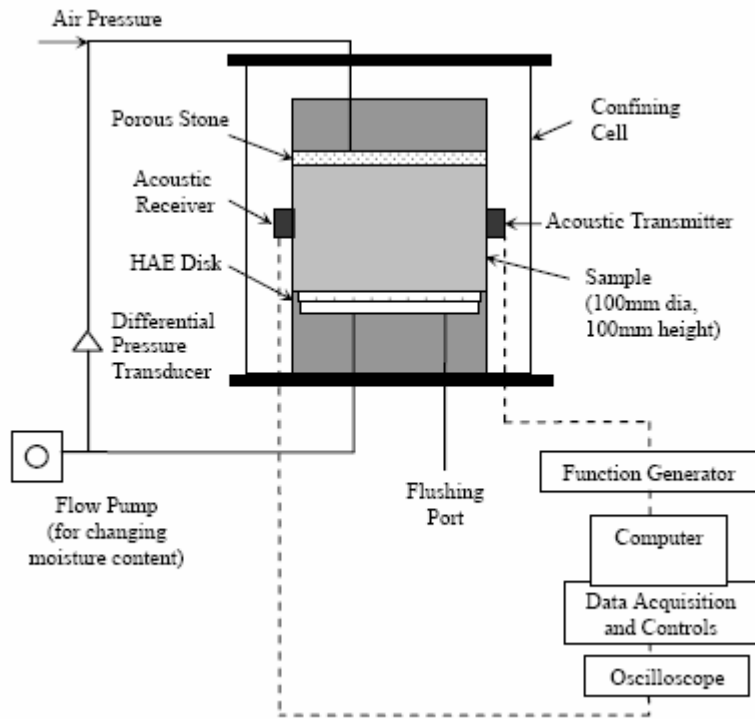


Figure 4-1: Schematic of the experimental apparatus

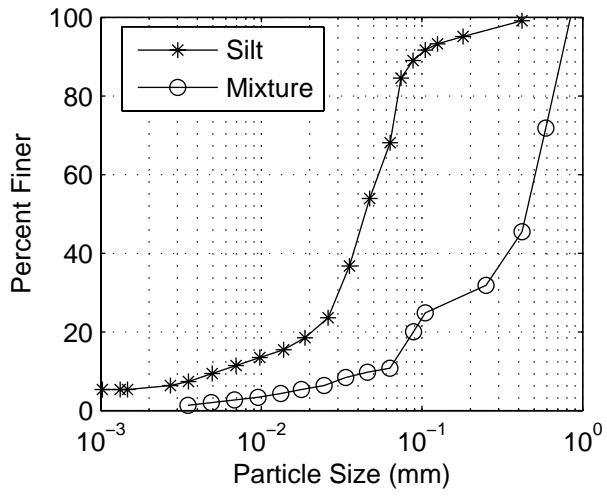


Figure 4-2: Grain size distribution for Bonny silt and heterogeneous soil mixture

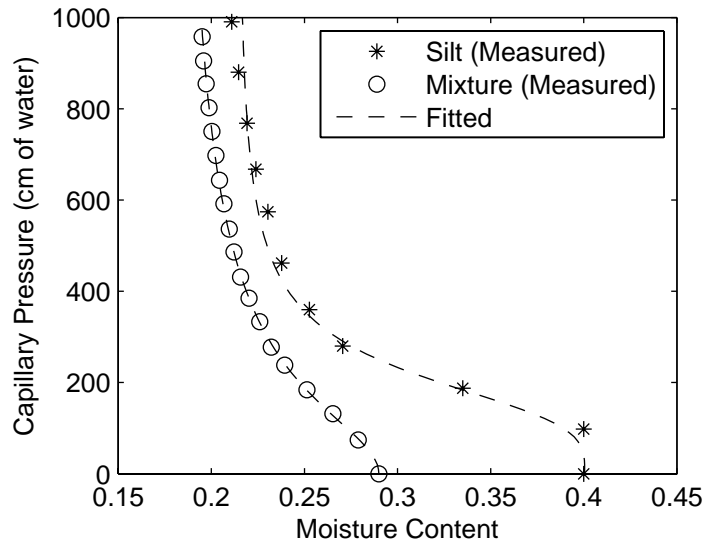


Figure 4-3: Capillary pressure functions fitted with a Van Genuchten function

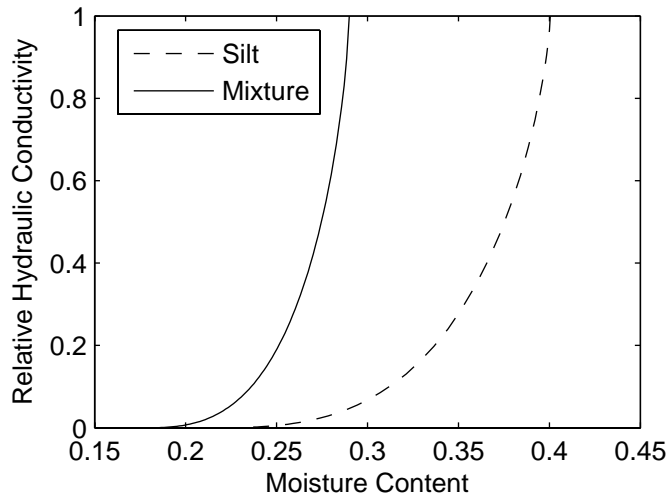
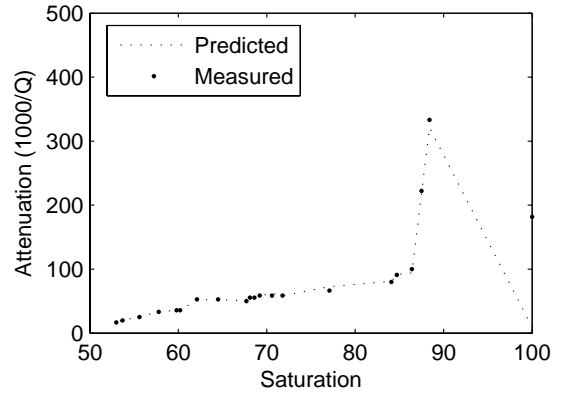
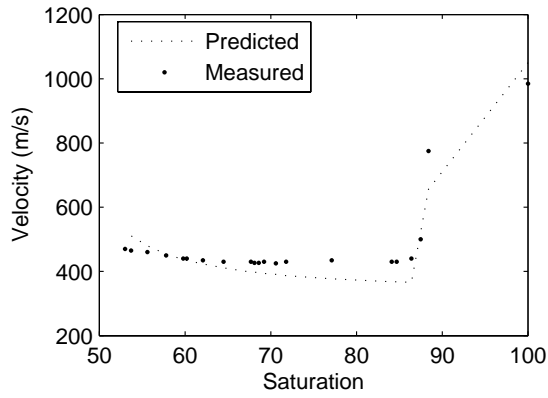
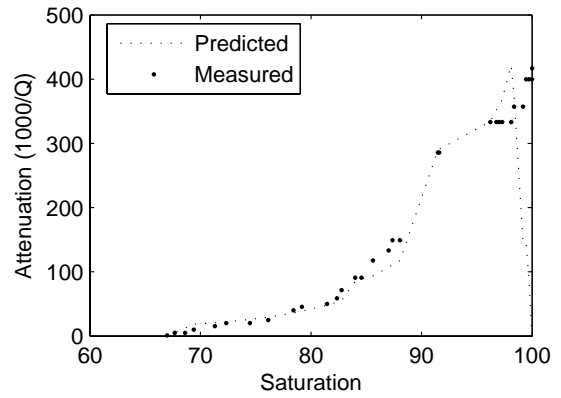
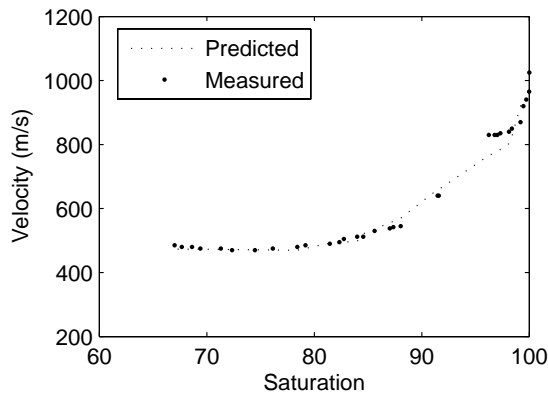


Figure 4-4: Unsaturated hydraulic conductivity functions found with inverse modeling

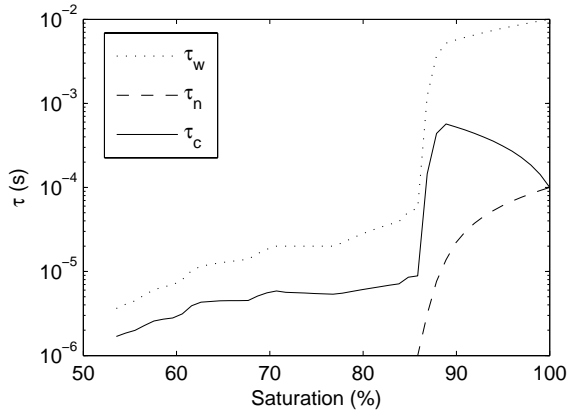


(a) Bonny silt

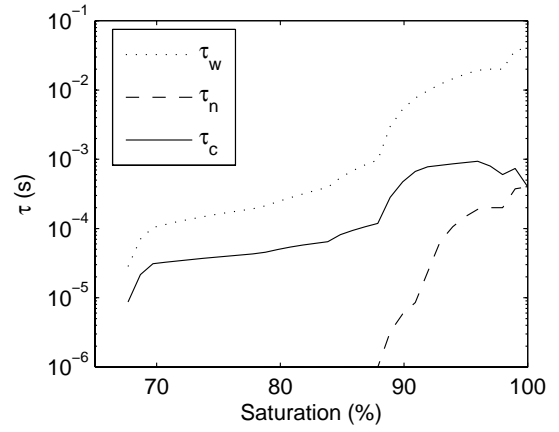


(b) Heterogeneous soil mixture

Figure 4-5: Comparisons of measured Compressional wave velocity and attenuation with predicted values for (a) Bonny silt and (b) Heterogeneous soil mixture

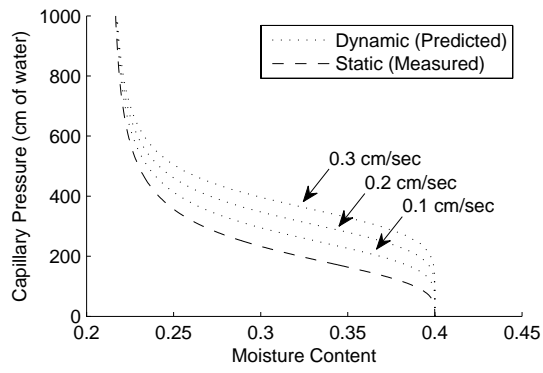


(a) Bonny silt

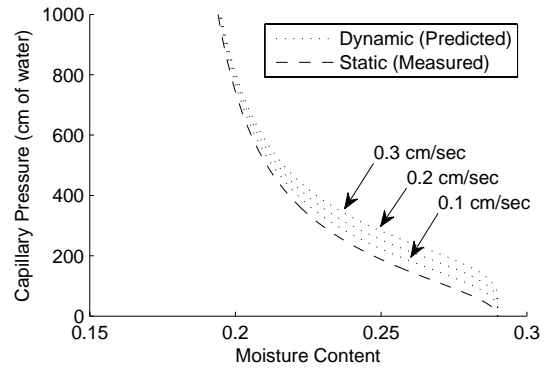


(b) Heterogeneous soil mixture

Figure 4-6: Capillary relaxation time versus saturation for (a) Bonny Silt and (b) Heterogeneous soil mixture



(a) Bonny silt



(b) Heterogeneous soil mixture

Figure 4-7: Predicted dynamic curves for (a) Bonny silt and (b) Heterogeneous soil mixture

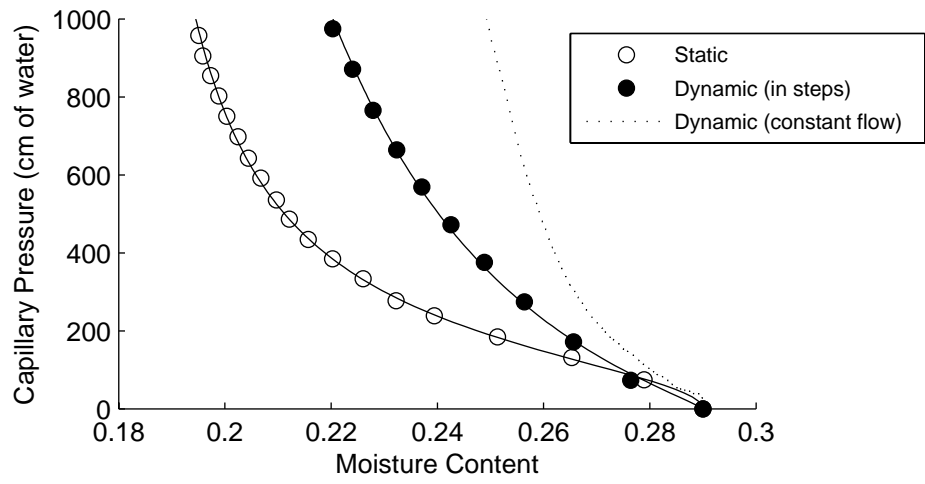


Figure 4-8: Experimentally measured dynamic curves on heterogeneous soil mixture

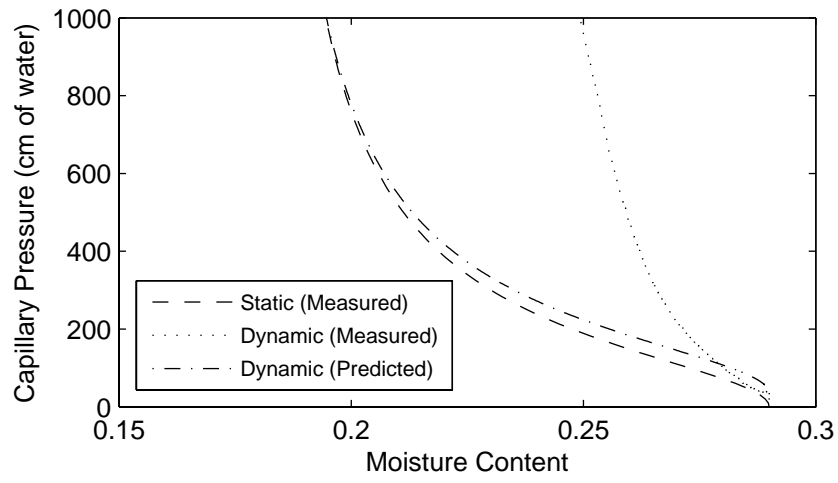


Figure 4-9: Measured and predicted constant flow dynamic curves on heterogeneous soil mixture

4.10 References:

- Bourbie, T., Coussy, O., and Zinszner, B. (1987). *Acoustics of Porous Media*, Editions Technip Paris.
- Cadoret, T., Marion, D., and Zinszner, B. (1995). "Influence of frequency and fluid distribution on elastic wave velocities in partially saturated limestones." *Journal of Geophysical Research*, 100(B6), 9789-9803.
- Chen, L., Miller, G. A., and Kibbey, T. C. (2007). "Rapid Pseudo-Static Measurement of Hysteretic Capillary Pressure-Saturation Relationships in Unconsolidated Porous Media " *Geotechnical Testing Journal*, 30(6), DOI: 10.1520/GTJ100850.
- Constantz, J. (1993). "Confirmation of Rate-Dependent Behavior in Water Retention During Drainage in Nonswelling Porous Materials." *Water Resour. Res.*, 29(4), 1331-1334.
- Davidson, J. M., Nielsen, D. R., and Biggar, J. W. (1966). "The dependence of soil water uptake and release upon the applied pressure increment." *Soil Science Society of America Journal*, 30, 298-303.
- Flammer, I., Blum, A., Leiser, A., and Germann, P. (2001). "Acoustic assessment of flow patterns in unsaturated soils." *Journal of Applied Geophysics*, 46, 115-128.
- Hassanizadeh, S. M., and Gray, W. G. (1993). "Thermodynamic basis of capillary pressure in porous media." *Water Resour. Res.*, 29, 3389-3405.
- Knight, R., and Nolen-Hoeksema, R. (1990). "A Laboratory Study of the Dependence of Elastic Wave Velocities on Pore Scale Fluid Distribution." *Geophysical Research Letters*, 17(10), 1529-1532.

- Mohamed, M. H., and Sharma, R. S. (2007). "Role of Dynamic Flow in Relationships between Suction Head and Degree of Saturation." *Journal of Geotechnical and Geoenvironmental Engineering*, 133(3), 286-294.
- Molyneux, J. B., and Schmitt, D. R. (2000). "Compressional-wave velocities in attenuating media: A laboratory physical model study." *Geophysics*, 65(4), 1162-1167.
- Murphy, W. F. (1982). "Effects of partial water saturation on attenuation in Massilon sandstone and Vycor porous glass." *Journal of Acoustic Society of America*, 71(6), 1458-1468.
- O'Carroll, D. M., Phelan, T. J., and Abriola, L. M. (2005). "Exploring dynamic effects in capillary pressure in multistep outflow experiments." *Water Resour. Res.*, 41(W11419, doi:10.1029/2005WR004010).
- Schultze, B., Ippisch, O., Huwe, B., and Durner, W. "Dynamic Nonequilibrium During Unsaturated Water Flow." *Characterization and Measurement of the Hydraulic Properties of Unsaturated Porous Media; Proc. Intern. Workshop., Riverside, CA, 22-24 October, 1997*, Riverside, CA, 877-892.
- Šimůnek, J., M. Šejna, H. Saito, M. Sakai, and M. Th. van Genuchten. (2008). "The HYDRUS-1D Software Package for Simulating the Movement of Water, Heat, and Multiple Solutes in Variably Saturated Media, Version 4.0, HYDRUS Software Series 3." Department of Environmental Sciences, University of California Riverside, Riverside, California, USA.

- Toksoz, M. N., Johnston, D. H., and Timurr, A. (1979). "Attenuation of seismic waves in dry and saturated rocks: 1. Laboratory measurements." *Geophysics*, 44(4), 681-690.
- Topp, G. C., Klute, A., and Peters, D. B. (1967). "Comparison of Water Content-Pressure Head Data Obtained by Equilibrium, Steady-State, and Unsteady-State Methods." *Soil Science Society of America Journal*, 31, 312-314.
- Vachaud, G., Vauclin, M., and Wakil, M. (1972). "A study of the uniqueness of the soil moisture characteristic during desorption by vertical drainage." *Soil Science Society of America Journal*, 36, 531-532.
- Wei, C., and Dewoolkar, M. "A Continuum Theory of Nonequilibrium Two-Phase Flow through Porous Media with Capillary Relaxation." *Advances in Unsaturated Soil, Seepage, and Environmental Geotechnics, Proceedings of Sessions of GeoShanghai, Shanghai, 6-8 June 2006*, Shanghai, 246-254.
- Wei, C., and Muraleethanan, K. K. (2006). "Acoustic characterization of fluid-saturated porous media with local heterogeneities: Theory and application." *International Journal of Solids and Structures*, 43, 982-1008.
- Wei, C., and Muraleetharan, K. K. (2007). "Linear viscoelastic behavior of porous media with non-uniform saturation." *International Journal of Engineering Science*, 45, 698-715.
- Wildenchild, D., Hopmans, J. W., Vaz, C. M. P., Rivers, M. L., Rikard, D., and Christensen, B. S. B. (2002). "Using X-ray computed tomography in hydrology: systems, resolutions, and limitations." *Journal of Hydrology*, 267, 285-297.

5. CONCLUSIONS

The purpose of this research was to satisfy three specific research objectives: (1) to develop an apparatus and procedure to collect acoustic waveforms on laboratory sized unsaturated soil samples, (2) to develop a forward modeling technique using a one-dimensional wave propagation model as an alternative analysis method for waves collected in small laboratory sized samples, and (3) to apply the theory to the measured acoustic data in an attempt to predict the dynamic behavior of the capillary pressure relationship. As shown in this dissertation, the three objectives have been satisfied and the conclusions are summarized in the following.

The development of a new type of laboratory device capable of making simultaneous measurements of acoustic signatures and hydraulic properties on relatively large soil specimens was presented in Chapter 2. The acoustic properties included the compressional and shear wave speeds and attenuations for two soils. A complete set of these measurements over a full range of saturations was presented. The results were found to be consistent with previously published data collected on unsaturated rocks. The soil water characteristic curve and the unsaturated hydraulic conductivity function were also measured and presented. The data collected using the apparatus developed were used in the meeting both objectives (2) and (3).

A forward modeling technique was used to interpret the compressional and shear waveforms in Chapter 3. The acoustic wave velocities and attenuations found using this

method were compared to the values obtained using more traditional methods, i.e. “manually-picking” arrival times for velocity and spectral ratios for attenuation. A one dimensional model was used in this forward modeling technique and it was shown that this model reduced computational time and provided essentially same results as a two dimensional model. The one dimensional model was able to capture the wave behavior over the first quarter cycle of the received wave. This means that the model was able to capture the arrival and the amplitude of the first peak, which was considered sufficient to quantify the velocity and attenuation of the sample. This forward modeling technique provided less subjective results than the traditional methods, and was able to find both the velocity and attenuation of the wave simultaneously.

The acoustic data collected and analyzed through this research was then used to attempt to verify existing theories of wave propagation and the dynamic soil water characteristics. The data presented in Chapter 4 suggested that the theories may be lacking in two areas. First, the wave propagation theory attributes all attenuation seen to local flow and ignores all other mechanisms of attenuation. It was found that this may be an inadequate assumption for unconsolidated porous media. The model of wave propagation proposed by Wei and Muraleetharan (2007) could be improved to include attenuation from other sources if it is applied to unconsolidated porous media. This is a difficult task due to the complex interactions of the soil grains and the lack of understanding of other mechanisms of attenuation. Second, the model of the dynamic soil water characteristics should include the effects of Darcy’s macroscopic flow on the dynamic behavior. If the height of

the sample was very short (on the order of 2-3 cm) the assumption could be made that the measurements being taken are representative of a point, and the effect of macroscopic flow could be neglected. Since the acoustic measurements require a large sample height, the effect of Darcy's flow should be included in the analysis.

It is difficult to make conclusions concerning the validity of the dynamic capillary pressure model. This model requires a measure of attenuation based on local flow only from which the capillary relaxation time can be found. If it was possible to measure the attenuation due to local flow only, the validity of this model could be tested. It may be possible to use much lower frequency waves (~5 to 10 kHz) on a larger sample (~50 cm in diameter) to reduce the effects of scatter and increase the effects of local flow on the wave propagation. It may be possible to use acoustics to obtain an accurate measure of capillary relaxation in consolidated porous media, as has been shown previously (Wei and Dewoolkar 2006). This dynamic capillary pressure model could then be applied with the acoustic data to predict the dynamic effects in consolidated media, such as rocks. This may not be of great interest to geotechnical and environmental engineer, but it may be of interest to the petroleum industry.

APPENDIX A: Evolution of the Experimental Apparatus

A.1 Apparatus:

The following figure (Figure A-1) is a schematic of the apparatus used initially in this research. It included two high air entry disks on both the top and the bottom of the sample. Initially, air was introduced through the tube shown at the bottom and entered the sample at a single point at the end of the tube. This approach was questioned. A uniform distribution of air throughout the sample was desired, and it was thought that repeatable results could not be attained if the air entered at only one point. A phenomenon was noticed in the data which could possibly be explained by air entering the sample in discrete bubbles. Where the bubbles would enter the sample, grow in size and become disconnected from the air supply. This approach was also criticized because it was possible that the air phase would become disconnected between the pressure transducer and the air within the sample. This would result in inaccurate measurements of the pore air pressure. The first attempt to rectify these issues was to create an air distribution element, shown in Figure A-2, it is also what is depicted in the first schematic (Figure A-1).

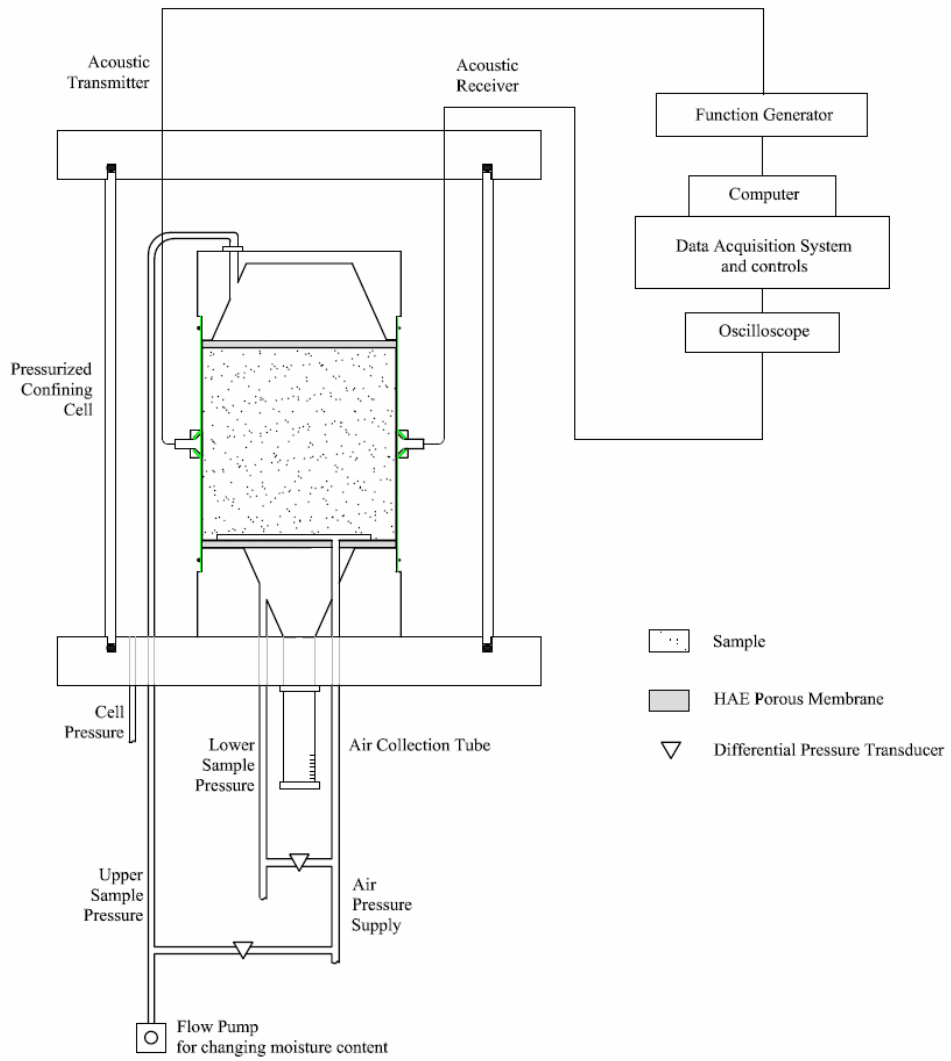


Figure A-1: Schematic of apparatus (early version)

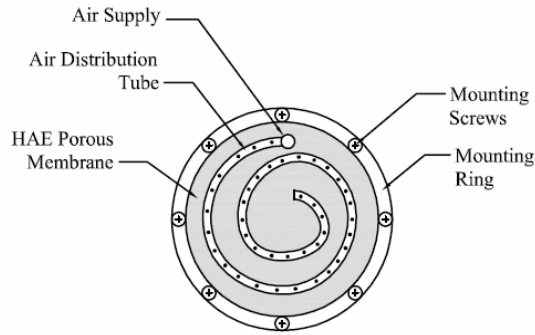


Figure A-2: Air distribution element in lower cap

It was proposed that this air distribution element would aid in creating a uniform distribution of air throughout the sample. The air would enter the bottom of the sample, and buoyancy would cause the air to travel vertically. Water would be withdrawn from the top of the sample. When an experiment was conducted with this configuration, it was found that there was no capillary pressure detected in the bottom of the sample and only expected capillary pressures in the top of the sample. The capillary pressures in the top of the sample looked accurate while withdrawing water at a constant, slow rate of 0.01-0.005 cc/min, but as soon as the pump was shut off the capillary pressures were lost. It was concluded that the experiment was not performing as planned and there were a few ideas about why it did not work. First, it was believed that the air distribution element was creating an air layer at the bottom of the sample, which was isolating the water in the bottom reservoir from the water in the sample resulting in zero capillary pressure. And second, it is possible that the capillary pressure in the top cap were accurate, possibly dynamic, but accurate. When the pump was shut off it caused the water to redistribute

throughout the sample resulting in a loss of capillary pressure. Portions of the sample were being rewetted and other parts drained, because of hysteresis, this would cause very erratic results.

Because of the results and conclusions regarding the configuration of the apparatus and the techniques used, it was decided that the attempts to obtain a uniform distribution of moisture were not working, and possibly unnecessary. If it is assumed that there will be some variation in the distribution of saturation throughout the length of the sample, and it is accounted for, the test may be more accurate and simpler. The next configuration attempted is a more traditional configuration where air is introduced to the sample through a coarse porous stone at the top of the sample and the water is withdrawn from the bottom of the sample (see Figure A-3). The pressure in the water at the bottom of the sample is compared with the pressure in the air at the top of the sample to calculate the capillary pressure. The distribution in saturation due to a distribution in hydrostatic pressure must be accounted for, and this is done using a procedure developed by Liu and Dane (1995). The amount of change in saturation from the top to the bottom of the sample will depend on the material chosen and its pore size distribution. If the material is very uniform, and the pore size distribution is very small, there could be very large changes in saturation, but if the material has a large range of pore sizes, the change could be very small. A material was chosen which will provide for a minimal change in saturation from the top to the bottom. Since the distribution is not perfectly uniform, the acoustics will be taken through a range of saturations, but if the range is kept small, the

acoustics can be measured over the entire range of saturations. One thing to point out is that the acoustic measurements vary the most between 100 and 90% saturation, and in that range there are generally relatively large changes in capillary pressures, meaning that the distribution across the length of the sample at very high saturations should be small.

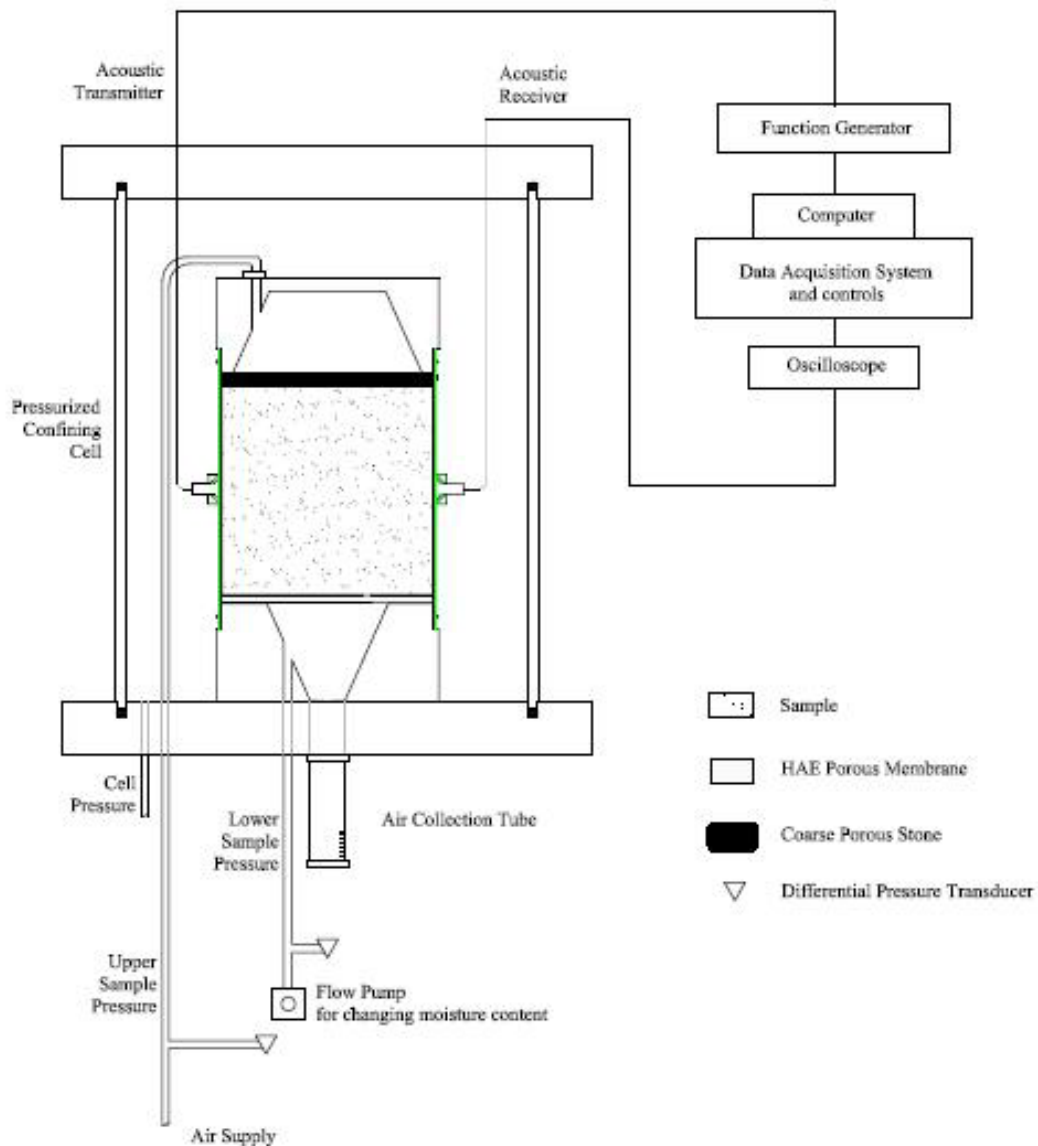


Figure A-3: Schematic of improved apparatus

A.2 Procedure for changing saturation:

There are many methods used for determining the capillary pressure saturation relationship in soils. Initially, a controlled volume technique with axis translation was chosen, withdrawing water fairly quickly in small steps and allowing time for equilibration. This technique may create a shock in the system. This technique also allowed for the sample to re-saturate in portions of the sample. It was desired to stay “on the drying side” of the curve throughout the whole test. To do this the technique was changed to withdrawing at a specified rate until a pressure level was obtained, then changing and maintaining that pressure until equilibrium was achieved. This was the method of Dorboslov Znidarcic at the University of Colorado in Boulder. This method seemed to work very well, and is recommended for future use.

The procedure was slightly modified to aid in simplicity of the inverse modeling used for determining the hydraulic conductivity function. HYDRUS-1 [http://www.pc-progress.cz/Pg_Hydrus_1D.htm] was chosen as a software package, and if the pressure is changed at the bottom of the sample in a stepwise manner, the software can model this system very easily. This is very similar to a multi-step outflow experiment; it actually may be exactly how some run their multi-step outflow experiments. This method required that the pressure is changed instantaneously at the bottom of the sample, and then that pressure is maintained. The flow pump has a built in function (maintain pressure) which will almost instantaneously withdrawn the required amount of water to reach the specified pressure, and then continue withdrawing whatever is necessary to maintain that

pressure. Equilibrium is achieved when the flow pump stops withdrawing water. This method worked very well and was fairly simple using the GeoComp flow pumps.

A.3 High Air Entry disks:

Originally the high air entry disks were capable of housing the static pressure line which would be used in hydraulic conductivity testing. The dimensions of those disks are shown in the figure below (Figure A-4); the approach was modeled after Lu et al. (2006). The purpose of the 0.25” hole drilled through the disk is to apply air to the sample, and the center 0.2” diameter hole houses the static pressure line. The thickness of the disk below the static pressure line is reduced to lower the head loss across the membrane. Lu et al. (2006) performed a finite element simulation to optimize the various dimensions to reduce the head loss. The thickness of these disks is undesirable for the apparatus used in this experiment; they are fragile and can easily be broken in the flexible membrane. The disks were improved for this application by removing the static pressure line housing. The thickness of the disk was also increased to 0.25” to improve the strength. The thicker disk may increase the time to equilibrium by slowing the flow of water out of the sample.

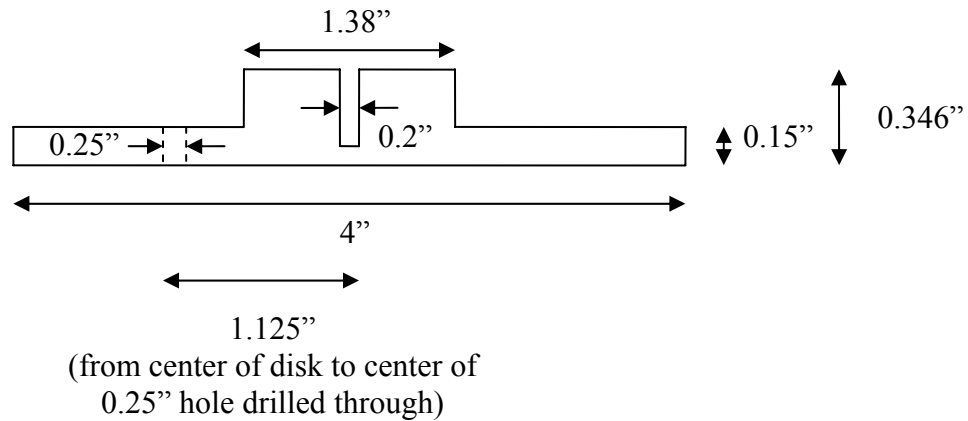


Figure A-4: First bottom high air entry disk design

Problems with the ceramic high air entry disks continued, even after increasing the thickness. The disks would break during assembly, and leakage of air would occur around the air tube through the lower disk. Other materials were investigated which may alleviate some of these problems. Both porous metals and porous nylon membranes were investigated. The porous metals, such as stainless steel, were considerably more expensive than ceramic (quoted approximately \$950 per disk from the Mott Corporation). The literature on the stainless ceramic states that the pore size can be manufactured to 0.45 microns, which has been reported in other literature to have a bubbling pressure of over 20 psi, but upon further conversation with the representatives from the Mott Corporation we learned that the pore size is actually much larger than that, and that much lower bubbling pressures should be expected. The stainless steel porous plates option was abandoned because of the high cost and limiting bubbling pressures.

Porous filter membranes were found to be much more reasonably priced from GE Osmotics (Part #1221546 Model # A04SP10225 Type: GE CA (Cellulose Acetate) Membrane 0.45 micron 102 mm diameter 25 each \$80.00). These membranes have an approximate bubbling pressure of 30 psi. A machinist built a support for the membrane which utilized bronze porous plates from Geotest. The membranes are affixed to the support using RTV silicone caulking. Although, the membranes did get damaged during testing and leaked air. To get around this issue, two to three membranes were layered together for protection and insurance. Since then, filter membranes made from Teflon were discovered, and should be able to withstand the testing without getting damaged.

Many methods were attempted to get the porous membranes to work. The major problem with the membranes is damage during sample preparation and sealing the edges from air leakages. These membranes may be worth investigating in the future when loss across the high air entry media is of concern. For now, it was decided to go back to the high air entry ceramics. Dobroslav Znidarcic has had luck using the porous membrane with silt and clay materials, he still has problems damaging the membrane when using sands.

The final high air entry ceramic design is as follows. A disc slightly smaller than the bottom cap was chosen, a seat was machined out of the bottom cap to house the disc, which was epoxied in. An unsuccessful attempt was made to seal the HAE disc with an o-ring around the circumference. The bottom cap is depicted in the following figure (Figure A-5). The seat for the HAE disc was machined slightly larger than the disc to

allow for epoxy, which was spread on the seat and around the circumference. The epoxy was supplied by Soil Moisture Corp. This configuration has worked seamlessly since it was built.

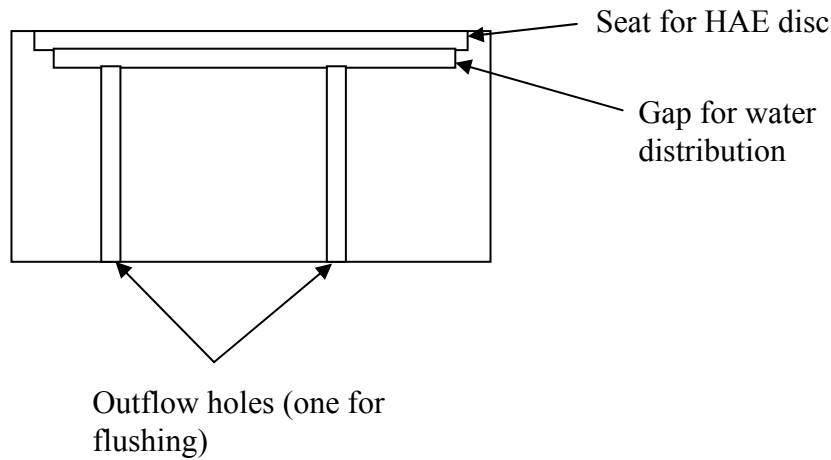


Figure A-5: Final bottom high air entry disk design

A.4 Coarse Porous Stone:

Originally the top cap of the apparatus utilized a coarse porous stone, both sintered bronze and aluminum were used. The major problem with using this material arose when calculating how long it would take to empty the top stone before the sample started to desaturate. It was always largely a guess to decide when the water was actually being withdrawn from the sample. It was also suggested that the smaller pores in the stone may not be emptied initially, meaning that the coarse porous stone acted as a source of water when higher suctions were applied to the water. The only reason to use a stone at the top of the sample is to allow for an even distribution of the air pressure at the top of the sample. This can be achieved using a screen instead of a porous stone. The screen would

not hold additional water and would have a minimal volume of water held in it, so that deciding when the sample started de-saturating would be easier. Two layers of screen were used to allow for a small air gap to distribute the air around the top of the sample, and grooves were machined in the upper cap to distribute the air. The final design is depicted in the following figure (Figure A-6). The dotted lines represent the screens and the small blue lines on the circumference represent the RTV sealant used to hold the screens in place. The solid black lines represent the grooves and the hole drilled through the top cap.

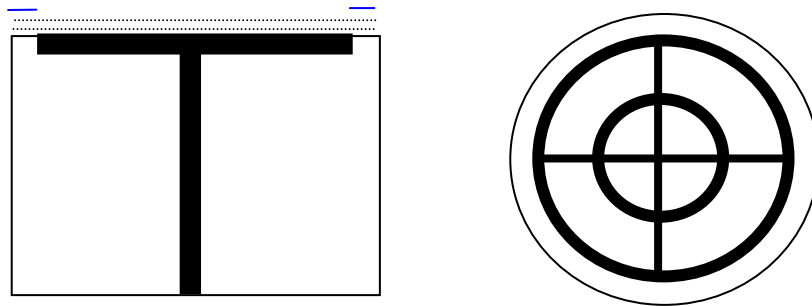


Figure A-6: Elevation and plan view of final upper cap

A.5 Flow Pump:

During the first experiment there were problems with the accuracy of the flow pump. This problem may have been due to residual air in the syringe of the flow pump. This problem was seen when using the controlled volume technique, where water was withdrawn and then the flow pump shut off. This problem was not a concern when the

maintain pressure command was used. If there is residual air in the syringe, it may cause the actual withdrawal to be different than the withdrawal measured by the flow pump motor steps. According to GeoComp (the flow pump manufacturer) the flow pump will lose pressure over time if it is not set to maintain pressure, which may result in unaccounted for volume change. When the flow pump is not in use it needs to be isolated from the sample using a quarter turn valve. When the valve is opened again, it was found that if the pressures between the sample water and the flow pump were matched, unaccounted flow could be eliminated. The recommended process is to first set the flow pump to match the water pressure, using the “Maintain constant pressure” command, then open the valve and watch to make sure the flow pump does not need to inject or withdraw water to maintain that pressure (meaning the pressures are equal). Then change the flow pump over to “maintain constant flow rate” set the desired flow rate, amount and pressure limit, withdraw the desired amount, and shut off the pump and close the valve simultaneously after the withdrawal is complete.

This procedure explained was only necessary when using the originally water withdrawal technique. When the technique was changed to the “change pressure instantaneously, then maintain pressure” option, the operation of the flow pump was simplified. The flow pump is always used in “Maintain pressure” mode, and when a new pressure level is desired the “Final Pressure” is changed to that desired new pressure level and “Maintain pressure” is started.

Data collection of the data on the flow pump is an issue. There is a built in memory which stored 1948 readings of the information collected by the flow pump. This is generally the time, volume withdrawn and pressure. In order to access the data on the flow pump, it needs to be hooked up to the computer which holds all of the software for all of the GeoComp equipment, or a GEO-NET card can be installed on any computer (approximately \$400 from GeoComp). The connection between all of the equipment and the computer is made through a cable which looks like a telephone cable, but it is wired slightly differently than telephone cable. The connection will not work, if a regular telephone cable is used. The cable needs to be wired “directly”. This means that one connector on one side of the cable needs to be put on opposite of the way it would be on a telephone cable. If two cable connectors are placed side by side, the colors of the wires are in the same order, compared to the connectors of a telephone cable side by side, the colors of wires are a mirror image of each other.

If the flow pump is properly connected to the computer, the DIAGS command program can be used to “talk” to the flow pump. Every time the flow pump is started on a specific function, such as “Maintain Pressure”, all of the data points in the memory are deleted and a fresh set of 1948 data points start to be collected. The sampling time can be set; usually 1 minute per sample is used, so that it can collect data for 32 hours without having to be reset. These data files can be saved in a text format. If more than 32 hours of data is needed for one function set on the flow pump, either the sampling interval can be

increased, or the flow pump needs to be restarted before the 32 hours is over in order to restart the data collection.

The data on the flow pump is important for recording the volume of water withdrawn from the sample over time. The reading on the flow pump LCD screen can be used to determine the total volume withdrawn from the sample, but if the volume over time needs to be recorded, it is necessary to take the data from the flow pump. We did have discussions with Geocomp about hooking the flow pump up to our National Instruments Data acquisition system. They were not interested in supporting our effort; because of the time it would take their programmers to help us. Basically a stand alone software package would have to be developed, like the shear or triaxial software. This would be very expensive. The method described to take the data off of the flow pump is “labor intensive”, but it is also simple and inexpensive compared to developing a new software package.

A.6 Electrical Feed-throughs:

The electrical feed-throughs caused some problem; originally one large compression type feed-through was used, in which all of the six wires for both transducers was fed (Omega MFT thermocouple feed through). Each wire had a Teflon compression type ferrule that sealed it between the inside and outside of the cell. There were two major problems with this approach. One was increased electrical noise created by the close proximity of the

transmitter and receiver wires. The second problem was that leakage of cell oil occurred through the stranded wire. This situation was improved by using two separate feed-throughs (LDS Vacuum products) and sheathing over the stranded wires which prevented any oil from entering the wire.

A.7 Electronic Pressure Regulator:

The electronic pressure regulator used to maintain constant confining stress was upgraded and replaced by a more accurate model. The accuracy of the first regulator was about 1% of the span, which resulted in a lag of approximately 0.3 psi. This lag was very noticeable on the pressure regulator data. The second regulator has an accuracy of 0.1% and was much better at maintaining the pressure at the desired value. The regulator was only one part of the problem. Initially, the house supplied air pressure was used. The compressor which supplies this pressure cycles on and off, which results in a noticeable change in the supply pressure to the regulator. Using compressed air cylinders and the more accurate electronic pressure regulator virtually eliminated any variations in pressure. The problem with the compressed air cylinders was their short life. A few cylinders would be used every week, and if one emptied unexpectedly before it was replaced, it could ruin the whole experiment.

In the final design the manual pressure regulators and the house air supply were used. A cylinder was added (for additional volume) and a second pressure regulator to “soften” the pressure variations that occur when the compressor turns on and off. This

configuration could be improved on with an electronic pressure regulator, but the concern is that the air must be very dry or else the electronic pressure regulators start malfunctioning. There is a dryer in the line before the lab, its reliability and the quality of it has been questioned. There is some water that comes into the system through the house air compressor.

APPENDIX B: Experimental Methods

B.1 Sample Preparation:

B.1.1 Material Choice:

Well graded materials were used because acoustic waves are highly dissipated through poorly graded, large grain sized materials. Ottawa sand may be the worst sample to use, due to reflections off of the grains. Heterogeneous material should show the most capillary relaxation. The distribution of moisture along the length of the sample also had to be considered. Uniformly graded sand will show a large variation in moisture from the top to the bottom of the sample, as if a front is traveling down the sample as it desaturates. This effect can be modeled, and the moisture content at mid height can be found using the HYDRUS-1 program. This should be compared to the overall average saturation which is calculated by the volume withdrawn.

It was concluded that local flow was not the dominating mechanism causing attenuation in Bonny Silt, a natural silt sample. Other mechanisms such as reflections or friction between grains were also dissipating wave energy.

B.1.2 Sample Preparation:

A static compaction method was used to prepare these samples. It was discovered that when a sample was prepared dry or near dry (10% moisture), the sample size shrank considerably during saturation under confinement. Hand compaction in layers did not work well, because the diameter of the sample reduced significantly during saturation. To circumvent this problem, astatic compaction method with over 1200 lbs of force was used. The sample was prepared at 10% moisture and then added to the mold in one lift. Pressure was applied to the top of the sample, and then the sample was flipped and pressure was applied to the bottom of the sample. This prevented significant loss in diameter during saturation. Specific sample preparation and compaction instructions are as follows:

B.1.3 Prepare rubber jacket and mold:

The upper cap of the apparatus is placed in the rubber jacket and the fittings from the top of the upper cap are removed. This will allow the upper cap to be used to compact the sample. Silicone grease (or Vaseline) is used to lubricate and seal between the upper cap and the rubber jacket. A filter paper cut to the size of the upper cap is placed inside the rubber jacket against the upper cap. The rubber jacket and upper cap is then placed

inside the split mold, which was specifically made for this apparatus. The split mold is held together with metal hose clamps. At this time, Canada Balsam is applied to the titanium heads of the transducers inside the rubber jacket.

B.1.4 Prepare soil:

10% water by weight is added to the sample and mixed thoroughly. The rubber jacket/mold is filled with the prepared soil; a spatula is used to force more soil into the mold without creating an interface by compacting from the top. The mold should be full to within $\frac{1}{4}$ " of the top. The "compaction cap" is placed into the rubber mold. The compaction cap is the same size and made of the same material (PVC) as the upper and lower caps, it is dark grey in color and has two $\frac{1}{8}$ " holes drilled through it. It is 4" in diameter and 2" in height. It also has a threaded tap in one side to accept a large eye bolt which can be used to remove the cap after compaction is complete.

The entire sample with split mold is placed in the loading frame. For this research approximately 1,500 lbs was applied to the sample. This number can change depending on the level of compaction desired. There are holes in the split mold for the transducers, and during compaction they need to be watched closely to insure that they do not hit the edge of the split mold. There will be some deformation of the jacket and the sample. The load is applied slowly and the entire sample needs to be visually monitored closely. Once the load has been applied to the "top" of the sample, the sample is flipped over and the load applied from the other side. Another note, the compaction cap and the lower cap in

the apparatus are the same height, but the lower cap in the apparatus is recessed approximately 1/8" into the bottom plate. Therefore when compaction is complete there should be at least 1/8" of the compaction cap exposed out of the jacket. This will allow for good contact between the bottom of the sample and the high air entry disk when the sample is placed in the apparatus.

After the sample has been prepared and compacted, the compaction cap can be removed, very carefully using the eye bolt to remove the cap by pulling it straight out of the jacket. If it is tilted too far to one side or the other, the sample may tend to crack and deform. Now the upper cap and the sample will be in the jacket, the jacket is carefully inverted and placed it in the apparatus on the high air entry disk. There should be lubricant on the lower cap and the high air entry disk should be saturated. It is easiest if the high air entry disk is saturated all the time. To do this, hook up the flow pump to the lower valve and set the flow pump to maintain a very small amount of pressure 0-1 kPa, as water evaporates from the top of the disk, more water is pushed in from the flow pump. If the pressure is set too high it will leak out of the top of the disk, and if the pressure is too low some drying will occur. It is better to have some water leaking over the top as long as the flow pump does not empty.

To complete inserting the sample and jacket into the apparatus, hose clamps need to be placed around the top and bottom caps. This is a problem area for leaks and it may be an area of improvement for this apparatus. In the worst cases RTV sealant can be used

instead of lubricant to complete the sealing of the jacket. Leakages have also been seen around the transducers recently. The epoxy used to seal the transducers to the jacket will eventually deteriorate further. Eventually, the transducers should be removed from the jacket, the jacket replaced, if necessary and the transducers re-sealed.

The confining cell is now placed over the sample, the acoustic wires connected to the top plate and the threaded rods tightened. The flow pump or the water supply should be attached to the lower cap valve, if it is not already. An air pressure line should be connected to the upper cap and an air pressure line connected to the confining valve. This would be a good time to insure that there are no air bubbles under the high air entry disk. This can be done by injected water with the flow pump and opening the second lower cap valve (flushing). At this time the omega differential pressure transducer should be attached to the data acquisition system. Data collection can begin now or after the sample is fully saturated. This completes the assembly of the apparatus.

B.1.5 Sample saturation strategy:

A vacuum saturation procedure has been used successfully for this apparatus, although others may also be acceptable. To saturate with a vacuum, the vacuum pump is attached to the top cap valve and the water supply to the lower cap valve. The vacuum pump is turned on before the valve to the water supply is opened. Once a significant vacuum is achieved (after about 10 seconds) the water supply valve is opened and water is allowed to flood the sample. The sample is said to be fully saturated when water starts coming out

of the top of the sample without air bubbles. This is the time when a leak in the jacket could be detected. If a constant amount of air bubbles is coming out with the vacuum, there is probably a leak in the jacket.

Confinement at 100kPa is added and the vacuum is removed, so that the sample still “feels” the same amount of confinement. If the test is going to be run with axis translation this is the time to add air pressure to the top of the sample while simultaneously adding the same amount of pressure to the confining air. Mineral oil has been used as a confining fluid in this apparatus. Mineral oil was chosen because of the electrical connections that would be in contact with the confining fluid. This fluid did not work when the acoustics were taken. It drastically changed the shape and arrival time of the acoustic waves. The acoustic waves may have been traveling through the confining fluid and not through the sample. If the acoustics are not being taken during the experiment, mineral oil may be used, and if another type of membrane is used and the acoustic wires are not in the apparatus, water could easily be used as the confining fluid.

B.2 Flow pump operation:

The start of the test is a little tricky, because of removing the water that is in the upper cap. The design of the upper cap has been modified so that the volume of water above the sample is limited. The recommended procedure is to set the “maintain pressure” to a low pressure below the expected air entry pressure, 1-3 kPa. Water will be withdrawn from

the apparatus, and if the air entry pressure has not been reached this water will be coming from above the sample, and not from within it. It may be useful to make a calculation of the total water which can be held in the top cap and the top water line. By increasing the pressure in small increments at the initial stages, the air entry pressure can be found with higher precision.

In a suction controlled test with axis translation, the flow pump is used to maintain the level of suction at the bottom of the sample. The air pressure at the top of the sample is maintained with an air regulator at a constant value throughout the test. The outlet valve on the flow pump should be open at the start of the test, and the value of flow pump pressure at rest can be determined. Then, that value is decreased and the amount it is decreased from the “at rest value” is equivalent to the capillary pressure. The test progresses as the flow pump pressure is lowered and the sample is desaturated in steps. The value of the steps depends on the material, generally the smaller the step, the shorter the equilibration time.

To set the value of pressure in the flow pump, the maintain pressure command is used. The manual for operation of the flow pump is available online, in the soils lab and on the documentation CD that came with the software. The value of final pressure is set to the desired pressure and the maintain pressure command is started. All of this is done using the keypad on the flow pump, it is a fairly user friendly interface. The final volume must

be set to a value which is much larger than what is expect to withdraw, or else it will trigger the end of the command.

The flow pump stores in its internal memory 1948 data points. Each data point includes, the reading number, the time elapsed, the volume withdrawn and the pressure. The flow pump needs to be connected to the computer which has the GeoComp software on it. The DIAGS program allows access to the internal memory of all of the machines. Flow pump #66 is currently connected to the apparatus, on the DIAGS screen this needs to be specified. The data can then be downloaded and shown on the screen in a text format. The memory only holds data from the function it is currently running. As soon as the function is changed on the flow pump a new data file is started and any data from previous functions is lost. The text file is saved under another filename on the computer, and then opened to see if equilibrium has been achieved, which will be explained later. If equilibrium has been achieved, that data file is saved, and the pressure step is changed on the flow pump. The flow pump holds 1,948 data points. The sampling rate is set at 1 sample per minute, so that a total of about 32 hours of data is collected. It also matches the sampling rate used on the omega pressure transducer.

To determine if equilibrium has been achieved, the data text file is opened in excel. The rate in cc/min (found by subtracting the volume withdrawn per minute from the value before it) is plotted versus the time. Once this rate fluctuates consistently between zero and the lowest value the flow pump is capable of, equilibrium has been achieved. In some

tests the rate will actually start fluctuating over zero, between injection and withdrawal.

An example of the figure produced is below (Figure B-1).

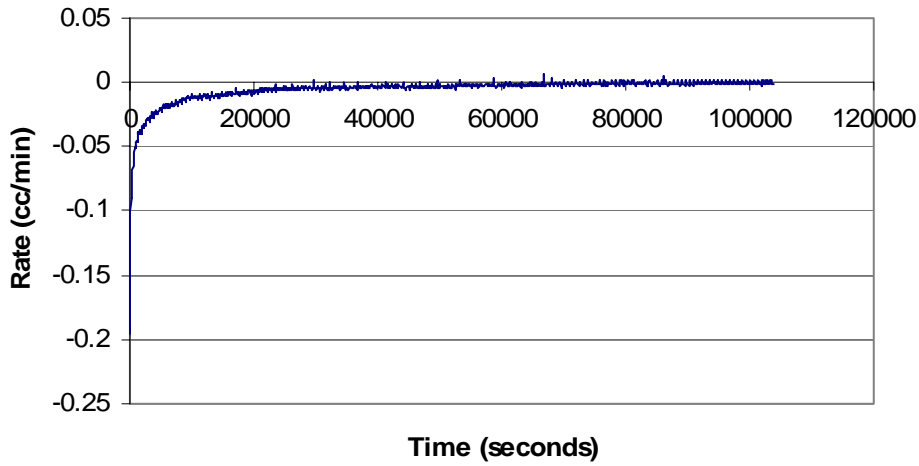


Figure B-1: Flow pump data, Rate versus Time

This figure of rate versus time coincides with the volume withdrawn versus time plot shown below (Figure B-2).

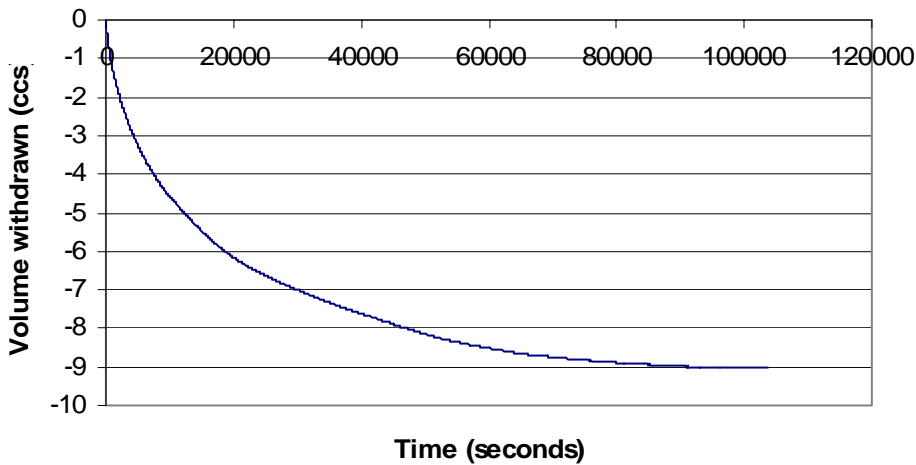


Figure B-2: Flow pump data, Volume withdrawn versus Time

The water has practically stopped being withdrawn by the time equilibrium has been declared.

B.3 Data Acquisition:

The entire time the experiment is running, the capillary pressure is being recorded using the omega pressure transducer that is placed between the upper air supply line and the lower water pressure line. This data is collected through a National Instruments Data Acquisition board that is hooked up to the white computer in the lab. The program CapPress writes the data to a file in a location the user specifies and controls the sampling rate. The data is written to an excel file that is opened and plotted using Matlab. When analyzing all the data at the end of the experiment, the data from the omega transducer are matched to the files produced from the flow pump. This results in a complete set of pressure and saturation data.

Electrical noise in the omega transducer has been a problem. It seems that the power supply was a large contributor, and it has been replaced a few times. The current power supply seems to work very well. Challenges with grounding also exist, and contribute significant noise. All of these issues have been addressed, and the noise has been reduced as much as possible. There is fluctuations in the pressure readings up to about 0.1 kPa, this is considered insignificant and could be averaged out of the data as it is only electrical noise.

B.4 Acoustic Data Acquisition:

The acoustic data is collected using the AutoLab system provided to us by New England Research, Inc. NER is a good source of information when using this equipment. There

are limited instructions available, if there are problems or questions NER can be contacted directly, and possibly come to UVM for a training day. There are three capabilities used in the autolab software related to this research; taking single acoustic measurements, taking acoustic measurements on a regular schedule, changing the frequency of the measurements taken. The user name and password to the acoustic equipment should be labeled on the computer, but if it is not the user name is uvm and the password is vermont, for administrative privileges use user name root password root*.

To make single low frequency acoustic measurements a section of the software called LFV is used. Open the autolab software using the Kelly wavelet icon on the bottom of the computer. Enter all the information about the experiment and sample, none of this information is used in calculations it is just there for the user. Open the LFV icon on the bottom-middle right side of the screen. Then initialize by pressing capture (preferably with the frequency levels and wave type chosen for your experiment). Now acoustic measurements can be taken by changing the pull down menu to capture and pressing the capture button. The waves that are being collected can be seen on the oscilloscope. After initialization the oscilloscope can be manually changed to any frequency level but these waveforms will not be collected. When all of the acoustic waves have been collected, press 'stop data acquisition' and start 'processing data'. The most current file created will be at the bottom of the list, they are all named with a time stamp. Highlight the file just created (or any other) and hit 'process traces'. This will allow the waveforms to be displayed, filters applied and arrival times to be picked. These features were not used in

this work, but can be used as a quick reference. Waveform files were created and analyzed in Matlab. To do this, choose 'Traces to spreadsheet', which creates a tss file that can be read by Matlab.

To make regularly scheduled measurements, follow the same steps as described in the previous section, until initialization. After initialized, go to Mode -> Script. Open and run any scripts that have been written. These scripts can be copied and modified. They contain information about the frequencies and wavetypes being collected, as well as specify the time between measurements.

To change the frequencies of the measurements collected the user file must be modified. The file is located at the following `/focus/autolab-5/etc/exptypes/user_lfv/user_lfv.tcl`
Change the values of the matrix labeled `flist.list`, the first column is the number that will show on the pull down menu and the second column is the actual frequency sent to the oscilloscope. There is one important inconsistency here. The frequency that is sent to the oscilloscope is not the actual center frequency of the wave it produces. The frequency sent needs to be multiplied by 2.87 to get the actual frequency. Usually, the label is set as the actual frequency and the frequency sent is that divided by 2.87.

APPENDIX C: Data Analysis

This appendix describes the analysis procedures used during the course of this research. The procedures are separated into two major sections; hydraulic data analysis and acoustic data analysis. Within the hydraulic data analysis section the determination of the capillary pressure function is described, and the determination of the unsaturated hydraulic conductivity function using inverse modeling. Within the acoustic data analysis section the use of taffy to model the experimental waveforms, the use of WAVE-UNSAT to determine the capillary relaxation time, and finally the Matlab program dynamic.m which predicts the dynamic capillary pressure function is described.

C.1 Hydraulic Data Analysis:

C.1.1 Capillary Pressure Function:

In the procedures section the methods used to collect the flow pump data and the omega differential pressure transducer data were described. These are the only two data types that are needed for the determination of the static capillary pressure function. But they are not taken using the same data acquisition system, so they need to be put together and synchronized using Matlab. The flow pump data is stringed together to make a continuous stream of volume data over the whole experiment. The volume data is converted into a moisture content once the porosity of the material is known. This can be found by determining the moisture content at the end of the experiment, destructively,

and back calculating the saturated porosity. When the data from the flow pump and the differential pressure transducer are combined, the result is similar to the following;

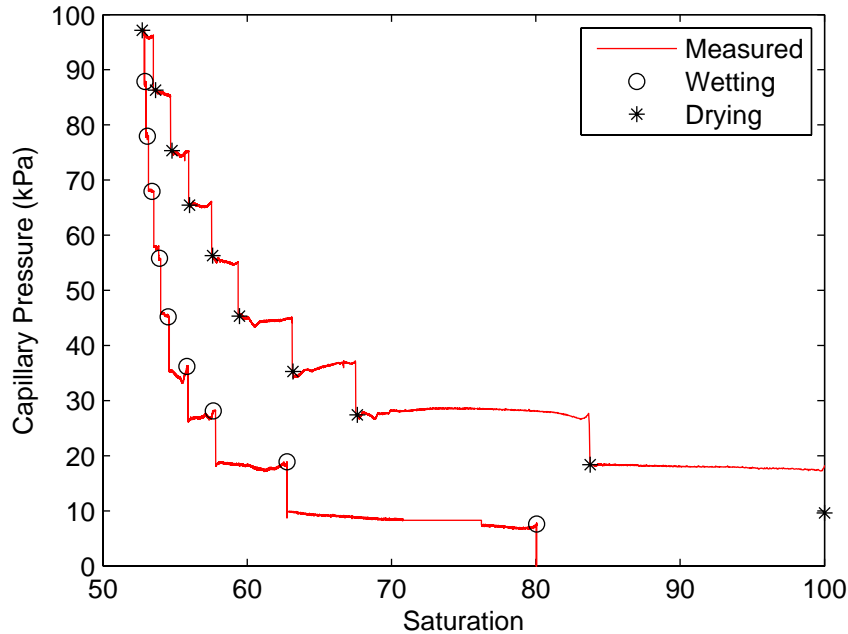


Figure C-1: Raw capillary pressure relationship data

The equilibrium points are shown on the figure and they are used to fit a van Genuchten or Brooks and Corey function. A program on the internet, swrc fit (<http://seki.webmasters.gr.jp/swrc/>) can be used to fit the function, but a fitting program can easily be written in Matlab or excel to do the same. The validity of the capillary pressure is also checked, since it is measured at two different points, the top air and the bottom water pressure. This procedure is explained in Chapter 2, but the program used is also available on the internet, the fitted capillary pressure function is input into the program and it shows if there is an effect. (<http://www.ag.auburn.edu/agrn/sp/truecell.html>). This program uses the Brooks and

Corey relationship, although, the inverse modeling procedure works better with van Genuchten parameters.

C.1.2 Unsaturated Hydraulic Conductivity Function:

The unsaturated hydraulic conductivity function is obtained through inverse modeling using the software HYDRUS-1 (http://www.pc-progress.cz/Fr_Hydrus.htm). The data needed for the inverse model can be obtained from the capillary pressure and volume data over time that was collected as described in the last section. The raw data needed for the inverse modeling includes the van Genuchten parameters for the capillary pressure function, points describing the pressure change at the bottom of the sample over time, and the function that we are trying to model, namely points from the volume withdrawn over time. All of this information can be reduced using Matlab to get a reasonable number of points that describe the experiment well. The optimization procedure is written into the program, so the parameters to optimize can be chosen and the optimization run. Problems were encountered when trying to use the Brooks and Corey relationship. This program comes with a really good manual and help menu, it should be self explanatory.

C.2 Acoustic Data Analysis:

C.2.1 Modeling Acoustic Waves:

The acoustic waves have been collected using the autolab software and then made into spreadsheet form and opened with a Matlab program for filtering and viewing. A Butterworth low pass filter is used to get rid of noise, but any low pass filter could work to get rid of the high frequency noise. Taffy is the program written by Martin Smith at NER that has been used for solving the one dimensional wave propagation equations. The instructions for building taffy on a unix machine are as follows. The program is installed to run on the machine named Rig in Votey. The files needed are included in the CD. NER has allowed this program to be open to the public.

Building taffy:

Make sure the machine has the packages fftw3 and lapack installed. If you're connected to the net, it should work to issue, as root, **yum install fftw3** and **yum install lapack**. Unpack the gzip'd tar file somewhere **tar xzvf ptaffy.tar.gz**. Cd to ptaffy and execute **make -f Makefile.pt** and it should crank around for a bit and leave the executable ptaffy in the directory. Try running a test with **ptaffy -P 1 -C TestCases/purepzt.couple.taffy** and after a little bit a bunch of ascii text containing trace data should race by on the screen. If you get that far, save the data into a file and see if you can connect the contents of the output file with the input file, TestCases/purepzt.couple.taffy. There are a couple of sample files (suffix'd .taffy). Run those and plot the traces you get.

To modify the input file use **nano folder/input.taffy**, if everything else in the input file is correct you can just modify the velocity and attenuation of the soil material to find the waveform that best matches the experimental one. To send the output to a file, use **ptaffy -C folder/input.taffy > output.out**. This output file can be read in Matlab and plotted against the experimental waveform.

More instructions for the program can be found in the manual page for taffy, this includes a description of inputs and outputs. To view the manual pages **cd ptaffy/ptaffy**, and use **nroff -man taffy.1**. A library of waveforms can be created and then searched through to find a match between the experimental and modeled waveforms.

C.2.2 Finding the capillary relaxation times using WAVE-UNSAT:

WAVE-UNSAT is a fortran code written by Changfu Wei, which estimates the velocity and attenuation of waves over a range of saturations based on given capillary relaxation times, both in the air and water. To use this program to find the capillary relaxation time, a trial and error approach is used, by adjusting the capillary relaxation times for each saturation until both the velocity and attenuation match the measured values. The inputs for the program are described in the following and the files needed to run the program are included in the CD.

1. A file with name “file.txt” must be created and put in the same folder as the executive file “WAVE_UN.S.EXE”. This file contains 4 lines:

1st line: the name of input file, this is a text file, e.g., you may write “input.txt”

2nd line: the name of output file, this is a text file, e.g., you may write

“output.txt”

3rd line: the name of soil water characteristic curve, a text file, e.g., “SWCC.txt”

4th line: the name of the original solution of a 3rd-order polynomial equation with complex coefficients, a text file, e.g., “solution.txt”

2. Input file

Name: input.dat (you can choose other names with extension “.txt” or “.dat” as specified above)

Line 1: iflag, itype

(iflag = 1 or 2; itype = 1)

Line 2: df

(If iflag = 1, df is the frequency; if iflag = 2, df is the saturation)

Line 3: $\rho^S, \rho^W, \rho^N, n$

(mass densities of solid material, wetting fluid and non-wetting fluid, respectively, all in kg/m³; n is the porosity)

Line 4: K_s, K_w, K_n

(bulk moduli of solid material, wetting fluid and nonwetting fluid, respectively, all in Pa) you may choose $K_s = 36\sim 39$ (x 10⁹ Pa)

Line 5: G (or ν), $K, \alpha_B, \tau_w, \tau_n$

(K is the (*undrained*) bulk modulus of the soil matrix, in Pa; α_B is the Biot effective stress coefficient; τ_W and τ_N are apparent relaxation times)

You can estimate these data (G and K) by fitting the acoustical velocity of the wetting sample.

Line 6: k_{sat}, η_W, η_N

(Saturated permeability [m^2], and dynamic viscosities [Pa.s])

Line 7: $i_{hydr}, p_b, \lambda, S_{rw}, S_{rm}$

(if $i_{hydr} = 1$, Brooks-Corey's equation is used)

3. Output file

Name: output.txt (you can choose other names with extension “.txt” or “.dat”)

This file contains 8 columns corresponding to:

Saturation, frequency, v1, 1000/Q1, v2, 1000/Q2, v3, 1000/Q3

Performing this trial and error procedure is challenging. Not only are the capillary relaxation times found using this program, but estimations of K, G, are also made. The best way to go about this is to start with the capillary relaxation times equal to zero, this will give the lower bound of the data. These numbers should be close to the lowest saturation values, if they are too low you will have a hard time getting up to the highest levels of saturation. Also try the upper bound of 1000 for each of the relaxation times. This will give a good first guess at K and G. Then start adjusting the capillary relaxation times. The capillary relaxation of the wetting fluid is always higher than the non wetting

fluid, and they both increase as saturation increases. It is easier to start at the lower saturations and work up in saturations.

C.2.3 Prediction of the dynamic capillary pressure function:

A Matlab program has been written which solves the dynamic capillary pressure relationship given in the Chapters 1 and 4, the m files are included in the CD. Inputs need to be changed in the m file for the porosity, irreducible and saturated moisture contents and the parameters for the Brooks-Corey capillary pressure relationship. The capillary relaxation times need to be input into an m file called Tau_c, which will perform a linear interpolation of the discrete points for all saturation levels. The rate of pressure change can be changed to the desired level and the dynamic capillary pressure relationships will be plotted. There are more instructions included in the text of the m-file.

COMPREHENSIVE BIBLIOGRAPHY:

- Adamchuk, V. I. (2006). "Characterizing Soil Variability Using On-the-go Sensing Technology." Site Specific Management Guidelines.
- Adamo, F., Andria, G., Atticissimo, F., and Giaquinto, N. (2004). "An Acoustic Method for Soil Moisture Measurement." IEEE Transactions on Instrumentation and Measurement, 53(4), 891-898.
- Aramahi, B., Alshibli, K., Fratta, D., and Trautwein, S. J. (2008). "A Suction-Controlled Apparatus for the Measurement of P and S-Wave Velocity in Soils." Geotechnical Testing Journal, 31(1), 12-23.
- Anderson, S. H., Gantzer, C. J., Boone, J. M., and Tully, R. J. (1988). "Rapid Nondestructive Bulk Density and Soil-Water Content Determination by Computed Tomography." Soil Science of America Journal, 52, 35-40.
- Arroyo, M., Wood, D. M., Greening, P. D., Medina, L., and Rio, J. (2006). "Effects of sample size on bender-based axial G₀ measurements." Geotechnique, 56(1), 39-52.
- Arulnathan, R., Boulanger, R. W., and Riemer, M. F. (1998). "Analysis of bender element tests." Geotechnical Testing Journal, 21(2), 120-131.
- Arya, L. M., and Paris, J. F. (1981). "A physico-empirical model to predict the soil moisture characteristic from particle size distribution and bulk density data." Soil Science Society of America Journal, 45, 1023-1030.

- Ataie-Ashtiani, B., Hassanizadeh, S. M., and Celia, M. A. (2002). "Effects of heterogeneities on capillary-pressure-saturation-relative permeability relationships." *Journal of Contaminant Hydrology*, 56, 175-192.
- Bachrach, R., and Nur, A. (1998). "High-resolution shallow-seismic experiments in sand, Part 1: Water table, fluid flow and saturation." *Geophysics*, 63(4), 1225-1233.
- Badri, M., and Mooney, H. M. (1987). "Q measurements from compressional seismic waves in unconsolidated sediments." *Geophysics*, 52(6), 772-784.
- Bardet, J. P. (1992). "A viscoelastic model for the Dynamic Behavior of Saturated Poroelastic Soils." *Transactions of the ASME*, 59, 128-135.
- Bardet, J. P., and Sayed, H. (1994). "Velocity and attenuation of compressional waves in nearly saturated soils." *Soil Dynamics and Earthquake Engineering*, 12, 391-401.
- Barry, D. A., Parlange, J. Y., Sander, G. C., and Sivaplan, M. (1993). "A class of exact solutions for Richards' equation." *Journal of Hydrology*, 142, 29-46.
- Bedford, A., and Stern, M. (1982). "A model for wave propagation in gassy sediments." *Journal of Acoustic Society of America*, 73, 409-417.
- Bentley, L. R., and Gharibi, M. (2004). "Two- and three-dimensional electrical resistivity imaging at a heterogeneous remediation site." *Geophysics*, 69(3), 674-680.
- Beresnev, I. A., and Johnson, P. A. (1994). "Elastic-wave simulation of oil production: a review of methods and results." *Geophysics*, 59(6), 1000-1017.
- Berge, P. A., and Bonner, B. P. (2002). "Seismic velocities contain information about depth, lithology, fluid content and microstructure." UCRL-JC-144792, DOE Lawrence Livermore National Laboratory.

- Besson, A., Cousin, I., Samouelian, A., Boizard, H., and Richard, G. (2004). "Structural Heterogeneity of the soil tilled layer as characterized by 2D electrical resistivity surveying " *Soil and Tillage Research*, 79(2), 239-249.
- Bicalho, K. V. (1999). "Modeling Water Flow in an Unsaturated Compacted Soil," PhD Thesis, University of Colorado, Boulder.
- Biot, M. A. (1955). "Theory of Propagation of Elastic Waves in a Fluid-Saturated Porous Solid. II. Higher Frequency Range." *The Journal of the Acoustical Society of America*, 28(2), 179-191.
- Biot, M. A. (1956). "Theory of Deformation of a Porous Viscoelastic Anisotropic Solid." *Journal of Applied Physics*, 27(5), 459-467.
- Biot, M. A. (1956). "Theory of Propagation of Elastic Waves in a Fluid-Saturated Porous Solid I. Low Frequency Range." *The Journal of the Acoustical Society of America*, 28(2), 168-178.
- Biot, M. A. (1972). "Mechanics of finite deformation of porous solids." *Indiana University Mathematical Journal*, 21, 597-620.
- Blewett, J., Blewett, I. J., and Woodward, P. K. (1999). "Measurement of shear-wave velocity using phase-sensitive detection techniques." *Canadian Geotechnical Journal*, 36, 934-939.
- Bocking, K. A., and Fredlund, D. G. "Limitations of the axis translation technique." *Fourth International Conference on Expansive Soils*, Denver, Colorado, 117-135.
- Bonner, B. P., Berge, P. A., Aracne-Ruddle, C. M., Bertete-Aguirre, H., Wildenchild, D., Trombino, C. N., and Hardy, E. D. (2000). "Linear and Nonlinear Ultrasonic

- Properties of Granular Soils." UCRL-JC-136207, DOE Lawrence Livermore National Laboratory.
- Bonner, B. P., Berge, P. A., and Wildenchild, D. (2001). "Compressional and Shear Wave Velocities for Artificial Granular Media Under Simulated Near Surface Conditions." UCRL-JC-142935, DOE Lawrence Livermore National Laboratory.
- Bourbie, T., Coussy, O., and Zinszner, B. (1987). *Acoustics of Porous Media*, Editions Technip Paris.
- Brignoli, E. G. M., Gotti, M., and Stokoe, K. H. (1996). "Measurement of Shear Waves in Laboratory Specimens by Means of Piezoelectric Transducers." *Geotechnical Testing Journal*, 19(4), 384-397.
- Brooks, R. H., and Corey, A. T. (1964). "Hydraulic properties of porous media." *Colorado State Univ, Fort Collins, Colorado*.
- Brown, J. M., Fonteno, W. C., Cassel, D. K., and Johnson, G. A. (1987). "Computed Tomographic Analysis of Water Distribution in Three Porous Foam Media." *Soil Science of America Journal*, 51, 1121-1125.
- Brutsaert, W. (1964). "The Propagation of Elastic Waves in Unconsolidated Unsaturated Granular Mediums." *Journal of Geophysical Research*, 69(2), 243-257.
- Buckingham, M. J. (1997). "Theory of acoustic attenuation, dispersion, and pulse propagation in unconsolidated granular materials including marine sediments." *Journal of Acoustic Society of America*, 102(5), 2579-2596.

- Cadoret, T., Marion, D., and Zinszner, B. (1995). "Influence of frequency and fluid distribution on elastic wave velocities in partially saturated limestones." *Journal of Geophysical Research*, 100(B6), 9789-9803.
- Cadoret, T., Mavko, G., and Zinszner, B. (1998). "Fluid distribution effect on sonic attenuation in partially saturated limestones." *Geophysics*, 63(1), 154-160.
- Carcione, J. M., Helle, H. B., and Pham, N. H. (2003). "White's model for wave propagation in partially saturated rocks: Comparison with poroelastic numerical experiments." *Geophysics*, 68(4), 1389-1398.
- Carcione, J. M., and Picotti, S. (2006). "P-wave seismic attenuation by slow-wave diffusion: Effects of inhomogeneous rock properties." *Geophysics*, 71, 1-8.
- Carcione, J. M., Seriani, G., and Gei, D. (2003). "Acoustic and electromagnetic properties of soils saturated with salt water and NAPL." *Journal of Applied Geophysics*, 52, 177-191.
- Celia, M. A., Bouloutas, E. T., and Zarba, R. L. (1990). "A General Mass-Conservation Numerical Solution for the Unsaturated Flow Equation." *Water Resour. Res.*, 26(7), 1483-1496.
- Chen, L., Miller, G. A., and Kibbey, T. C. (2007). "Rapid Pseudo-Static Measurement of Hysteretic Capillary Pressure-Saturation Relationships in Unconsolidated Porous Media " *Geotechnical Testing Journal*, 30(6), DOI: 10.1520/GTJ100850.
- Cheng, C. H., and Toksoz, M. N. (1981). "Elastic wave propagation in a fluid-filled borehole and synthetic acoustic logs." *Geophysics*, 46(7), 1042-1053.

- Cheng, N., Cheng, C. H., and Toksoz, M. N. (1995). "Borehole wave propagation in three dimensions." *Journal of Acoustic Society of America*, 97(6), 3483-3493.
- Cislerova, M., and Votrubova, J. (2002). "CT derived porosity distribution and flow domains." *Journal of Hydrology*, 267, 186-200.
- Claria, J. J., and Rinaldi, V. A. (2007). "Shear Wave Velocity of a Compacted Clayey Silt." *Geotechnical Testing Journal*, 30(5), 1-9.
- Clothier, B., and Scotter, D. (2002). "Unsaturated Water Transmission Parameters Obtained from Infiltration." *Methods of Soil Analysis, Part 4, Physical Methods*, J. H. Dane and G. C. Topp, eds., SSSA, Madison, WI, 879-898.
- Constantz, J. (1993). "Confirmation of Rate-Dependent Behavior in Water Retention During Drainage in Nonswelling Porous Materials." *Water Resour. Res.*, 29(4), 1331-1334.
- Coussy, O., Dormieux, L., and Detournay, E. (1998). "From Mixture theory to Biot's approach for porous media." *International Journal of Solids and Structures*, 35(34-35), 4619-4635.
- Crestana, S., Mascarenhas, S., and Pozzi-Mucelli, R. S. (1985). "Static and Dynamic Three-Dimensional Studies of Water in Soil Using Computed Tomographic Scanning." *Soil Science*, 40(5), 326-332.
- Dahle, H. K., Celia, M. A., and Hassanizadeh, S. M. (2005). "Bundle-of-Tubes Model for Calculating Dynamic Effects in the Capillary-Pressure-Saturation Relationship." *Transport in Porous Media*, 58, 5-22.

- Daley, T. M., Majer, E. L., and Peterson, J. E. (2004). "Crosswell seismic imaging in a contaminated basalt aquifer." *Geophysics*, 69(1), 16-24.
- Dane, J. H., and Topp, G. C. (2002). *Methods of Soil Analysis Part 4 Physical Methods*, Soil Science Society of America, Inc. , Madison, WI.
- Davidson, J. M., Nielsen, D. R., and Biggar, J. W. (1966). "The dependence of soil water uptake and release upon the applied pressure increment." *Soil Science Society of America Journal*, 30, 298-303.
- Delerue, J. F., Perrier, E., Timmerman, A., and Rieu, M. "New Computer tools to quantify 3D porous structures in relation with hydraulic properties." *Transport Processes in Soils*, Wageningen, Netherlands.
- Diagle, M., Fratta, D., and Wang, L. B. "Ultrasonic and X-ray Tomographic Imaging of Highly Contrasting Inclusions in Concrete Specimens." *Geo-frontiers*, Austin, Texas.
- Domenico, S. N. (1976). "Effect of brine-gas mixture on velocity in an unconsolidated gas reservoir." *Geophysics*, 41, 882-894.
- Durner, W., Schultze, D., and Zurmühl, T. "State-of-the-Art in Inverse Modeling of Inflow/Outflow Experiments." *International Workshop on Characterization and Measurement of the Hydraulic Properties of Unsaturated Porous Media*, Riverside, CA, 661-681.
- Dutta, N. C., and Odé, H. (1983). "Seismic reflections from a gas-water contact." *Geophysics*, 48, 148.

- Dutta, N. C., and Seriff, A. J. (1979). "On White's model of attenuation in rocks with partial gas saturation." *Geophysics*, 44, 1806.
- Dvorkin, J., and Nur, A. (1993). "Dynamic poroelasticity: A unified model with the squirt and the Biot mechanisms." *Geophysics*, 58(4), 524-533.
- Emmerich, H. a. K., M. . (1987). "Incorporation of attenuation into time-domain computations of seismic wave fields." *Geophysics*, 52(9), 1252-1264.
- Fetter, C. W. (1999). *Contaminant Hydrogeology*, Prentice Hall, Upper Saddle River.
- Flammer, I., Blum, A., Leiser, A., and Germann, P. (2001). "Acoustic assessment of flow patterns in unsaturated soils." *Journal of Applied Geophysics*, 46, 115-128.
- Fredlund, D. G., and Rahardjo, H. (1993). *Soil Mechanics for Unsaturated Soils*, John Wiley & Sons, Inc.
- Fredlund, M. D., Wilson, G. W., and Fredlund, D. G. "Indirect procedures to determine unsaturated soil property functions." 50th Canadian Geotechnical Conference, Ottawa, Ontario, Canada, 9.
- Garambois, S., Senechal, P., and Perroud, H. (2002). "On the use of combined geophysical methods to assess water content and water conductivity of near-surface formations." *Journal of Hydrology*, 259, 32-48.
- Garg, S. K., and Nayfeh, A. H. (1986). "Compressional wave propagation in liquid and/or gas saturated elastic porous media." *Journal of Applied Physics*, 60(9), 3045-3055.
- Gei, D., and Carcione, J. M. (2003). "Acoustic Properties of sediments saturated with gas hydrate, free gas and water." *Geophysical Prospecting*, 51, 141-157.

- George, L. A., Dewoolkar, M. M., and Wei, C. "A device for simultaneous measurement of acoustic and hydraulic properties in unsaturated soil." Proceedings of the First European Conference on Unsaturated Soils, E-UNSAT 2008, Durham, UK, 97-102.
- Ghose, R., and Slob, E. C. (2006). "Quantitative integration of seismic and GPR reflections to derive unique estimates for water saturation and porosity in subsoil." *Geophysical Research Letters*, 33(5).
- Ghosh, R. K. (1976). "Model of the soil moisture characteristic." *Journal of the Indian Society of Soil Science*, 24, 353-355.
- Gist, G. A. (1994). "Fluid effects on velocity and attenuation in sandstones." *Journal of Acoustic Society of America*, 96(2), 1158-1173.
- Gladwin, M. T., and Stacey, F. D. (1974). "Anelastic degradation of acoustic pulses in rock." *Physics of the Earth and Planetary Interiors*, 8, 332-336.
- Goertz, D., and Knight, R. (1998). "Elastic wave velocities during evaporative drying." *Geophysics*, 63(1), 171-183.
- Gray, W. G., and Hassanizadeh, S. M. (1989). "Averaging theorems and averaged equations for transport of interface properties in multiphase systems." *International Journal of Multiphase Flow*, 15(1), 81-95.
- Gregory, A. R. (1976). "Fluid saturation effects on dynamic elastic properties of sedimentary rock." *Geophysics*, 41, 895-921.
- Gregory, A. R. (1976). "Fluid saturation effects on dynamic elastic properties of sedimentary rocks." *Geophysics*, 41(895-921).

- Griffiths, D. H., and King, R. F. (1983). *Applied Geophysics for Geologists & Engineers*, Pergamon Press, Oxford.
- Guerin, R. (2005). "Borehole and surface-based hydrogeophysics." *Hydrogeology Journal*, 13, 251-254.
- Gurevich, B., Marschall, R., and Shapiro, S. A. (1994). "Effect of fluid flow on seismic reflections from a thin layer in a porous medium." *Journal of Seismic Exploration*, 3, 125-140.
- Gurevich, B., Zyrianov, V. B., and Lopatnikov, S. L. (1997). "Seismic attenuation in finely layered porous rocks: effects of fluid flow and scattering." *Geophysics*, 62(1-6).
- Guyonnet, D., Gourry, J.-C., Bertrand, L., and Amraour, N. (2003). "Heterogeneity detection in an experimental clay liner." *Canadian Geotechnical Journal*, 40, 149-160.
- Haeni, F. P. (1986). "Application of seismic-refraction techniques to hydrologic studies." U.S. Geol. Sur. Open File Report 84-0746.
- Hallenburg, J. K. (1998). *Introduction to Geophysical Formation Evaluation*, CRC Press, Boca Raton.
- Hallenburg, J. K. (1998). *Standard Methods of Geophysical Formation Evaluation* CRC Press, Boca Raton.
- Hamilton, E. L. (1970). "Reflection coefficients and bottom losses at normal incidence computed from pacific sediment properties." *Geophysics*, 35(6), 995-1004.

- Hanafy, S., and Hagrey, S. A. a. (2006). "Ground-penetrating radar tomography for soil-moisture heterogeneity." *Geophysics*, 71(1), k9-k18.
- Hassanizadeh, S. M., Celia, M. A., and Dahle, H. K. (2002). "Dynamic Effects in the Capillary Pressure-Saturation Relationship and its Impact on Unsaturated Flow." *Vadose Zone Journal*, 1, 38-57.
- Hassanizadeh, S. M., and Gray, W. G. (1979). "General Conservation Equations for multiphase systems: a & b." *Advances in Water Resources*, 2, 131-203.
- Hassanizadeh, S. M., and Gray, W. G. (1993). "Thermodynamic basis of capillary pressure in porous media." *Water Resour. Res.*, 29, 3389-3405.
- Haverkamp, R., and Vauclin, M. (1980). "A Comparative Study of Three Forms of the Richard Equation used for Predicting One-Dimensional Infiltration in Unsaturated Soils." *Soil Science Society of America Journal*, 45, 13-20.
- Healthcare, G. (2005). "CT Generation." *W*.
- Heijs, A. W. J., and Lange, J. d. (1997). "Determination of pore networks and water content distribution from 3-D computed tomography images of a clay soil." *Bioimaging*, 5, 194-204.
- Helle, H. B., Pham, N. H., and Cacione, J. M. (2003). "Velocity and attenuation in partially saturated rocks: poroelastic numerical experiments." *Geophysical Prospecting*, 51, 551-566.
- Helmig, R., Weiss, A., and Wohlmuth, B. (2007). "Dynamic capillary effects in heterogeneous porous media." *Computational Geoscience*, 11, 261-274.

- Hilf, J. W. (1956). "An Investigation of Pore-water Pressure in Compacted Cohesive Soils, PhD dissertation." US Department of the Interior, Bureau of Reclamation, Design and Construction Division, Denver, Colorado.
- Ho, C. K., Lindgren, E. R., Rawlinson, K. S., McGrath, L. K., and Wright, J. L. (2003). "Development of a Surface Acoustic Wave Sensor for In-situ Monitoring of Volatile Organic Compounds." *Sensors*, 3, 236-247.
- Hopmans, J. W., Vogel, T., and Koblik, P. D. (1992). "X-ray Tomography of Soil Water Distribution in One-Step Outflow Experiments." *Soil Science of America Journal*, 56, 355-362.
- Horton, R., Wierenga, O. J., and Nielson, D. R. (1982). "A rapid technique for obtaining uniform water content distributions in unsaturated soil columns." *Soil Science*, 133(6), 397-399.
- Hubbard, S., Grote, K., and Rubin, Y. (2002). "Mapping the volumetric soil water content of a California vineyard using high-frequency GPR ground wave data." *The Leading Edge*, 553-559.
- Imhof, M. G. (2003). "Scale dependence of reflection and transmission coefficients." *Geophysics*, 68(1), 322-336.
- Jakobsen, M., Johansen, T. A., and McCann, C. (2003). "The acoustic signature of fluid flow in complex porous media." *Journal of Applied Geophysics*, 54(3-4), 219-246.
- Johnson, D. L. (2001). "Theory of frequency dependent acoustics in patchy-saturated porous media." *Journal of the Acoustic Society of America*, 110(2), 682-694.

- Jovicic, V., Coop, M. R., and Simic, M. (1996). "Objective criteria for determining Gmax from bender element tests." *Geotechnique*, 46(2), 357-362.
- Keys, W. S. (1997). *A Practical Guide to Borehole Geophysics in Environmental Investigation*, CRC Press, Boca Raton.
- Khanzode, R. M., Fredlund, D. G., and Vanapalli, S. K. "An alternative method for the measurement of soil-water characteristic curves for fine grained soils."
- Kibblewhite, A. C. (1989). "Attenuation of sound in marine sediments: A review with emphasis on new low-frequency data." *Journal of Acoustic Society of America*, 86(2), 716-738.
- Kimura, M., and Tsurumi, T. (2004). "Acoustic wave reflection from the transition layer of surficial marine sediment." *Acoustical Science and Technology*, 25(3), 188-195.
- Klimentos, T., and McCann, C. (1990). "Relationships among compressional wave attenuation, porosity, clay content and permeability in sandstones." *Geophysics*, 55(8), 998-1014.
- Klute, A. (1986). "Methods of Soil Analysis: Part 1 Physical and Mineralogical Methods." *Hydraulic Conductivity and Diffusivity: Laboratory Methods*, C. D. A. Klute, ed., American Society of Agronomy, Inc. Soil Science Society of America, Inc, Madison, 687-734.
- Knight, R., and Nolen-Hoeksema, R. (1990). "A Laboratory Study of the Dependence of Elastic Wave Velocities on Pore Scale Fluid Distribution." *Geophysical Research Letters*, 17(10), 1529-1532.

- Knight, R. J., and Endres, A. L. (2005). "An Introduction to Rock Physics Principles for Near-Surface Geophysics." Near-Surface Geophysics, D. K. Butler, ed., Society of Exploration Geophysicists, Tulsa, 31-65.
- Knopoff, L. (1964). "Q." Reviews of Geophysics, 2(4), 625-660.
- Kowalsky, M. B., Finsterle, S., and Rubin, Y. (2004). "Estimating flow parameter distributions using ground-penetrating radar and hydrological measurements during transient flow in the vadose zone." Advances in Water Resources, 27, 583-599.
- Krasovec, M. K., D. R. Burns, M. E. Willis, S. Chi, and M. N. Toksöz (2004). "3-D Finite Difference Modeling for Borehole and Reservoir Application." In MIT-ERL Reservoir Delineation Consortium Report.
- Lee, D. H., and Abriola, L. M. (1999). "Use of the Richards equation in land surface parameterizations." Journal of Geophysical Research, 104(d22), 27519-27526.
- Lee, J., and Santamarina, J. C. (2005). "Bender Elements: Performance and Signal Interpretation " Journal of Geotechnical and Geoenvironmental Engineering, 131(9), 1063-1069.
- Lee, M. (2004). "Elastic velocities of partially gas-saturated unconsolidated sediments." Marine and Petroleum Geology, 21(6), 641-650.
- Leij, F. J., Schaap, M. G., and Arya, L. R. (2002). "Indirect methods." Methods of Soil Analysis, Part 4:3.6.3. SSSA Book Series 5, J. H. Dane, Topp, C.G., ed., SSSA, Madison, WI.

- Leong, E.-C., Yeo, S.-H., and Rahardjo, H. (2004). "Measurement of wave velocities and attenuation using an ultrasonic test system." *Canadian Geotechnical Journal*, 41, 844-860.
- Lesmes, D. P., Decker, S. M., and Roy, D. C. (2002). "A multiscale radar-stratigraphic analysis of fluvial aquifer heterogeneity." *Geophysics*, 67(5), 1452-1464.
- Li, X., Zhong, L., and Pyrak-Nolte, L. J. (2001). "Physics of Partially Saturated Porous Media: Residual Saturation and Seismic-Wave Propagation." *Annual Review of Earth and Planetary Sciences*, 29, 419-460.
- Liu, H. H., and Dane, J. H. (1995). "Improved Computational Procedure for Retention Relations of Immiscible Fluids Using Pressure Cells." *Soil Science Society of America Journal*, 59, 1520-1524.
- Liu, Z., Rector, J. W., Nihei, K. T., Tomutsa, L., Myer, L. R., and Nakagawa, S. (2001). "Extensional wave attenuation and velocity in partially saturated sand in the sonic frequency range." Paper LBNL-50301, Lawrence Berkeley National Laboratory.
- Lo, W., Yeah, C., and Tsai, C. (2007). "Effect of soil texture on the propagation and attenuation of acoustic waves at unsaturated conditions." *Journal of Hydrology*, 338, 273-284.
- Lu, N., Wayllance, A., Carrera, J., and Likos, W. J. (2006). "Constant Flow Method for Concurrently Measuring Soil-Water Characteristic Curve and Hydraulic Conductivity Function " *Geotechnical Testing Journal*, 29(3), 256-266.
- Lu, Z., Hickey, C. J., and Sabatier, J. M. (2004). "Effects of Compaction on the Acoustic Velocity in Soils." *Soil Science of America Journal*, 68, 7-16.

- Majer, E. L., Williams, K. H., Peterson, J. E., and Daley, T. M. (2002). "High Resolution Imaging of Vadose Zone Transport Using Crosswell Radar and Seismic Methods." Lawrence Berkley National Laboratory
- Malone, M. K. (1987). "The Influence of Groundwater on Slope Stability," M. S. Thesis, University of Colorado, Boulder.
- Mavko, G., and Mukerji, T. (1998). "Bounds on low-frequency seismic velocities in partially saturated rocks." *Geophysics*, 63(3), 918-924.
- Mavko, G., and Nur, A. (1979). "Wave attenuation in partially saturated rocks." *Geophysics*, 44(2), 161-178.
- Mirzaei, M., and Das, D. B. (2007). "Dynamic effects in capillary pressure-saturation relationships for two-phase flow in 3D porous media: Implications of micro-heterogeneities." *Chemical Engineering Science*, 62, 1927-1947.
- Mohamed, M. H., and Sharma, R. S. (2007). "Role of Dynamic Flow in Relationships between Suction Head and Degree of Saturation." *Journal of Geotechnical and Geoenvironmental Engineering*, 133(3), 286-294.
- Mohsin, M. K., and Airey, D. W. "Automating Gmax measurements in triaxial apparatus." Lyon '03 International symposium on deformation behavior of Geomaterials.
- Molyneux, J. B., and Schmitt, D. R. (2000). "Compressional-wave velocities in attenuating media: A laboratory physical model study." *Geophysics*, 65(4), 1162-1167.

- Monsen, K., and Johnstad, S. E. (2004). "Improved understanding of velocity-saturation relationships using 4D computer-tomography acoustic measurements." *Geophysical Prospecting*, 53, 173-181.
- Moran, K., Altmann, V., O'Regan, M., and Ashmankas, C. (2007). "Acoustic Compressional Wave Velocity as a Predictor of Glacio-marine Sediment Grain Size " *Geotechnical Testing Journal*, 30(4), 1-7.
- Moret, G. J. M., Knoll, M. D., Barrash, W., and Clement, W. P. (2006). "Investigating the stratigraphy of an alluvial aquifer using crosswell seismic traveltime tomography." *Geophysics*, 71(3), B63-B73.
- Mukunoki, T., Otani, J., Obara, Y., Sugawara, K., and Hirata, A. "New Methodology using X-Ray CT data to characterize the engineering property of Geomaterials." 5th North American Rock Mechanics Symposium [NARMS] and 17th Tunneling Association of Canada [TAC] conference, Toronto, Ontario, Canada.
- Muller, T. M., and Gurevich, B. (2004). "One-dimensional random patchy saturation model for velocity and attenuation in porous rocks." *Geophysics*, 69(5), 1166-1172.
- Muller, T. M., and Gurevich, B. (2005). "Wave-induced fluid flow in random porous media: Attenuation and dispersion of elastic waves." *Journal of the Acoustic Society of America*, 117(5), 2732-2741.
- Muraleetharan, K. K., and Nedunuri, P. R. "A bounding surface elastoplastic constitutive model for monotonic and cyclic behavior of unsaturated soils." 12th Engineering Mechanics Conference, La Jolla, Ca, 1331-1334.

- Muraleetharan, K. K., and Wei, C. (1999). "Dynamic Behavior of Unsaturated Porous Media: Governing Equations using the Theory of Mixtures with Interfaces (TMI)." *International Journal of Analytical Methods in Geomechanics*, 23, 1579-1608.
- Murphy, W. F. (1982). "Effects of partial water saturation on attenuation in Massillon sandstone and Vycor porous glass." *Journal of Acoustic Society of America*, 71(6), 1458-1468.
- Murphy, W. F. (1984). "Acoustic Measures of Partial Gas Saturation in Tight Sandstones." *Journal of Geophysical Research*, 89(B13), 11,549-11,559.
- Murphy, W. F., Winkler, K. W., and Klienber, R. L. (1986). "Acoustic relaxation in sedimentary rocks: Dependence on grain contacts and fluid saturation." *Geophysics*, 51(3), 757-766.
- Muthukrishniah, K., Zachariah, R., Murthy, G. R. K., and Nair, P. V. (1995). "Relationship between geophysical and geotechnical properties of marine sediments using Biot-Stoll model." *Marine Georesources & Geotechnology* 13(3), 243-261.
- O'Connell, R. J., and Budiansky, B. (1977). "Viscoelastic properties of fluid-saturated cracked solids." *Journal of Geophysical Research*, 82(36), 5719-5736.
- O'Carroll, D. M., Phelan, T. J., and Abriola, L. M. (2005). "Exploring dynamic effects in capillary pressure in multistep outflow experiments." *Water Resour. Res.*, 41(W11419, doi:10.1029/2005WR004010).

- Oelze, M. L., O'Brien, W. D., and Darmody, R. G. (2002). "Measurement of Attenuation and Speed of Sound in Soils." *Soil Science Society of America Journal*, 66, 788-796.
- Olhoeft, G. "Geophysical Detection of Hydrocarbon and Organic Chemical Contamination." USGS.
- Olsen, H. W., Willden, A. T., Kiusalaas, N. J., Nelson, K. R., and Poeter, E. P. (1994). "Volume-Controlled Hydrologic Property Measurements in Triaxial Systems." *Hydraulic Conductivity and Waste Contaminant Transport in Soil*, ASTM STP 1142, D. E. Daniel and S. J. Trautwein, eds., American Society for Testing and Materials, Philadelphia, 482-504.
- Oza, A., Vanderby, R., and Lakes, R. S. (2003). "Interrelation of creep and relaxation for nonlinearly viscoelastic materials: application to ligament and metal." *Rheol Acta*, 42, 557-568.
- Paffenholz, J., and Burkhardt, H. (1989). "Absorption and Modulus Measurements in the Seismic Frequency and Strain Range on Partially Saturated Sedimentary Rocks." *Journal of Geophysical Research*, 94(B7), 9493-9507.
- Paillet, F. L., and White, J. E. (1982). "Acoustic modes of propagation in the borehole and their relationship to rock properties." *Geophysics*, 47(8), 1215-1228.
- Pan, C. (1998). "Spectral ringing suppression and optimal windowing for attenuation and Q measurements." *Geophysics*, 63(2), 632-636.

- Panfilov, M. B., and Panfilova, I. V. (1998). "Averaged model with capillary nonequilibrium effects for two-phase flow through a highly heterogeneous porous medium." *Fluid Dynamics*, 33(3), 373-381.
- Panfilov, M. B., and Tchijov, A. (2000). "Splitting the saturation and heterogeneity for time dependent effective phase permeabilities." *Computational Methods for Flow and Transport in Porous Media* J. M. Crolet, ed., 115-140.
- Parlange, J. Y., Barry, D. A., Parlange, M. B., Hogarth, W. L., Haverkamp, R., Ross, P. J., Ling, L., and Steenhuis, T. S. (1997). "New Approximate analytical technique to solve Richards equation for arbitrary surface boundary conditions." *Water Resour. Res.*, 33(4), 903-906.
- Parra, J. O., Hackert, C. L., and Sablik, M. J. (1999). "Dispersion and attenuation of acoustic waves in randomly heterogeneous media." *Journal of Applied Geophysics*, 42(2), 99-115.
- Petrovic, A. M., Siebert, J. E., and Rieke, P. E. (1982). "Soil Bulk Density Analysis in Three Dimensions by Computed Tomographic Scanning." *Soil Science of America Journal*, 46(3), 445-450.
- Prevost, J. (1980). "Mechanics of Continuous Porous Media." *International Journal Of Engineering Science*, 18(6).
- Pride, S. R., Berryman, J. G., and Harris, J. M. (2004). "Seismic attenuation due to wave-induced flow." *Journal of Geophysical Research*, 109(B1).
- Pride, S. R., Harris, J. M., and Johnson, D. L. (2003). "Permeability dependence of seismic amplitudes." *The Leading Edge*, 22, 518-525.

- Richards, L. A. (1931). "Capillary conduction of liquids in porous mediums." *Physics*, 1, 318-333.
- Robb, G., Best, A.I., Dix, J.K., Leighton, T.G., Harris, A., Riggs, J.S., Bull, J.M. and White, P.R. . "Frequency dependence of acoustic waves in marine sediments." Sixth European Conference on Underwater Acoustics, Gdansk, Poland, 43-49.
- Rogasik, H., Crawford, J. W., Wendroth, O., Young, I. M., Joschko, M., and Ritz, K. (1999). "Discrimination of Soil Phases by Dual Energy X-ray Tomography." *Soil Science of America Journal*, 63, 741-751.
- Rose, M. E. (1983). "Numerical Methods for Flows Through Porous Media, I." *Mathematics of Computation*, 40(162), 435-467.
- Ross, P. J., and Smettem, K. R. J. (2000). "A simple treatment of physical nonequilibrium water flow in soils." *Soil Society of America Journal*, 64, 1926-1930.
- Sabatier, J. M., Sokol, D. C., Fredrickson, C. K., Romkens, M. J. M., Grissinger, E. H., and Shipps, J. C. (1996). "Probe Microphone instrumentation for determining soil physical properties: testing in model porous material." *Soil Technology*, 8, 259-274.
- Sams, M., and Goldberg, D. "Short Note: The validity of Q estimates from borehole data using spectral ratios." *Geophysics*, 97-101.
- Schultze, B., Ippisch, O., Huwe, B., and Durner, W. "Dynamic Nonequilibrium During Unsaturated Water Flow." *Characterization and Measurement of the Hydraulic Properties of Unsaturated Porous Media; Proc. Intern. Workshop., Riverside, CA, 22-24 October, 1997, Riverside, CA, 877-892.*

- Sharma, P. V. (1997). *Environmental and Engineering Geophysics*, University Press, Cambridge.
- Siddiqui, S. I., Drnevich, V. P., and Deschamps, R. J. (2000). "Time Domain Reflectometry Development for Use in Geotechnical Engineering." *Geotechnical Testing Journal*, 23(1), 9-20.
- Šimůnek, J., M. Šejna, H. Saito, M. Sakai, and M. Th. van Genuchten. (2008). "The HYDRUS-1D Software Package for Simulating the Movement of Water, Heat, and Multiple Solutes in Variably Saturated Media, Version 4.0, HYDRUS Software Series 3." Department of Environmental Sciences, University of California Riverside, Riverside, California, USA.
- Šimůnek, J., Jarvis, N. J., Genuchten, M. T. v., and Gradenas, A. (2003). "Review and comparison of models for describing non-equilibrium and preferential flow and transport in the vadose zone."
- Singha, K., and Moysey, S. (2006). "Accounting for spatially variable resolution in electrical resistivity tomography through field-scale rock-physics relations." *Geophysics*, 71(4), A25-A28.
- Smith, M. L. (1993). *Ultrasonic Waveform Matching*, NER Application Note AN93-1, AutoLab Users Manual, New England Research, Inc.
- Spencer, J. W. (1979). "Bulk and Shear Attenuation in Berea Sandstone: The Effects of Pore Fluids." *Journal of Geophysical Research*, 84(B13), 7521-7523.

- Stewart, M., and North, L. (2006). "A borehole geophysical method for detection and quantification of dense, non-aqueous phase liquids (DNAPL) in saturated soils." *Journal of Applied Geophysics*, 60(2), 87-99.
- Stoll, R. D. (1985). "Marine Sediment Acoustics." *Journal of Acoustic Society of America*, 77, 1789-1799.
- Stoll, R. D., and Bryan, G. M. (1969). "Wave Attenuation in Saturated Sediments." *The Journal of the Acoustical Society of America*, 47(5 (Part 2)), 1440-1447.
- Tang, X. M., and Cheng, A. (2004). *Quantitative Borehole Acoustic Methods*, Elsevier, Amsterdam.
- Taylor, S. R., and Knight, R. J. (2003). "An inclusion-based model of elastic wave velocities incorporating patch-scale fluid pressure relaxation." *Geophysics*, 68(5), 1503-1509.
- Toksoz, M. N., Johnston, D. H., and Timurr, A. (1979). "Attenuation of seismic waves in dry and saturated rocks: 1. Laboratory measurements." *Geophysics*, 44(4), 681-690.
- Toms, J., Muller, T. M., Ciz, R., and Gurevich, B. (2006). "Comparative review of theoretical models for elastic wave attenuation and dispersion in partially saturated rocks." *Soil Dynamics and Earthquake Engineering*, 26, 548-565.
- Topp, G. C., Klute, A., and Peters, D. B. (1967). "Comparison of Water Content-Pressure Head Data Obtained by Equilibrium, Steady-State, and Unsteady-State Methods." *Soil Science Society of America Journal*, 31, 312-314.

- Tortorella, M. (1990). "Closed Newton-Cotes Quadrature Rules for Stieltjes Integrals and Numerical Convolution of Life Distributions." *SIAM J. Sci. Stat. Comput.*, 11(4), 732-748.
- Tortorella, M. (2005). "Numerical Solutions of renewal-type integral equations." *INFORMS Journal on Computing*, 17(1), 66-74.
- Tracy, F. T. (2006). "Clean two- and three-dimensional analytical solutions of Richard's equation for testing numerical solvers." *Water Resour. Res.*, 42(W08503), doi:10.1029/2005WR004638.
- Tserkovnyak, Y., and Johnson, D. L. (2002). "Can one hear the shape of a saturation patch?" *Geophysical Research Letters*, 29(7), 12.
- Tserkovnyak, Y., and Johnson, D. L. (2003). "Capillary forces in the acoustics of patchy-saturated porous media." *Journal of the Acoustic Society of America*, 114(5), 2596-2606.
- Tsukamoto, Y., Ishihara, K., Nakazawa, H., Kamada, K., and Huang, Y. (2002). "Resistance of partly saturated sand to liquefaction with reference to longitudinal and shear wave velocities." *Soils and Foundations*, 42(6), 93-104.
- Tuncay, K., and Corapcioglu, M. Y. (1996). "Body waves in poroelastic media saturated by two immiscible fluids." *Journal of Geophysical Research*, 101(B11), 25,149-25,159.
- Tuncay, K., and Corapcioglu, M. Y. (1997). "Wave Propagation in Poroelastic Media Saturated by Two Fluids." *Journal of Applied Mechanics*, 64, 313-320.

- Turgut, A., and Yamamoto, T. (1990). "Measurement of acoustic wave velocity and attenuation in marine sediments." *Journal of Acoustic Society of America*, 87(6), 2376-2383.
- Vachaud, G., Vauclin, M., and Wakil, M. (1972). "A study of the uniqueness of the soil moisture characteristic during desorption by vertical drainage." *Soil Science Society of America Journal*, 36, 531-532.
- van Genuchten, M. T. (1980). "A Closed-form Equation for Predicting the Hydraulic Conductivity of Unsaturated Soils." *Soil Science Society of America Journal*, 44, 892-898.
- Velea, D., Shields, F. D., and Sabatier, J. M. (2000). "Elastic Wave Velocities in Partially Saturated Ottawa Sand: Experimental Results and Modeling." *Soil Science Society of America Journal*, 4, 1226-1234.
- Viggiani, G., and Atkinson, J. H. (1995). "Interpretation of bender element tests." *Geotechnique*, 45(1), 149-154.
- Visscher, W. M., Migliori, A., Bell, T. M., and Reinert, R. A. (1991). "On the normal modes of free vibrations on inhomogeneous and anisotropic elastic objects." *Journal of Acoustic Society of America*, 90(4), 2154-2162.
- Wei, C., and Dewoolkar, M. "A Continuum Theory of Nonequilibrium Two-Phase Flow through Porous Media with Capillary Relaxation." *Advances in Unsaturated Soil, Seepage, and Environmental Geotechnics, Proceedings of Sessions of GeoShanghai, Shanghai, 6-8 June 2006, Shanghai*, 246-254.

- Wei, C., and Dewoolkar, M. (2006). "Rate-Dependent Behavior of Soil Moisture Retention Characteristics." In Progress.
- Wei, C., and Muraleethanan, K. K. (2006). "Acoustic characterization of fluid-saturated porous media with local heterogeneities: Theory and application." *International Journal of Solids and Structures*, 43, 982-1008.
- Wei, C., and Muraleetharan, K. K. (2002). "A continuum theory of porous media saturated by multiple immiscible fluids: II. Lagrangian description and variation structure." *International Journal of Engineering Science*, 40, 1835-1854.
- Wei, C., and Muraleetharan, K. K. (2002). "A continuum theory of porous media saturated by multiple immiscible fluids: I. Linear Poroelasticity." *International Journal of Engineering Science*, 40, 1807-1833.
- Wei, C., and Muraleetharan, K. K. (2007). "Linear viscoelastic behavior of porous media with non-uniform saturation." *International Journal of Engineering Science*, 45, 698-715.
- White, J. E. (1975). "Computed seismic speeds and attenuation in rocks with partial gas saturation." *Geophysics*, 40, 224-232.
- Wildenchild, D., Hopmans, J. W., Rivers, M. L., and Kent, A. J. R. (2005). "Quantitative Analysis of Flow Processes in a Sand Using Synchrotron-Based X-ray Microtomography." *Vadose Journal*, 4, 112-126.
- Wildenchild, D., Hopmans, J. W., and Simunek, J. (2001). "Flow rate dependence of Soil Hydraulic Characteristics." *Soil Science of America Journal*, 65, 35-48.

- Wildenchild, D., Hopmans, J. W., Vaz, C. M. P., Rivers, M. L., Rikard, D., and Christensen, B. S. B. (2002). "Using X-ray computed tomography in hydrology: systems, resolutions, and limitations." *Journal of Hydrology*, 267, 285-297.
- Wingham, D. j. (1985). "The dispersion of sound in sediment." *Journal of Acoustic Society of America*, 78(5), 1757-1760.
- Winkler, K., and Nur, A. (1979). "Pore Fluids and Seismic Attenuation in Rocks." *Geophysical Research Letters*, 6(1), 1-4.
- Winkler, K. W., and Nur, A. (1982). "Seismic attenuation: Effects of pore fluids and frictional sliding." *Geophysics*, 47, 1-15.
- Wong, R. C. K., and Wibowa, R. (2000). "Tomographic Evaluation of Air and Water Flow Patterns in Soil Column." *Geotechnical Testing Journal*, 23(4), 413-422.
- Wösten, J. H. M., and Genuchten, M. T. v. (1988). "Using texture and other soil properties to predict the unsaturated soil hydraulic functions." *Soil Science of America Journal*, 52, 1762-1770.
- Wulff, A., and Mjaaland, S. (2002). "Seismic monitoring of fluid fronts: An experimental study." *Geophysics*, 67(1), 221-229.
- Yamamoto, T. (2001). "Imaging the permeability structure within the near-surface sediments by acoustic crosswell tomography." *Journal of Applied Geophysics*, 47(1), 1-11.
- Yamamoto, T., Nye, T., and Kuru, M. (1994). "Porosity, permeability, shear strength: Crosswell tomography below an iron foundry." *Geophysics*, 59(10), 1530-1541

- Zadler, B. J., Rousseau, J. H. L. L., Scales, J. A., and Smith, M. L. (2004). "Resonant Ultrasound Spectroscopy: theory and application." *Geophysical Journal International*, 156, 154-169.
- Zagzebski, J. A. (1996). *Essentials of Ultrasound Physics*, Mosby Inc.
- Zamanek, J., and Rudnick, J. (1961). "Attenuation and dispersion of elastic waves in a cylindrical bar." *Journal of Acoustic Society of America*, 33, 1283-1288.
- Zienkiewicz, O. C. a. S., T. (1984). "Dynamic behavior of saturated porous media: the generalized Biot formulation and its numerical solution." *Int. J. Numer. Anal. Methods Geomech.*, 8, 71-96.